Università degli Studi di Ferrara

PH.D. Course
in
Evolutionary Biology and Ecology

In cooperation with:
Università degli Studi di Parma
Università degli Studi di Firenze

CYCLE XXXI

COORDINATOR Prof. Guido Barbujani

Population genetics meets dendrochronology: joint approaches to the exploration of growth and reproductive success in Norway spruce

Scientific/Disciplinary Sector (SDS) BIO/07

Candidate
Dott. Camilla Avanzi

Supervisor
Prof. Stefano Leonardi

Co-Supervisor
Dott. Andrea Piotti

Table of contents

Abstract p. 3

Chapter 1. Introduction p. 5

Chapter 2. Overview of the data p. 11
- 2.1 Study species p. 11
- 2.2 Study sites and sampling activities p. 11
- 2.3 Genetic data p. 14
- 2.4 Standard genetic analyses p. 16
- 2.5 Dendrochronological data p. 19
- 2.6 Climatic data p. 22

Chapter 3. Disentangling the effects of spatial proximity and genetic similarity on individual growth performances p. 23
- 3.1 Introduction p. 23
- 3.2 Materials and methods p. 25
- 3.3 Results p. 30
- 3.4 Discussion p. 40

Chapter 4. Do dendrophenotypic traits influence individual reproductive success? p. 46
- 4.1 Introduction p. 46
- 4.2 Materials and methods p. 48
- 4.3 Results p. 55
- 4.4 Discussion p. 62

Chapter 5. Do SNP loci putatively under selection have an influence on individual reproductive success? p. 70
- 5.1 Introduction p. 70
- 5.2 Materials and methods p. 72
- 5.3 Results p. 77
- 5.4 Discussion p. 86

Chapter 6. Conclusions and future insights p. 89

References p. 91

Appendix 1 p. 109

Abstract

Predicting the fate of forest tree species is crucial to adopt forest management strategies that could effectively mitigate the effects of climate change. To this aim, tree-ring time series can be used to investigate growth dynamics and responses to climate and environmental stressors. The potentialities of tree-ring data have been recently acknowledged by the scientific community and tree-ring research is experiencing a "*renaissance*" of new uses. In particular, there is a raising interest in linking dendrochronological and genetic data to shed light on the genetic basis of local adaptation.

My PhD thesis aims at developing a comprehensive framework to jointly analyse dendrochronological and genetic data in forest tree populations. By embracing the change in perspective proposed by recent dendrochronological literature, I switched from the classical, population-based dendrochronological approach to an extensive individual-based exploration of growth dynamics. To this aim, I exhaustively sampled the genetic and dendrophenotypic variance of five Norway spruce (*Picea abies*) populations. Within each population, I sampled individuals from two age cohorts following the requirements for parentage analysis and collecting a total of 518 adults and 604 seedlings. All individuals were genotyped at both neutral and potentially adaptive genetic markers. Taking advantage of dendrochronological techniques, all adult trees were phenotyped scoring a large set of dendrophenotypic traits.

My thesis is structured in six chapters. After an overview of the state of the art in Chapter 1, in Chapter 2 I described the studied species, the sampling sites and the datasets used.

In Chapter 3, I combined dendrochronological, genetic and spatial data to disentangle the relative importance of genetic similarity and spatial proximity on individual growth performances. The modelling approach used successfully captured a large fraction of variance in growth, which was mainly embedded in inter-individual differences. Genetic similarity did not explain variation in the individual parameters describing growth. In contrast, up to 29% of the variance of individual parameters was due to the spatial location of individuals. These results showed the advantages of modelling dendrochronological data at the individual level to study growth determinants and the relevance of micro-environmental variation for individual growth patterns.

In Chapter 4, I combined dendrochronological, genetic and spatial data to investigate the determinants of individual reproductive success. I tested a large set of dendrophenotypic traits against reproductive success to quantify the effect of aging, tree growth rate and

climate sensitivity on the number of offspring sired by each adult tree. I found that, regardless the number of reproductive seasons they have been through, trees with the highest reproductive success had higher growth rates, in particular when temperature of the previous vegetative season is potentially limiting. These results suggested that individuals with higher growth rates better compensate reproductive costs by increasing their resource intake and/or through other compensatory mechanisms.

Finally, in Chapter 5 I searched for genetic signatures of local adaptation both in the adult and seedling cohorts, by using an integrated approach based on F_{ST}-based tests and environmental association analysis. I identified three and four SNPs as putative loci under selection in adults and seedlings, respectively. I then assessed if these SNP loci influence individual reproductive success. Although no evidence of such an influence was found, I showed how evaluating the effect of SNP loci on reproductive success might be a straightforward strategy to validate results from classical approaches to the study of local adaptation.

The main conclusions and most promising perspectives of my work, together with the methodological innovations propounded are summarized in Chapter 6.

Chapter 1

Introduction

Both average temperature and frequency of extreme climatic events (*e.g.* extreme droughts, heat waves, late frosts, heavy rains) have increased over the last decades (Jones *et al.*, 2001) and are expected to further increase during the upcoming century (IPCC, 2013). Among other consequences, such changes have started a complex spatial rearrangement of the distribution of climatic conditions (*e.g.* Loarie *et al.*, 2009), niche envelopes (*e.g.* McKenney *et al.*, 2014) and species ranges as well (*e.g.* Parmesan and Yohe, 2003; Parmesan, 2006; Lenoir *et al.*, 2008; Chen *et al.*, 2011). Understanding and predicting the fate of forest tree species is a vital concern because of the important roles they play in natural systems and for the ecosystem services they provide (Bonan, 2008; Allen *et al.*, 2010). In addition, since they are sessile, long-lived organisms with overlapping generations, they are considered to be particularly vulnerable to shifts in ecological conditions (Kremer *et al.*, 2012). Forest tree populations can adopt three strategies to respond to a changing environment. They can migrate towards new favourable habitats through seed dispersal, persist *in situ* by adjusting their phenotype and/or adapt to the new local conditions (Aitken *et al.*, 2008). These strategies are often considered as alternative responses but they will likely occur simultaneously, intermingling their effects (Kremer *et al.*, 2012). Forest tree populations will persist in their current sites depending on their sensitivity to current perturbations and their adaptive potential to future climatic and environmental changes (Aubin *et al.*, 2016). High genetic variation for traits involved in responses to climate, large effective population sizes and the possibility for adaptive gene flow are expected to ensure the best long-term evolutionary potential to populations (Alberto *et al.*, 2013). Although trees are supposed to have a generally strong potential for evolutionary changes (Savolainen *et al.*, 2007), it is actually still debated whether long-term genetic adaptation and migration will be fast enough to keep pace with the unprecedented velocity of the ongoing climate change (*e.g.* Hamrick, 2004; Jump and Peñuelas, 2005; Aitken *et al.*, 2008; Kremer *et al.*, 2012; Alberto *et al.*, 2013; Corlett and Westcott, 2013).

A population is considered locally adapted if it has a higher fitness at its home site than non-local populations originating from other sites (Kawecki and Ebert, 2004). Strong evidence that forest tree populations are generally locally adapted to climate has been accumulating

through a long history of common garden and reciprocal transplant experiments (*e.g.* Langlet, 1971; Savolainen *et al.*, 2007). In such experiments fitness was often evaluated by measuring dendrometric traits (*e.g.* tree diameter and height). Nevertheless, the genetic and ecophysiological mechanisms that shape trees' responses to climate are still largely unknown (Aubin *et al.*, 2016; Housset *et al.* 2018). Filling these gaps of knowledge is crucial to predict the fate of forest tree species and adopt effective forest management strategies to mitigate the effects due to climate change. For instance, detailed knowledge of local adaptation dynamics is required to successfully translocate individuals from pre-adapted populations toward other parts of the species range (*i.e.* assisted gene flow) or even outside the species current distribution (*i.e.* assisted colonization) (Aitken and Whitlock, 2013). To elucidate the genetic architecture of climate adaptation throughout a tree lifespan, a tree-centred approach based on tree-ring time series has been recently proposed together with a conceptual framework to evaluate tree responses to past oscillations of environmental and climatic conditions (Housset *et al.* 2018).

Tree rings are natural archives of past environmental conditions, as their morphological and anatomical properties are shaped by the interplay of several intrinsic and extrinsic variables (Carrer *et al.*, 2015). These wood characteristics can be measured to generate retrospective multi-decade to multi-century time series of individual annual growth. Such tree-ring time series can be used to investigate tree growth dynamics and responses to climate and environmental stressors. For instance, correlating growth time series and monthly climatic variables has allowed dendroecologists to shed light on the factors that limit growth and the time of the year (month or season) which trees are particularly sensitive to (Fritts, 1976). The huge amount of information embedded in tree rings can be distilled in a multitude of tree-ring-based traits (*i.e.* dendrophenotypes, as defined in Heer *et al.*, 2018) that represents an exceptional resource for addressing global change questions (Evans *et al.*, 2018). Potentialities of tree-ring data have been recently acknowledged by the scientific community and tree-ring research is now experiencing "*a renaissance of new uses*" (Evans *et al.*, 2018) and it is expanding far beyond its initial aims (Büntgen, 2019). Among others, there is a raising interest in linking dendrochronological and genetic data (Franks *et al.*, 2014). First attempts in this direction were made by analysing growth-climate correlations in common garden experiments, exploring the effect of genetic variation among provenances on growth patterns (*e.g.* Taeger *et al.*, 2013; Montwé *et al.,* 2016) as well as signatures of genetic adaption to climate (Housset *et al.* 2018; Trujullo-Moya *et al.*, 2018). Common gardens represent a powerful experimental set-up to assess among-population genotypic divergence in controlled environmental conditions (Alberto *et al.*, 2013). However, they have some

well-known drawbacks: *i*) they are not available for most non-commercial species; *ii*) they are limited to a set of soil and climatic conditions that may not reflect the actual native environmental conditions; *iii*) provenances are usually from a low number of fecund mother trees that might not be representative of the genetic variation of the entire population; *iv*) in long-lived species such as trees, traits are prevalently studied on seedlings or saplings, thus shedding light only on early-stage dynamics. For all these reasons, comprehensive investigations in natural populations are required to complement the information gathered from common garden experiments and increase our knowledge on local adaptation in natural settings (Bontemps *et al.*, 2016).

To my knowledge, only few studies have combined dendrochronological and genetic data in natural settings. The influence of the genetic layout of populations on tree growth synchronicity (King *et al.,* 2013; Latutrie *et al.*, 2015), average growth rates (Babushkina *et al.*, 2016) and growth-climate correlations (Bosela *et al.*, 2016) have been investigated at different spatial scales. For instance, significant differences in growth patterns and climate sensitivity were found among *Abies alba* populations belonging to different post-glacial genetic lineages (Bosela *et al.*, 2016). However, this study did not control for the effect of potential confounding environmental features (*e.g.* soil, elevation) that can shape growth dynamics as well. Effective strategies that account for such confounding environmental factors are essential to avoid misleading conclusions regarding the link between genetics and growth in natural populations (Housset *et al.*, 2016). However, this has been addressed only in very few studies. Housset *et al.* (2016) investigated the correlation between population genetic structure and climate responses of *Thuja occidentalis* both within and among populations. The authors assessed the relative contribution of genetic structure, climate and environmental conditions to growth-climate correlations by using a statistical approach that merged model selection and variance partitioning. Heer et al. (2018) explored the genetic basis of individual silver fir responses to the 1970s stress episode that caused a large-scale forest dieback in Central Europe. These authors accounted both for micro- and macro-environmental variation by first normalizing tree-ring series and then standardizing the metrics used to measure the magnitude of the stress episode on growth.

Besides the relevance of studying local adaptation in natural settings, another aspect that should be stressed is the need for an individual-based exploration of growth dynamics. In fact, the classical dendrochronological approach typically has a population-based focus, mainly aimed at extracting and enhancing the common climatic signal while removing the noise introduced by inter-individual variation in growth patterns (Cook, 1985). Such approach is efficient as long as tree-ring time series are used to reconstruct past climate or

to date events. However, it prevents any characterization of the whole spectrum of individual growth performances, which is essential for a better understanding of tree species dendroecology (Carrer, 2011). On the contrary, an individual-based exploration of growth dynamics would allow to disentangle the role of several drivers of growth, such as age, competition and climatic and environmental variables (*e.g.* Primicia *et al.*, 2015; Rozas, 2015) as well as the individual genetic background. The benefits of such a change in perspective have been discussed in the recent dendrochronological literature (*e.g.* Carrer, 2011; Galvan *et al.*, 2014; Redmond *et al.*, 2017). To this purpose, the adoption of new experimental approaches has been suggested (Galvan *et al.*, 2014). In particular, an exhaustive sampling of the within-population dendrophenotypic variance seems a promising strategy to correctly describe the spectrum of possible growth dynamics.

Understanding the link between individual growth and its determinants is a first step towards a deeper understanding about how trees' genotypes survive, thrive or succumb in their environment. However, from an evolutionary point of view it is essential to dig deeper in the genetic consequences of growth patterns, that is the outcome of each individual in terms of its representation in the next generations. To maximize its fitness, that is the number of surviving offspring produced by each individual, an individual should invest in *i*) growth, in order to win against its competitors, *ii*) defences, in order to avoid predation and *iii*) reproduction (Obeso, 2002). These different investments are tightly interdependent, so that the existence of trade-offs between such life history traits (*i.e.* growth, survival, reproduction) has been postulated since long time (Williams, 1966; Levins, 1968). For instance, perennial polycarpic plants often show an inverse correlation between vegetative growth and seed production (Harper, 1977). The same negative relationship has been reported in forest tree species (*e.g.* Pukkala, 1987; Viglas *et al.*, 2013; Davi *et al.*, 2016). However, studies on the costs associated to reproduction in plants have often relied on indirect measures of fitness, quantified through the amount of resources invested in reproductive structures (*e.g.* biomass/number of seeds, pollen grains, flowers, fruits) (Oddou-Muratorio *et al.*, 2018a). The development of marker-based approaches to paternity and parentage analysis has represented a powerful tool to quantify individual fitness in terms of number of gametes produced by each adult tree (Meagher and Thompson, 1987). Such marker-based measures of fitness are considered more reliable than the resource-based ones, as they account, at least partially, for all those dispersal and post-dispersal processes that may decouple individual fecundity from individual effective reproductive success (*e.g.* pre- and post-zygotic selection, spatial arrangements of favourable microsites for regeneration, early mortality rates) (Schoen and Stewart, 1986; Bernasconi, 2003; Amm *et al.*, 2012).

These processes play a crucial role in shaping population dynamics, as they determine the initial template for plant regeneration and drive the transmission of genetic variation across generations (Bontemps *et al.*, 2013). However, obtaining lifetime measures of individual fitness is extremely demanding in long-lived species such as trees, because they require a long-term monitoring far beyond the duration of most studies (Steinitz *et al.*, 2011). Life-stage studies usually rely on a diachronic approach (*i.e.* survey of the same cohort throughout the recruitment process; Augspurger, 1983) or on a synchronic one (*i.e.* survey of different distinct cohorts, generally seeds and recruited seedlings) (Bontemps *et al.*, 2013). Both approaches are resource- and time-consuming, especially if they are replicated in multiple sites. Replicating these studies is essential for moving from case-study evidence towards generalization at the species level.

Reproductive dynamics have a critical importance for the maintenance, demography and adaptation of forest tree populations (Hampe and Petit, 2005). Reproductive success is highly unequal within populations, with generally few individuals overwhelmingly contributing to the next generation and many local offspring fathered and/or mothered by adult trees located outside the study population (*e.g.* Schnabel *et al.*, 1998; González-Martinez *et al.*, 2006; Steinitz *et al.*, 2011; Moran and Clark, 2012; Gerzabek *et al.*, 2017). The phenotypic determinants that are most frequently tested against reproductive success are tree size (*e.g.* Schnabel *et al.*, 1998; Piotti *et al.*, 2009; Leonarduzzi *et al.*, 2016; Chybicki and Oleska, 2018), investments in reproductive structures (*e.g.* Meagher and Thompson, 1987; Morgan and Conner, 2001; González-Martínez *et al.*, 2006) and flowering phenology (*e.g.* Burczyk and Prat, 1997; Piotti *et al.*, 2012). However, the determinants of reproductive success as well as their interactions are still largely under-documented (Oddou-Muratorio *et al.*, 2018b). In particular, the relationship between growth and reproduction has been rarely assessed (González-Martínez *et al.*, 2006; Moran and Clark, 2012; Oddou-Muratorio *et al.*, 2018b). Considering the tight link between individual growth and reproductive output and the major consequences that both these processes have on the evolutionary dynamics of populations (Obeso, 2002), studying such relationship represents a promising research topic to deepen our understanding of the adaptive responses of forest trees to climate and environmental changes.

In my PhD thesis, I built a comprehensive framework to combine dendrochronological and genetic data, aiming at unravelling the tight link between individual growth and reproductive dynamics in natural populations of Norway spruce (*Picea abies* (L.) Karst). To this purpose, I carried out a genetic and phenotypic characterization of a large sample of trees from two

study sites in southern and central Europe (a detailed description of study sites and data is provided in Chapter 2). Within each study site, multiple plots were established at different altitudes. Within each plot, individuals from two age cohorts (adults and seedlings) were sampled following the requirements for parentage analysis. All individuals were then genotyped at both neutral and potentially adaptive genetic markers. Taking advantage of dendrochronological techniques, all adult trees were phenotyped scoring a large set of tree-ring-based phenotypic traits. First, I assessed the influence of genetic relatedness among individuals on growth performances (Chapter 3). I tested whether more genetically related individuals exhibit more similar growth performances. To answer this research question, I developed an analytical framework which allowed me to properly account for the confounding effects of other drivers of growth (*i.e.* age, temperature, precipitation, microenvironmental heterogeneity). Second, I performed a detailed investigation of the phenotypic basis of reproductive success in Norway spruce (Chapter 4). To this purpose, I tested a large set of dendrophenotypic traits against individual reproductive success to quantify the effect of aging, tree growth rate and climate sensitivity on the number of offspring sired by each adult tree. Finally, I explored patterns of allele frequencies to detect signals of local adaptation in the two sampling sites (Chapter 5). An integrated approach based on F_{ST}-based tests and environmental association analysis was used to identify genetic markers potentially under selection in both age cohorts. The results of these classical methods for the study of local adaptation were validated using an innovative approach, that is testing whether these genetic markers potentially under selection influence individual reproductive success.

Chapter 2

Overview of the data

2.1 Study species

Norway spruce is one of the key European forest tree species both for its high ecological and economical relevance (Bucci and Vendramin, 2000). It is a monoecious, predominantly outcrossed and anemophilous conifer, capable of long-distance pollen and seed dispersal (Xie and Knowles, 1994; Burczyk *et al.*, 2004; Piotti *et al.*, 2009). It generally reaches flowering maturity around 30-40 years and starts seed production after 50 years (Giesecke and Bennett, 2004). Its geographical distribution is divided into a northern and a southern part (**Fig. 1**), which correspond to as many genetically differentiated groups (Lagercrantz and Ryman, 1990; Tollefsrud *et al.*, 2008). In the north, the species forms a wide continuum covering both the entire Scandinavia and European Russia, until the Ural Mountains. In the south, it mainly occurs along the mountains of central and south-eastern Europe, from Western Alps until the Balkan peninsula. Norway spruce modern range essentially results from the post-glacial demographic events of the last 13000 years, but it also has been influenced by the intensive planting activities occurred in the last 200 years (Bucci and Vendramin, 2000). Although the species vegetates within a wide range of climatic and environmental conditions, Norway spruce is a continental tree which tolerates high summer temperatures but initiates bud and shoot growth at relatively low temperatures (Partanen *et al.*, 1998). It prefers moist acid soils with high seasonal water storage (Sutinen *et al.*, 2002) mainly because of its shallow root system that makes water supply more demanding. Such root system exposes the species also to the risks of windthrow, as recently seen during the storm "Vaia" that occurred in north-eastern Italy in October 2018 causing the loss of eight million m^3 of standing trees (mainly spruces) (Motta *et al.*, 2018).

2.2 Study sites and sampling activities

The first study site is located within the Campolino Natural Reserve (northern Apennines, Italy), which hosts the Italian southernmost autochthonous Norway spruce population (Chiarugi, 1936; Ravazzi, 2002; Vescovi *et al.*, 2010; Magri *et al.*, 2015). Here, three plots were established at different elevations (**Table 1**). The first plot (CAMH, ~1730 m a.s.l.) is a recent recolonization area within an abandoned wooded pasture at the upper forest limit. It

is a pure, highly dense and relatively young *Picea abies* stand, with abundant regeneration. The second plot (CAME, ~1615 m a.s.l.) is a mature stand, where spruce is mixed with silver fir (*Abies alba* Mill.) and beech (*Fagus sylvatica* L.). The third plot (CAML, ~1475 m a.s.l.) is a mixed forest with prevalence of beech and silver fir, where spruce occurs scatteredly. The second study site is located in the Bavarian National Park (Bohemian Massif, Germany). Here, two plots were established at the local altitudinal extremes of Norway spruce distribution (**Table 1**). The first plot (BAVH, ~1300 m a.s.l.) is a pure spruce forest while the second one (BAVL, ~730 m a.s.l.) is a mixed stand with beech and silver fir.

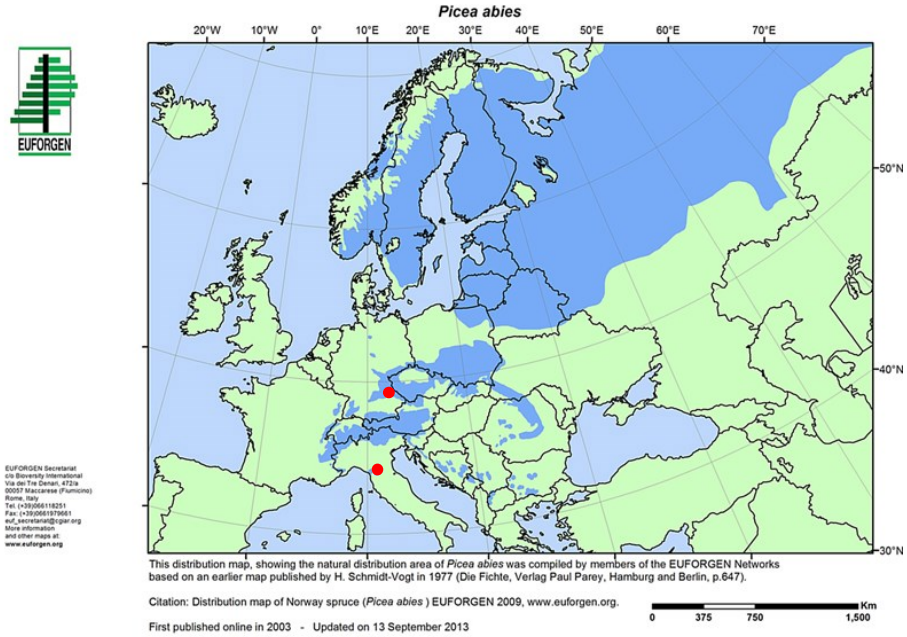

Fig. 1 Map of *Picea abies* geographical distribution. Red dots are approximate locations of the two study sites.

Table 1 Geographic coordinates and stand characteristics of the five *Picea abies* plots.

Characteristic	Unit	CAMH	CAME	CAML	BAVH	BAVL
Country		Italy	Italy	Italy	Germany	Germany
Latitude	°N	44°06'36"	44°06'47"	44°07'07"	49°05'04"	49°05'55"
Longitude	°E	10°39'44"	10°39'47"	10°40'18"	13°17'06"	13°13'39"
Mean elevation	m	1730	1615	1475	1300	730
Area	ha	0.25	0.83	1.95	0.38	1.46
Conspecific density	ind ha^{-1}	648	127	28	263	68
Mean temperature	°C	4.81	5.35	6.19	2.84	5.92
Mean precipitation	mm	1937	1906	1762	1141	933
Adults sampled	ind	159	105	54	100	100
Seedlings sampled	ind	148	100	63	150	150

In each of the five plots data collection was done following the same sampling scheme which consisted in delimiting a roughly circular area and sampling all the adult trees within, as well

as a subset of seedlings (**Fig. 2**), for a total of 518 and 611 individuals, respectively (**Table 1**). Trees were identified as adults based both on their size and the presence of cones. Seedlings were collected from different cohorts (average basal diameter: 5.7±0.2 cm; average height: 36.4±1.5 cm; **Fig. 3**), accordingly to local densities. Fresh needles were collected from all individuals for genetic analyses. Adult tree stems were cored at 1.3 m using a Pressler increment borer and taking one increment core in the Italian plots and two in the German ones. Spatial positions of both adults and seedlings were recorded using compass and laser distancimeter in the Italian plots and a GPS device in the German ones. Diameter at breast height (DBH) and basal diameter were recorded for all adults and seedlings, respectively.

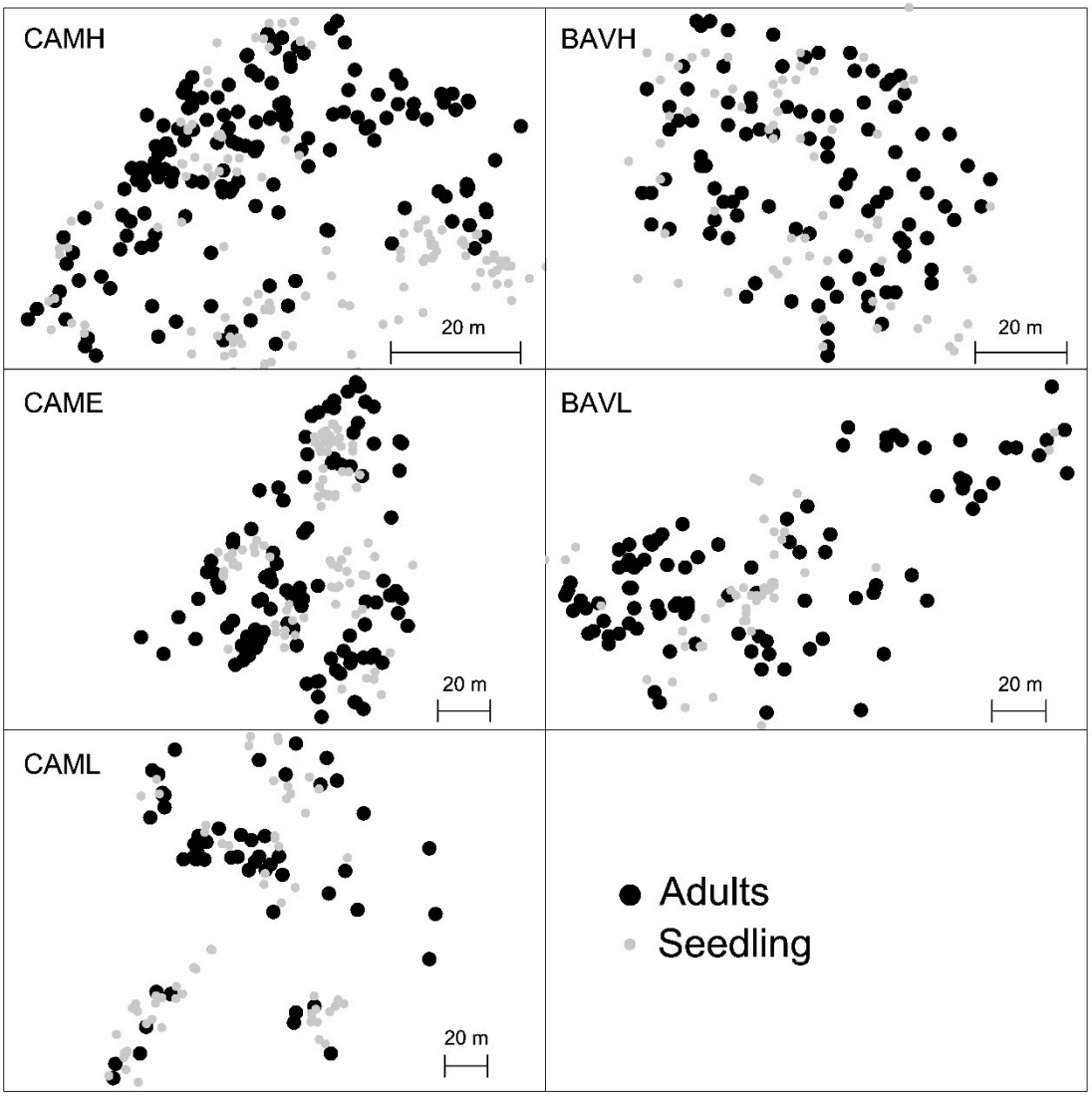

Fig. 2 Maps of the five *Picea abies* plots. Adults are represented by black dots, while seedlings by grey ones.

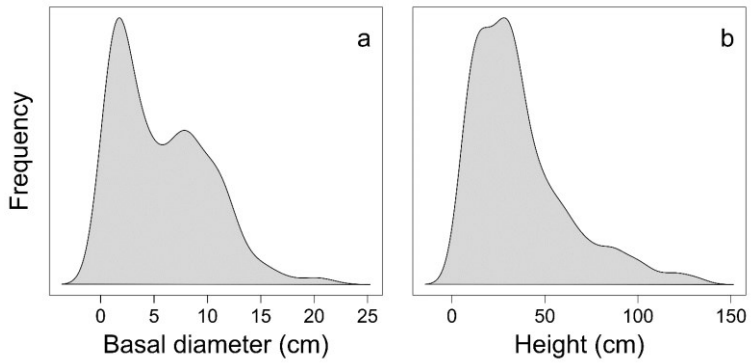

Fig. 3 Frequency distribution of (**a**) basal diameter and (**b**) height of all sampled seedlings.

2.3 Genetic data

DNA was extracted from 50 mg of frozen needles using the DNeasy 96 Plant Kit (Qiagen) following the manufacturer's instructions. Adults and seedlings were genetically characterized by using both neutral and potentially adaptive genetic markers (**Table 2**).

Table 2 Number of individuals genotyped with neutral (SSR) and potentially adaptive (SNP) genetic markers.

	CAMH	CAME	CAML	BAVH	BAVL	Total
Adults genotyped at SSR loci	159	105	54	100	100	518
Seedlings genotyped at SSR loci	148	100	63	148	145	604
Adults genotyped at SNP loci	152	103	52	100	100	507
Seedlings genotyped at SNP loci	142	100	63	150	150	605
Adults genotyped with SNP after filtering procedure	138	86	47	93	88	452
Seedlings genotyped with SNP after filtering procedure	126	93	59	130	148	556
Non-admixed[a] adults for which SNP are available	115	77	25	79	73	369
Non-admixed[a] seedlings for which SNP are available	109	85	36	101	123	454

[a]The level of admixture was evaluated on STRUCTURE results on SSR data. Individuals were considered non-admixed whether they had a q_I <0.2 or >0.8.

Neutral genetic markers

All sampled individuals were genotyped with 11 nuclear microsatellite markers (nSSR) (Pa05, Pa28, Pa44: Fluch *et al.*, 2011; SpAGG03: Pfeiffer *et al.*, 1997; WS0092.A19, WS0022.B15, WS0016.O09, WS00111.K13, WS0023.B03: Rungis *et al.*, 2004; EATC1E03, EATC2G05: Scotti *et al.*, 2002) and three chloroplast ones (cpSSR) (Pt26081, Pt63718, Pt71936: Vendramin *et al.*, 1996). The 14 microsatellite markers were multiplexed in four PCRs using the Type-it Microsatellite PCR kit (Qiagen), optimizing the final volume of PCRs to 6 µl. The PCR mix was 3 µl of Type-it Multiple PCR Master Mix, 0.6 µl of

primers premix, 1.4 µl of RNase-free water and 1 µl of DNA (~10 ng/µl). The amplification profile required an initial step at 95 °C for 5 min, followed by 30 cycles at 95 °C for 30 s, 57 °C for 90 s and 72 °C for 30 s, with a final 30 min extension step at 60 °C. All PCRs were performed on a GeneAmp PCR System 9700 thermal cycler (Perkin Elmer) and PCR products were run on AB 3500 sequencer (Applied Biosystems, USA), with LIZ-500 as internal size standard. Allele calling and binning were performed manually using GeneMarker (Softgenetics).

Potentially adaptive markers

Sampled individuals were genotyped with a set of 135 single nucleotide polymorphisms (SNPs). Such SNPs were located within candidate genes which were likely involved in wood formation, growth and phenology (Heuertz *et al.*, 2006; Chen *et al.*, 2010, 2012a, 2012b, 2016; Pavy *et al.*, 2013; Källman *et al.*, 2014; Heer *et al.*, 2016; **Table 3**). SNP genotyping was done using PCR-based KASP^{TM} genotyping assays at LGC Genomics Ltd. (Hoddesdon, UK).

Table 3 Sources of 135 SNPs used in the KASP assays.

Number of SNPs	Reference
70	Pavy *et al.* (2013)
22	Chen *et al.* (2012b)
16	Chen *et al.* (2012a)
13	Heer *et al.* (2016)
7	Heuertz *et al.* (2006), Chen *et al.* (2010), Källman *et al.* (2014)
6	Chen *et al.* (2016)
1	http://dendrome.ucdavis.edu/NealeLab/crsp/

The dataset was initially filtered by removing SNPs that were not called correctly for the majority of the dataset (>80% of missing data) because they may interfere with subsequent filtering steps. Then, individuals and SNPs with more than 20% of missing data, as well as monomorphic SNPs, were removed. Finally, all SNPs with a minor allele frequency (MAF) <2% were removed. At the end of the filtering procedure, the SNP dataset was made up of 1008 individuals and 115 SNP markers (**Table 2**; **Appendix 1**).

2.4 Standard genetic analyses

Linkage disequilibrium

Presence of within-population linkage disequilibrium among SSR loci was tested with Genepop 4.7 (Rousset, 2008), using log-likelihood ratio statistics (G test) with Bonferroni correction. The 11 SSRs used were unlinked.

Within-plot genetic variation

For each plot and demographic stage and both on nSSR and SNP datasets, standard genetic parameters (*Na*, H_E, H_O, F_{IS}) were calculated by using GenAlEx v6.5 (Peakall and Smouse, 2012). Allelic richness (*Ar*) was calculated both on nSSR and SNP datasets using HP-RARE v1.0 (Kalinowski, 2005) based on a minimum sample size of 50 and 40 diploid individuals, respectively. Diversity indexes for cpSSR (*h* = number of haplotypes, *Pb* = haplotypic richness) were calculated by using Contrib (Petit *et al.*, 1998). All these calculated parameters were reported in **Table 4**.

Pairwise genetic differentiation

To assess genetic differentiation, pairwise G'_{ST} values (Hedrick, 2005) between each stand and demographic stage were calculated with GenAlEx using 999 permutations on nSSR data, while pairwise F_{ST} values on SNP data (**Table 5**). The picture of genetic differentiation emerging from the two datasets was consistent. In particular, *i*) no significant genetic differentiation was found across generations within each plot, *ii*) the two study sites showed the highest genetic differentiation values (average pairwise G'_{ST} of 0.0843 and average pairwise F_{ST} of 0.026), and *iii*) the German site was more genetically homogeneous with respect to the Italian one (average pairwise G'_{ST} of 0.024 *vs.* 0.034; average pairwise F_{ST} of 0.005 *vs.* 0.011).

Genetic structure

Two approaches were applied to assess the existence of genetic structure within or between study sites. Preliminarily, a Principal Coordinates Analysis (PCoA) was carried out both on SSR and SNP datasets to provide a visual representation of the genetic distance relationships among the sampled Norway spruce trees. Such analysis was performed using GenAlEx. Point clouds resulting from PCoA showed a slight genetic differentiation between the two study sites (**Fig. 4**) on both datasets.

Table 4 Averaged genetic diversity parameters calculated for each plot and demographic stage, both on nSSR and SNP datasets. *Na*: number of alleles, *Ar*: allelic richness, H_O: observed heterozygosity, H_E: expected heterozygosity, F_{IS}: fixation index, *h*: number of haplotypes, *Pb*: haplotypic richness.

Marker	Plot	*Na*	*Ar*	H_O	H_E	F_{IS}	*H*	*Pb*
SSR	CAMHa	10.18 (2.10)	8.82 (2.66)	0.63 (0.09)	0.65 (0.09)	0.03 (0.01)	13	8.46
	CAMHs	9.91 (2.12)	8.6 (2.59)	0.65 (0.10)	0.65 (0.10)	-0.003 (0.01)	15	8.91
	CAMEa	8.73 (1.79)	7.74 (2.33)	0.64 (0.09)	0.64 (0.09)	-0.005 (0.02)	11	7.40
	CAMEs	8.73 (1.84)	7.7 (2.32)	0.60 (0.10)	0.62 (0.09)	0.07 (0.04)	12	7.97
	CAMLa	8.72 (1.76)	8.65 (2.61)	0.61 (0.09)	0.63 (0.09)	0.03 (0.02)	11	9.63
	CAMLs	9.36 (1.96)	9.03 (2.72)	0.63 (0.09)	0.64 (0.09)	0.01 (0.02)	15	12.67
	BAVHa	12.45 (2.62)	11.05 (3.33)	0.52 (0.07)	0.65 (0.09)	0.16 (0.03)	20	13.69
	BAVHs	13.27 (2.67)	11.42 (3.44)	0.56 (0.08)	0.66 (0.09)	0.13 (0.03)	17	11.26
	BAVLa	12.09 (2.75)	10.84 (3.27)	0.62 (0.09)	0.66 (0.10)	0.05 (0.02)	18	11.64
	BAVLs	13.18 (2.75)	11.19 (3.37)	0.61 (0.08)	0.66 (0.09)	0.07 (0.02)	19	9.96
SNP	CAMHa	1.98 (0.01)	1.90 (0.02)	0.29 (0.02)	0.31 (0.02)	0.07 (0.02)		
	CAMHs	1.97 (0.02)	1.89 (0.02)	0.29 (0.02)	0.31 (0.02)	0.06 (0.01)		
	CAMEa	1.96 (0.02)	1.89 (0.02)	0.30 (0.02)	0.31 (0.02)	0.04 (0.02)		
	CAMEs	1.98 (0.01)	1.89 (0.02)	0.31 (0.02)	0.31 (0.02)	0.02 (0.01)		
	CAMLa	1.97 (0.01)	1.94 (0.02)	0.30 (0.02)	0.32 (0.02)	0.05 (0.02)		
	CAMLs	1.97 (0.01)	1.94 (0.02)	0.32 (0.02)	0.32 (0.02)	0.002 (0.02)		
	BAVHa	2.00 (0)	1.96 (0.01)	0.32 (0.02)	0.33 (0.01)	0.04 (0.02)		
	BAVHs	2.00 (0)	1.97 (0.01)	0.33 (0.02)	0.33 (0.01)	0.01 (0.01)		
	BAVLa	2.00 (0)	1.97 (0.01)	0.34 (0.02)	0.34 (0.01)	0.005 (0.01)		
	BAVLs	2.00 (0)	1.97 (0.01)	0.34 (0.02)	0.34 (0.01)	0.01 (0.01)		

Table 5 Matrix of pairwise values of genetic differentiation among each stand and demographic stage. G'_{ST} values were calculated on nSSR dataset and are reported below the diagonal, while F_{ST} were calculated on SNP dataset and reported above. All parameters were statistically different from zero, based on AMOVA with 999 permutations.

	CAMH ad	CAMH sdl	CAME ad	CAME sdl	CAML a	CAML sdl	BAVH ad	BAVH sdl	BAVL ad	BAVL sdl
CAMH ad	-	0.002	0.007	0.007	0.015	0.014	0.028	0.024	0.025	0.023
CAMH sdl	0.0003	-	0.006	0.008	0.016	0.016	0.030	0.026	0.026	0.024
CAME ad	0.0135	0.0160	-	0.004	0.018	0.018	0.030	0.026	0.024	0.024
CAME sdl	0.0150	0.0175	0.0006	-	0.017	0.018	0.030	0.026	0.025	0.025
CAML ad	0.0339	0.0399	0.0536	0.0486	-	0.005	0.030	0.028	0.027	0.025
CAML sdl	0.0360	0.0378	0.0539	0.0537	0.0031	-	0.029	0.026	0.024	0.022
BAVH ad	0.0877	0.0838	0.1140	0.1077	0.0790	0.0759	-	0.003	0.009	0.006
BAVH sdl	0.0709	0.0700	0.0945	0.0931	0.0660	0.0650	0.0036	-	0.007	0.003
BAVL ad	0.0788	0.0793	0.1009	0.0991	0.0890	0.0939	0.0240	0.0144	-	0.003
BAVL sdl	0.0729	0.0704	0.0944	0.0915	0.0740	0.0720	0.0100	0.0084	0.0027	-

Next, the Bayesian clustering algorithm implemented in STRUCTURE v.2.3.4 (Pritchard *et al.*, 2000) was used to *i*) determine the most likely number of genetic clusters (K) in which sampled individuals can be divided an *ii*) quantifying the probability (*q* value) of each individual to belong to each of the identified genetic clusters. The analysis was performed both on SSR and SNP datasets, running the standard admixture model with correlated allele frequencies. K ranged from one to ten, and ten runs were replicated for each K. Burn-in period consisted of 5×10^4 and 1×10^4 iterations for SSR and SNP data, respectively. Similarly, data collection consisted of 2×10^5 and 5×10^4 iterations. Convergence toward reliable *q* value estimates was assessed by checking whether log-likelihood and alpha parameter trends were constant. The most likely K was selected calculating the empirical statistic ΔK (Evanno *et al.*, 2005), which is implemented in the STRUCTURE HARVESTER software (Earl and vonHoldt, 2012). The CLUMPAK online software was used for coordinating the different runs and obtaining *q* values averaged over the runs (Kopelman *et al.*, 2015). The Bayesian clustering analysis showed the presence of a genetic structure with optimal grouping at K = 2 both on nSSR and SNP datasets (**Fig. 5**). Such grouping globally distinguished the German plots from the Italian ones (**Fig. 5**). However, CAML showed the largest signal of admixture. Based on SSR data, 19% of individuals were clearly assigned to the German cluster, while the percentage of individuals that were hybrids between the two inferred genetic clusters (*i.e.* $0.2< q_1 <0.8$) reached 41%. Numbers of individuals that were clearly assigned to one of the two inferred genetic cluster (*i.e.* $q_1 \leq 0.2$ or $q_1 \geq 0.8$) are reported in **Table 2**.

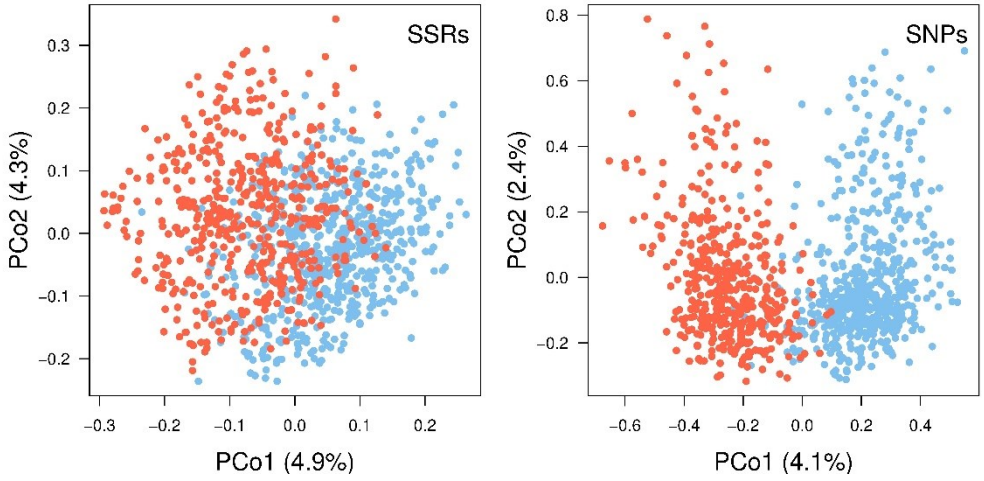

Fig. 4 First two axes of the PCoA performed on both nSSR and SNP datasets.

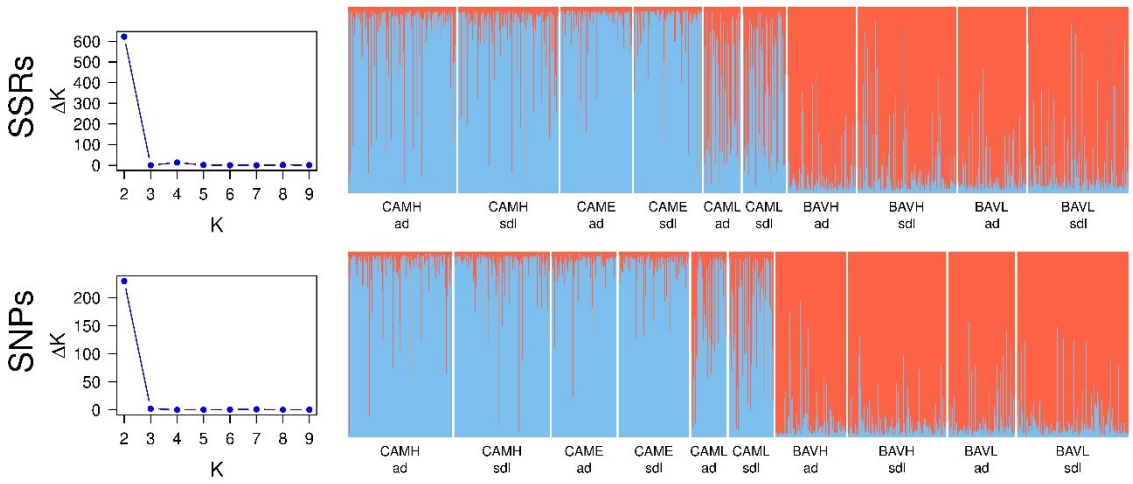

Fig. 5 Results of STRUCTURE analyses on SSR (*above*) and SNP (*below*) data. The most likely grouping of individuals was consistently found at K = 2, as it is clearly shown by the scatterplot of K *vs*. ΔK. In the barplots, each bar represents the probability of each individual to belong to the two identified genetic clusters.

2.5 Dendrochronological data

Increment cores were processed following standard dendrochronological techniques (Schweingruber, 1988). Tree-ring width (TRW) was measured with a LINTAB device (Rinntech, Germany) to a precision of 0.01 mm. All time series were visually and statistically crossdated using COFECHA (Holmes, 1983). In the German plots, TRW time series from each of the two increment cores were averaged to obtain a unique time series per tree (**Fig. 6**).

TRW time series were converted to basal area increment (BAI) time series with the function *bai.in* of the R package *dplR* (Bunn, 2008). BAI describes growth variations better than linear measurements such as TRW, because it takes into account the geometrical bias introduced by the age-related stem circumference increase (Biondi and Qeadan, 2008). The annual BAI was calculated as:

$$BAI = \pi(r_t^2 - r_{t-1}^2), \qquad (1)$$

where r_t and r_{t-1} were the stem radii in the current (t) and previous ($t-1$) years.

TRW time series were also standardized applying 20-year long spline functions with 50% frequency response with the program ARSTAN (Cook and Kairiukstis, 1990) (**Fig. 7**). Such standardization method converts TRW into dimensionless tree-ring indexes (RWI), removing low-frequency growth trends in periods longer than decades. In this way, high-frequency growth variability is retained and can be correlated with climatic fluctuations. For each plot, a mean standardized chronology was calculated, using a bi-weight robust estimate of the mean (Cook, 1985) with the program ARSTAN.

For 36 trees, core could not be analysed due to a high number of fractures or missing segments. In this way, dendrochronological data were successfully produced for 482 trees (**Table 6**). By a rough analysis of tree age data, it emerged that the five plots were characterized by different age structures (**Fig. 8**; **Table 6**). In CAMH and CAML, 81% and 64% of the trees were younger than 60 years, with a median age of 42 and 53 years, respectively. In the other three plots, the percentage of trees < 60 years was markedly lower (CAME: 16%; BAVH: 3%; BAVL: 20%) and the median age ≥100.

Table 6 Number of individuals successfully phenotyped. Minimum, median and maximum values of age and diameter at breast height (DBH) are reported, as well as average individual growth rates calculated both on tree-ring width (TRW) and basal area increment (BAI) time series.

	Unit	**CAMH**	**CAME**	**CAML**	**BAVH**	**BAVL**
Adults sampled	ind	159	105	54	100	100
Adults successfully phenotyped	ind	156	102	52	98	74
Minimum age	years	13	37	33	32	31
Median age	years	42	131	53	174	98
Maximum age	years	140	162	164	247	249
Minimum DBH	cm	11	17	20	18	15
Median DBH	cm	25	47	33	46	69
Maximum DBH	cm	56	89	122	87	136
Average TRW	mm	2.97	1.78	2.81	1.31	3.08
Average BAI	mm^2	1240	1178	1652	766	2643

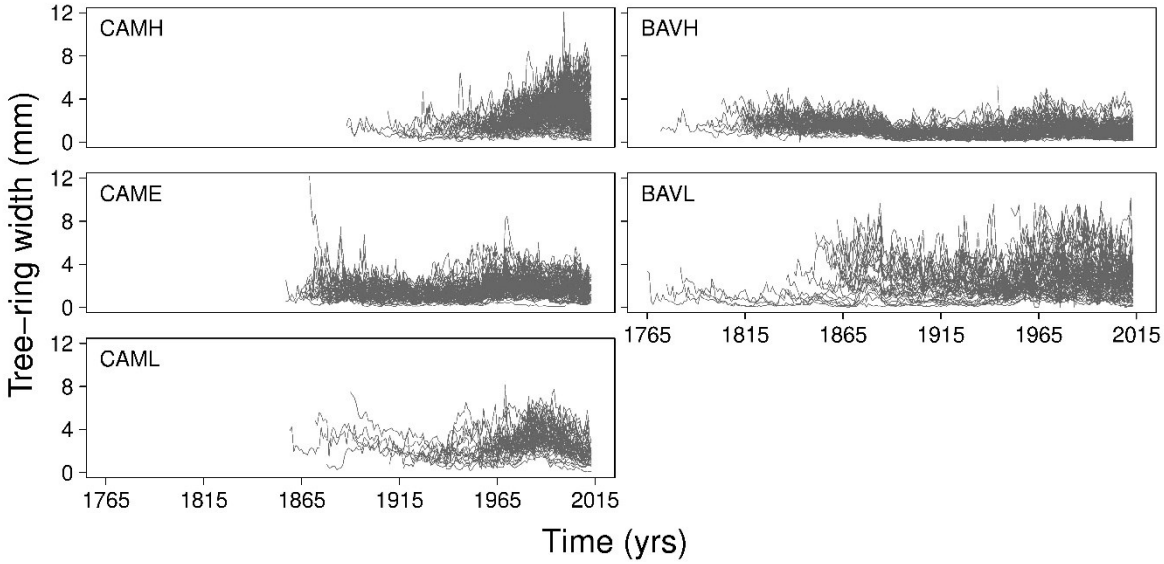

Fig. 6 Individual raw tree-ring width (TRW) time series within each plot.

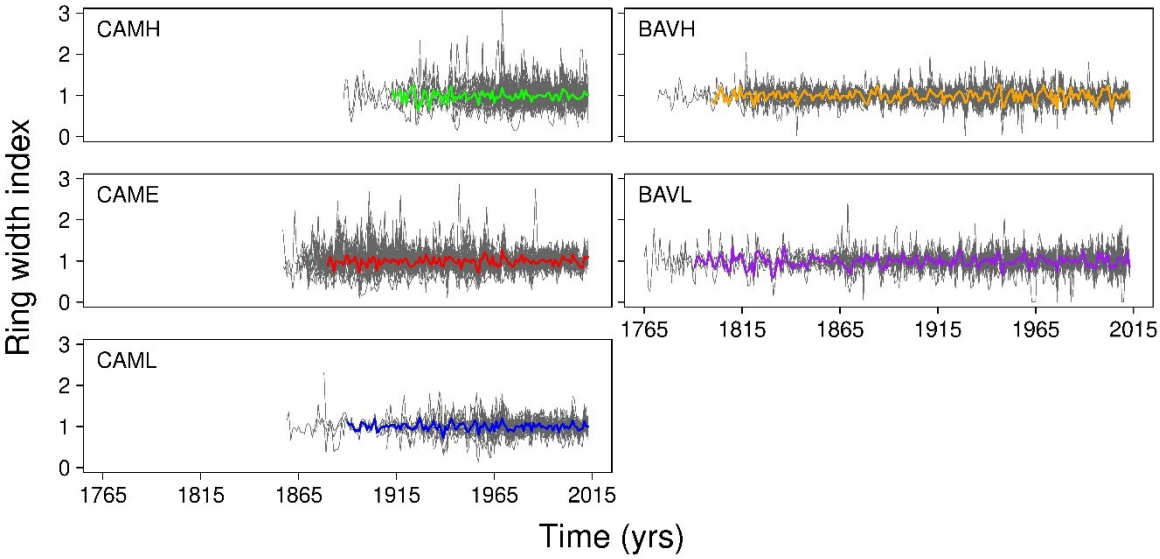

Fig. 7 Individual tree-ring index (RWI) time series (*grey lines*) and plot mean standardized chronology (*coloured lines*).

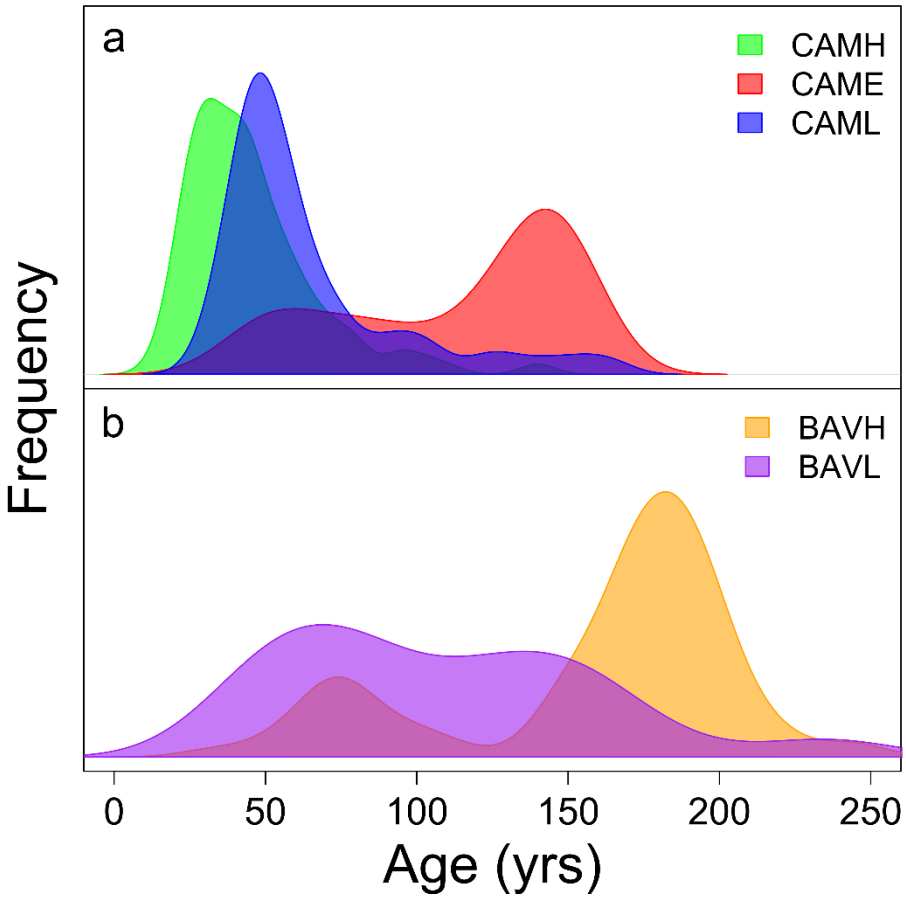

Fig. 8 Age distribution in (**a**) Italian and (**b**) German site.

2.6 Climatic data

Monthly mean temperature and total precipitation data for the 1901-2013 period were obtained from the CRU TS V.4.0 database with 0.5° steps through the Climate Explorer application (Harris *et al.*, 2014). The CRU data were extracted from the grid point closest to each study site (Apennine grid centre: 44°15'0" N, 10°45'0" E; Bavarian grid centre: 49°15'0" N, 13°15'0" E). To obtain plot-specific climatic data, the gridded data were successively corrected for the coordinates and altitude of each plot, using the climate software ClimateEU v.4.63 (Hamann *et al.*, 2013).

Chapter 3

Disentangling the effects of spatial proximity and genetic similarity on individual growth performances

3.1. Introduction

Cambial growth is a complex phenotypic trait influenced by several determinants such as climate, tree age, competition, disturbances (*e.g.* pathogen outbreaks, management, wildfires) as well as individual microenvironmental conditions and genetic background (Cook *et al.*, 1990; Schweingruber, 1996). Although recent advances in genomics have discovered some genetic and epigenetic factors involved in growth processes of model plants (Busov *et al.*, 2008), most of the genetic architecture of growth traits is still unknown for forest tree species (Grattapaglia *et al.*, 2009). However, the available literature about common garden experiments and progeny trials showed that growth traits (*e.g.* height, diameter, tree ring width, wood density) have moderate to high values of heritability (Cornelius, 1994; Hannrup *et al.*, 2004; Martinez Meier *et al.*, 2008; Klisz *et al.*, 2016; Mihai and Mirancea, 2016; Quesada *et al.*, 2017; Lind *et al.*, 2018). The heritability of a phenotypic trait is the essential prerequisite for potentially adaptive responses (Ritland and Ritland, 1996; Lind *et al.*, 2018). Heritability should be ideally estimated in situ (Ritland, 1996; Kremer *et al.*, 2014), because it can be easily overestimated when assessed under controlled environmental conditions, and this bias can be even larger for complex traits (Ritland, 2000; Castellanos *et al.*, 2015). A potential first step in this direction is to jointly analyse quantitative trait variation and genetic relatedness in natural conditions (Ritland, 1996, 2000). The extent of relatedness between two individuals reflects their coancestry (that is how many common ancestors do they share and how much these ancestors are distant in time) and the resulting probability of their alleles being identical by descent (Weir *et al.*, 2006; Wang, 2017). Related individuals have more similar genotypes with respect to unrelated ones and, thus, they are expected to show also more similar phenotypes for quantitative traits (Falconer and Mackay, 1996). Over the last decades, substantial improvements in genotyping techniques and genetic analyses gave to population genetic studies a greater power to address ecological questions (Selkoe and Toonen, 2006). Although hyper-variable microsatellites often do not provide any information about potentially

adaptive responses (King *et al.*, 2013), they are considered as almost ideal markers to estimate relatedness, and study demographic processes in general, with high resolution power (Hardy, 2003; Weir *et al.*, 2006).

Generating genetic data is currently far easier than obtaining a deep phenotypic characterization of numerous individuals (Araus and Cairns, 2014). The recent development of high throughput phenotyping techniques has started to fill this gap, at least in controlled conditions for annual species or, for forest trees, at the seedling stage (Furbank and Tester, 2011; Fiorani and Schurr, 2013; Araus and Cairns, 2014). However, a deep phenotyping of a large number of forest trees in natural conditions remains challenging. An available option is taking advantage of dendrochronology to characterize growth performances through individual annual tree-ring width (TRW) data (Heer *et al.*, 2018). For this purpose, a shift in the classical dendrochronological perspective is required. Indeed, the traditional dendrochronological approach mainly aims at finding the within population common climatic signal, by reducing the amount of unwanted noise through some useful but potentially controversial procedures (for a detailed discussion of their advantages and limitations see Carrer (2011)). In dendrochronological studies few individuals per site are usually sampled (~ 20/site), preferentially selecting old dominant trees, which are supposed to present the best signal to noise ratio (Fritts, 1976). Tree-ring time series are then standardized to remove age-related and low-frequency trends determined by non-climatic factors, and to homogenize growth rates and variances (Cook, 1985). Finally, standardized tree-ring time series are usually averaged into a unique site chronology (Cook and Kairiukstis, 1990). Whereas this approach is ideal for reconstructing past climate, it prevents characterizing the whole range of individual growth performances and responses to climate (Carrer, 2011) and eventually predicting how trees may cope with climate change (Redmond *et al.*, 2017). Carrer (2011) proposed an individual-based dendrochronological approach after finding out that investigating the whole range of individual responses outperforms the classical method to obtain more robust and reliable estimates of mean growth-climate correlations. Additionally, Galvan *et al.* (2014) suggested the adoption of new protocols for sampling all adult trees within a circumscribed area, to better quantify how climate affects individual tree growth.

Recent dendrochronological studies underlined the relevance of individual-based linear mixed-effects models to quantify and disentangle the effects of different drivers of growth (Linares *et al.*, 2010; Hereş *et al.*, 2012; Galvan *et al.*, 2014; Macalady and Bugmman, 2014; Primicia *et al.*, 2015; Redmond *et al.*, 2017). Such individual-based models offer the possibility of estimating model parameter both at the population and individual level.

However, the above-mentioned studies were mainly focused on the mean effect of each driver at the population level, whereas inter-individual variation was poorly investigated. In contrast, I argue that the individual parameters obtained by such modelling approach can be considered as a new type of tree-ring based traits (see Housset *et al.*, 2018). In fact, such parameters describe how individual trees respond to specific yearly-based drivers of growth (*e.g.* age, climate), while holding constant the others. In this way, inter-individual variation of sensitivities to drivers of growth could be explicitly quantified (Albert *et al.*, 2011) and linked to factors that are time-constant (*e.g.* genotypes) or measured occasionally (*e.g.* microenvironmental features, competition).

In this chapter, I assess whether sharing the same microenvironment and/or genetic characteristics influence inter-individual variation of growth performances within natural populations of Norway spruce. To my knowledge, King *et al.* (2013) is the only study that tried to answer a similar question, assessing whether genetic relatedness or climate affect TRW variation along forest trees' altitudinal transects. In their work, 115 Norway spruce individuals from five populations were genotyped with five nSSR markers. The authors visually compared genetic relatedness and growth synchronicity, concluding that among-population TRW variation is more climate- than genetic-driven at regional scale. Here, I embrace the change in perspective suggested by recent dendrochronological literature to switch from a classical population-based approach to a deep individual-based exploration of growth dynamics. Five plots were intensively sampled collecting dendrochronological data from 482 trees. All individuals were genotyped at 11 nSSR to thoroughly characterize the genetic structure within each plot. I developed an individual-based analytical framework to quantify inter-individual variation of TRW and assess the effects of different growth determinants. Specifically, the aims were *i*) disentangling the effects of age and climate vf on TRW at both individual and population level, *ii*) assessing whether genetic similarity and spatial proximity (used as a proxy for microenvironmental heterogeneity) determining similar individual growth performances, and *iii*) quantifying the extent of the fine-scale spatial arrangement of phenotypes.

3.2 Materials and methods

Study sites and datasets have been already presented in Chapter 2. In the following paragraphs, I will give some details about estimates of genetic relatedness among individuals (3.2.1) and dendrochronological measures at the individual level (3.2.2). After that, I will exhaustively describe the two-step analytical framework developed to assess whether Norway spruce growth performances were influenced by the spatial proximity among

individuals (hereafter, spatial structure) and the genetic similarity or relatedness among individuals (hereafter, genetic structure). First, the effects of climate and age on TRW were estimated using a random slope mixed-effects model (3.2.3). This primary step allowed us to obtain individual parameters which summarize individual growth performances, taking into account the effects of climate and age simultaneously. After that, individual parameters were tested against genetic and spatial variables by two alternative methods (3.2.4). Finally, the existence and the extent of fine-scale spatial arrangements of individual parameters were investigated through both correlograms and kriging (3.2.5).

3.2.1 A measure of genetic relatedness

Using SSR data, pairwise relatedness coefficients and their confidence intervals were estimated within each study site using the triadic likelihood estimator by Wang (2007) as implemented in the R package *related* (Pew *et al.*, 2015).

3.2.2 Dendrochronological measures at the individual level

Cross-correlation coefficients among all pairs of individuals within each study site were calculated using both TRW and RWI data, to measure the strength of synchronicity in growth. A Spearman correlation was used to avoid problems of heteroscedasticity between series. Growth-climate correlations were calculated using Pearson's correlation coefficient both on individual time series and mean chronologies, using the length of the individual time series and the common interval 1915-2013, respectively. Correlations were computed between RWI and monthly temperature and precipitation, for a biological year extending from April of the previous year to October of the current year.

3.2.3 A random slope mixed-effects model

A linear random slope mixed-effects model was used to quantify the effects of age and climate on TRW at both population and individual level. Preliminary analyses carried out on the whole dataset showed a high number of significant interactions between a plot factor and the other variables, suggesting the existence of significant differences among plots. Thus, the analyses were performed separately for each plot, using the *nlme* package (Pinheiro *et al.*, 2018) of the R statistical suite.

Since it is well known that growth is non-linearly affected by tree age (Cook, 1985), both a linear and a quadratic term for age (A, A^2) were included in the model as fixed-effect variables. In the classical dendrochronological approach, the age effect is removed by applying detrending techniques (Cook *et al.*, 1990). However, the use of raw data could give

three significant advantages: *i*) avoiding transformation to RWI, which are dimensionless values with a less clear biological meaning (Redmond *et al.*, 2017); *ii*) preserving low-frequency variations associated to long-term trends (Esper *et al.*, 2002); *iii*) retaining all the information recorded by the rings during the entire tree lifetime, thus maximizing inter-individual variation. Two climatic variables (total precipitation (P) and mean temperature (T) of the vegetative season, from April to September) and all two-way interactions (P:T, P:A, T:A) were also included in the model as fixed effects. To avoid collinearity problems due to the inclusion of interaction terms, all explanatory variables were centred and the variance inflation factor (VIF) was calculated for each variable using the R package *car* (Fox and Weisberg, 2011). VIF values were always ≤ 1.25, confirming the absence of collinearity problems (Zuur *et al.*, 2010).

A random factor TreeID was included in the model to estimate inter-individual variances of intercept and slopes ($\sigma^2_{I,i}$). These variances provide conditional individual parameters (b_i), which represent how each tree responds to climate and age. As TreeID contributes to both intercept and slopes (*i.e.* random slope model), the assumed theoretical model (Pinheiro and Bates, 2000) is the following:

$$y_{ki} = (\beta_0 + b_{0i}) + (\beta_1 + b_{1i})x_{ki} + \cdots + \varepsilon_{ki}, \qquad (2)$$

where y_{ki} is the TRW of the k-th year of the i-th tree, β_0 and β_1 are, respectively, the fixed intercept and slope parameters (*i.e.* the common effect for all trees in the plot), b_{0i} and b_{1i} are the random intercept and slope of the i-th tree (*i.e.* the effect for each individual tree), x_{ki} is one of the explanatory variables measured in k-th year for the i-th tree and ε_{ki} is the within-tree error which is assumed to be normally distributed ($\varepsilon_{ki} \sim N(0, \sigma^2)$). To correct for autocorrelation in time between multiple measurements on each tree, which causes the residuals not to be independent, a first-order autoregressive correlation structure (using the corAR1 constructor in the lme function) was also included in the model. In this way, a Φ parameter was estimated, which represents the within-tree temporal TRW autocorrelation. *ACF* function of the R package *nlme* was used to check whether temporal autocorrelation pattern was successfully removed (Pinheiro and Bates, 2000).

If all the explanatory variables are expressed, (2) becomes:

$$y_{ki} = (\beta_0 + b_{0i}) + (\beta_P + b_{Pi})\,P_k + (\beta_T + b_{Ti})\,T_k + (\beta_A + b_{Ai})\,A_{ki} + (\beta_{A^2} + b_{A^2})\,A_{ki}^2 + \beta_{P:T}P_kT_k + \beta_{P:A}P_kA_{ki} + \beta_{T:A}T_kA_{ki} \qquad (3)$$

where

$$b_i = \begin{bmatrix} b_{0i} \\ b_{Pi} \\ b_{Ti} \\ b_{Ai} \\ b_{A^2 i} \end{bmatrix} \sim \mathbb{N}\,(0, \Psi_I) \qquad (4)$$

Independency of the different random effects was assumed, so that the variance-covariance matrix Ψ_I is:

$$\Psi_i = \begin{bmatrix} \sigma^2_{I,0} & 0 & 0 & 0 & 0 \\ 0 & \sigma^2_{I,P} & 0 & 0 & 0 \\ 0 & 0 & \sigma^2_{I,T} & 0 & 0 \\ 0 & 0 & 0 & \sigma^2_{I,A} & 0 \\ 0 & 0 & 0 & 0 & \sigma^2_{I,A^2} \end{bmatrix} \qquad (5)$$

For each plot, the model selection procedure is a slightly modified version of the top-down strategy proposed by Zuur *et al.* (2009): *i*) it started from the beyond optimal model (3), which contains all explanatory variables and pairwise interactions; *ii*) using maximum likelihood estimation, each fixed variable was dropped whether the Likelihood Ratio Test on nested models indicated that a simpler model structure was more parsimonious; *iii*) the final optimal model was presented using restricted maximum likelihood estimation. All random effects were purposely kept in each model, regardless whether their variances ($\sigma^2_{I,i}$) were significantly >0, to obtain a coherent quantification of heterogeneity among individuals (Bolker *et al.*, 2008) ending up with the same set of individual parameters for all five plots. Normality and homoscedasticity of normalised residuals were checked (Zuur *et al.*, 2009) and both marginal and conditional R^2 were calculated (respectively, the variance proportion explained by only fixed effects and by both random and fixed effects; Nakagawa and Schielzeth, 2013), using the R package *piecewiseSEM* (Lefcheck, 2016).

3.2.4 Testing the influence of genetic and spatial structure on individual parameters

Two approaches were used to investigate the effects of genetic and spatial structure on growth performances. In the first one, genetic structure was included as the matrix of pairwise relatedness coefficients, whereas spatial structure as the matrix of pairwise spatial distances. Spatial proximity was thus considered a proxy for shared microenvironmental conditions. Since relatedness coefficients and spatial distances are pairwise data, dendrochronological data needed to be pairwise too. Thus, matrices of pairwise absolute differences of individual parameters (*b*) were calculated. The rationale was to check whether smaller differences in individual parameters were exhibited by more genetically related or

spatially closer trees. The correlation between *i*) relatedness and dendrochronological matrices and *ii*) spatial and dendrochronological matrices was tested by Mantel test using the R package *vegan* (Oksanen *et al.*, 2018).

Although this first approach based on pairwise data allowed to make a more direct comparison with King *et al.* (2013)'s study, Mantel test suffers from some limitations. In fact, it just performs a simple correlation between two similarity/dissimilarity matrices, and requires often unmet assumptions about the linearity and homoscedasticity of distance-distance relationships (Legendre *et al.*, 2015). Therefore, variance partitioning (Legendre and Legendre, 2012) was used as a second approach. This statistical method allowed us to partition the explanatory power (adjusted R^2) of two sets of explanatory variables (*i.e.* genetic and spatial structure) on a response data table (*i.e.* individual parameters). Genetic structure was included through a principal component analysis on genotypes, using the *dudi.pca* function of the R package *adegenet* (Jombart and Ahmed, 2011). In each plot, only principal components accounting for more than 50% of the variance in genotypes were used. Spatial structure was instead modelled by a distance-based Moran's eigenvectors map (dbMEM, Dray *et al.*, 2006), which has been proposed as a powerful and informative method of spatial analysis by Legendre *et al.* (2015). In each plot, only the statistically significant eigenfunctions modelling positive spatial autocorrelation, as estimated by the *mem* function of the R package *adespatial* (Dray *et al.*, 2018), were retained. The relative contributions of genetic and spatial structure in explaining the variance of individual parameters were assessed using the *varpart* function of the R package *vegan*, following the procedure described in Borcard *et al.* (2011). Significance of the variance components was calculated through ANOVA-like permutation test for redundancy analysis (RDA) and partial redundancy analysis pRDA based on 1×10^4 permutations (Legendre and Legendre, 2012).

3.2.5 Investigating the fine-scale spatial arrangement of individual parameters

The fine-scale spatial arrangement of individual parameters and relatedness coefficients was investigated through Moran's I correlograms, using the R package *spdep* (Bivand and Piras, 2015) and SPAGeDi v1.2 (Hardy and Vekemans, 2002), respectively. Ten distance classes with even sample size were used. For relatedness coefficients, 95% confidence intervals were calculated by 1×10^4 permutations of individual spatial coordinates to test the statistical significance of observed Moran's I values. Finally, ordinary kriging with an isotropic global neighbourhood was applied to identify the existence and extent of within-plot clusters of trees exhibiting similar individual parameters. Input parameters for kriging *(i.e.* partial sill, range and nugget size) were obtained by fitting a theoretical exponential curve on variograms

with a restricted maximum likelihood approach. All analyses were performed using the R package *geoR* (Ribeiro and Diggle, 2016).

3.3 Results

3.3.1 Relatedness coefficients

The highest average relatedness coefficients were recorded in CAME (0.103 ± 0.124 SD) and CAML (0.115 ± 0.143 SD) while the lowest one in BAVL (0.065 ± 0.097 SD) (**Fig. 9a**). The proportion of pairs of individuals with relatedness coefficients significantly higher than 0 (*i.e.* CI lower limit not overlapping 0) ranged from 0.063 in BAVL to 0.179 in CAML.

3.3.2 Dendrochronological measures at the individual level

The frequency distributions of within-plot cross-correlation coefficients calculated on TRW were generally platykurtic, with a percentage of tree pairs with negative cross-correlation coefficients ranging from 14% in BAVH to 37% in CAMH (**Fig. 9b**). Average cross-correlation coefficients varied from 0.115 (± 0.398 SD) in CAMH to 0.398 (± 0.346 SD) in CAML. Average cross-correlation coefficients calculated on RWI were similar to the ones from TRW, but generally showed a lower proportion of negative values and a lower standard deviation (**Fig. 9b**).

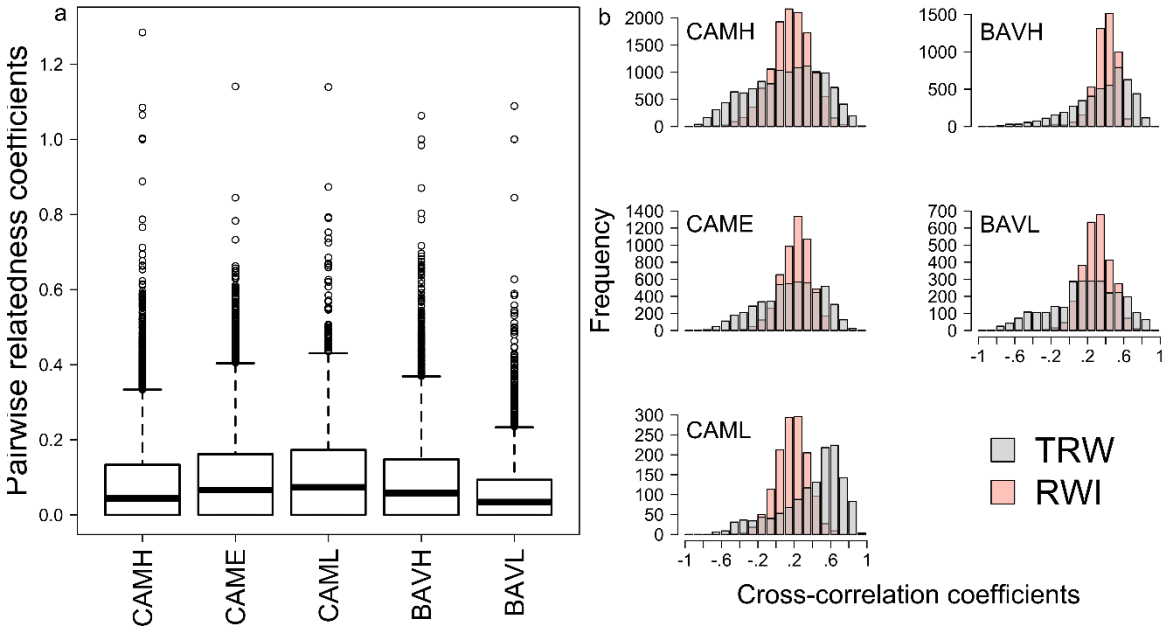

Fig. 9 Boxplot of pairwise relatedness coefficients calculated within each plot (**a**) and frequency distributions of cross-correlation coefficients (**b**). Grey bars represent cross-correlation coefficients calculated on raw tree-ring width (TRW) data, while pink bars cross-correlation coefficients calculated on standardized data (RWI).

Growth-climate correlations showed a large inter-individual variation, both for monthly temperature and precipitation responses. Only 1% of the individual growth-climate correlations was larger than ±0.4 (**Fig. 10**). Growth-climate correlations calculated on mean chronologies were globally low and heterogeneous among plots, confirming the absence of a strong common climatic signal among plots. In addition, 11 out of 190 growth-climate correlations calculated on mean chronologies are >90th or <10th percentile of the distribution of individual growth-climate correlations (**Fig. 10**).

3.3.3 Effects of age and climate on tree-ring width at population and individual level

At the population level, TRW was mainly determined by age, but the shape of this relationship was different among plots: in CAMH, CAME and BAVL there was a quadratic dependency, with downward concavity for CAMH and CAME and upward concavity for BAVL, whereas this relationship was linear and negative in CAML and BAVH (**Fig. 11**). TRW was positively associated with the mean temperature of the vegetative season and this relationship was consistent among plots, with slopes ranging from 0.0608 mm/°C in BAVL to 0.1168 mm/°C in CAML (**Table 7**; **Fig. 12**). TRW was also influenced by total precipitation of the vegetative season. The linear relationship was negative in the Italian plots and positive in the German ones. Slope parameters were statistically different from 0 but extremely small, ranging from -0.00006 mm/mm in CAMH to 0.00039 mm/mm in BAVL (**Table 7**; **Fig. 12**).

Table 7 REML-estimated parameters significant after the model selection procedure: β_0, ..., β_7 are the parameters of fixed effects, $\sigma_{I,0}$, ..., $\sigma_{I,4}$ are the standard deviations of random effects, Φ_1 is the within-tree temporal autocorrelation. Marginal and conditional R^2 are also reported.

	CAMH	**CAME**	**CAML**	**BAVH**	**BAVL**
β_0	3.18	1.81	2.56	9.81×10^{-1}	2.33
β_P	-6.01×10^{-5}	-6.67×10^{-5}	-8.78×10^{-5}	1.15×10^{-5}	3.99×10^{-4}
β_T	6.72×10^{-2}	7.99×10^{-2}	1.17×10^{-1}	8.30×10^{-2}	6.08×10^{-2}
β_A	-6.33×10^{-3}	1.10×10^{-3}	-9.69×10^{-3}	1.67×10^{-3}	-1.42×10^{-2}
β_A^2	-1.27×10^{-3}	-7.98×10^{-5}	-	-	1.21×10^{-4}
$\beta_{P:T}$	1.96×10^{-4}	7.55×10^{-5}	7.28×10^{-5}	7.28×10^{-5}	7.29×10^{-4}
$\beta_{P:A}$	-	1.31×10^{-6}	2.19×10^{-6}	2.19×10^{-6}	-6.01×10^{-6}
$\beta_{T:A}$	-1.63×10^{-3}	-4.62×10^{-4}	4.03×10^{-4}	4.03×10^{-4}	-8.39×10^{-4}
$\sigma_{I,0}$	1.29	6.07×10^{-1}	3.17×10^{-1}	5.02×10^{-1}	1.33
$\sigma_{I,P}$	2.31×10^{-6}	1.27×10^{-8}	1.60×10^{-7}	1.04×10^{-7}	9.19×10^{-7}
$\sigma_{I,T}$	3.07×10^{-4}	1.08×10^{-4}	5.78×10^{-5}	4.37×10^{-2}	3.88×10^{-2}
$\sigma_{I,A}$	4.41×10^{-2}	8.79×10^{-3}	9.90×10^{-3}	6.93×10^{-3}	2.49×10^{-2}
$\sigma_{I,A}^2$	1.28×10^{-3}	5.94×10^{-5}	-	-	2.42×10^{-4}
Φ_1	5.39×10^{-1}	7.89×10^{-1}	8.78×10^{-1}	6.17×10^{-1}	6.43×10^{-1}
Marg R^2	0.29	0.02	0.05	0.02	0.06
Cond R^2	0.94	0.56	0.17	0.79	0.86

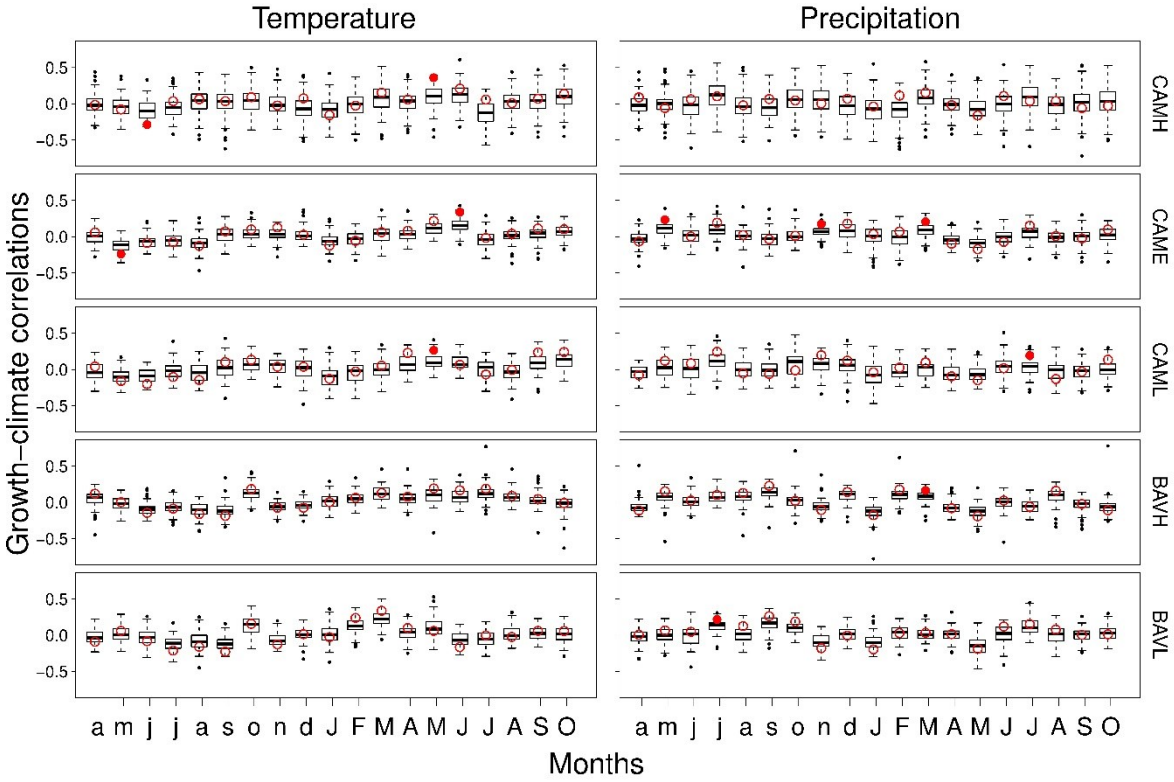

Fig. 10 Boxplot of individual growth-climate correlations calculated between standardized tree-ring time series and monthly temperatures and precipitations, from previous April up to current October. Months are abbreviated with lowercase and uppercase letters for the previous and current year of growth, respectively. Red dots are the growth-climate correlations calculated on mean chronologies built for each plot for the common period 1915-2013. Red dots are filled when the correlation values are below the 10th or above the 90th percentile of the distribution of individual growth-climate correlations.

Most of the total TRW variance was explained by random effects. Except for CAML, conditional R^2 values were high (ranging from 0.56 in CAME to 0.94 in CAMH) and much larger than marginal R^2 values (**Table 7**). Among individual parameters, the intercepts and the parameters describing the growth-age relationship showed a standard deviation significantly different from 0 (**Table 7**). Several trees showed very different behaviours in the individual sensitivity to age with respect to the overall effect observed at the population level (**Fig. 11**). The standard deviation of remaining individual parameters were negligible, with the only exception of the growth-temperature relationship in BAVH.

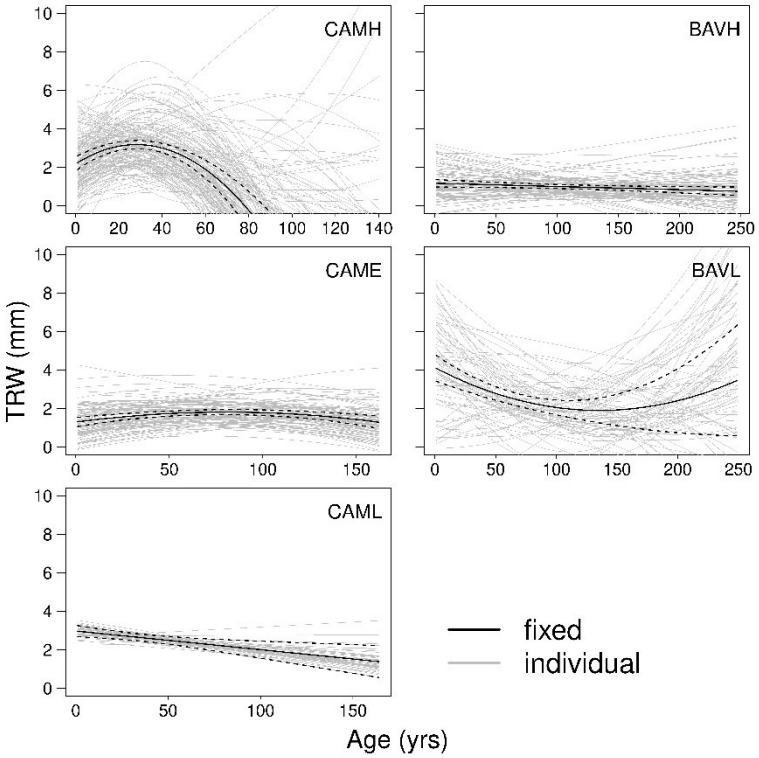

Fig. 11 Growth-age relationship for each plot. Black solid lines represent the effect of age on tree-ring width at the population level, dashed lines are the limits of 95% confidence intervals. Grey lines represent the individual sensitivity to age.

3.3.4 Influence of genetic and spatial structure on individual parameters

Genetic structure had no influence on growth performances. In fact, none of the Mantel tests performed between the relatedness matrix and the matrices of pairwise differences among individual parameters were significant, except for the intercept of CAML ($r = 0.117$, $P < 0.01$) (**Fig. 13**). On the other hand, spatial structure had a larger effect in determining similar growth responses. In fact, seven out of 23 Mantel tests between the spatial matrix and the matrices of pairwise differences among individual parameters were significant (**Fig. 14**), with positive correlation values ranging from 0.076 to 0.205.

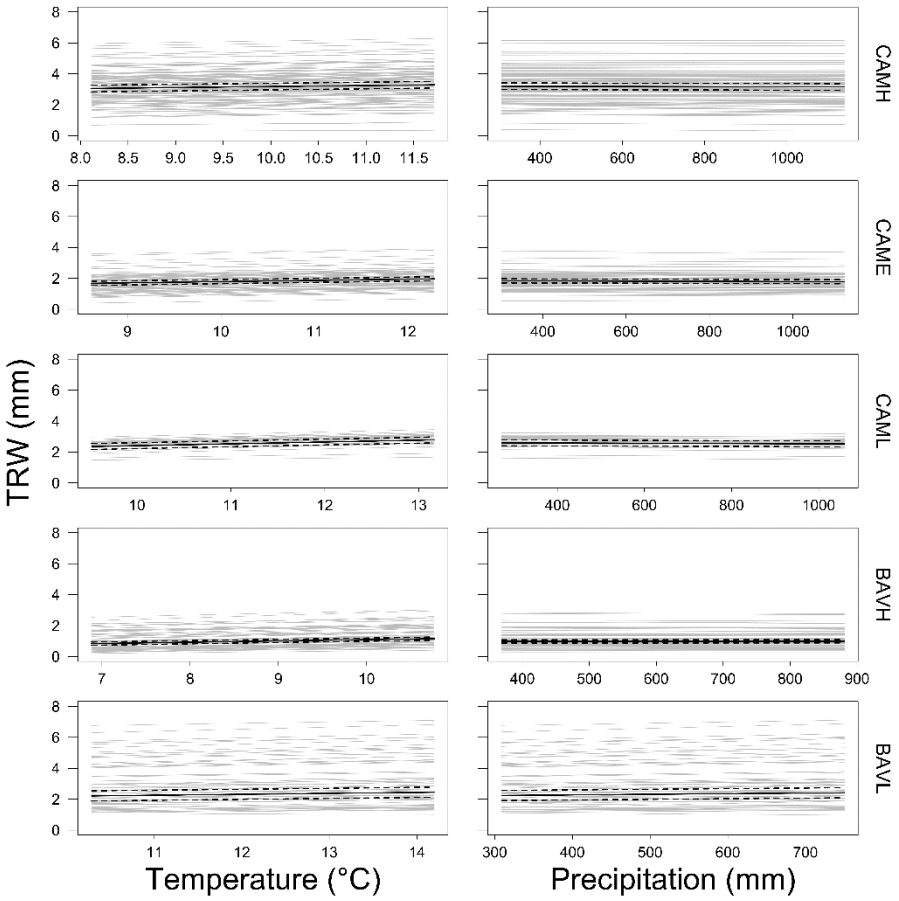

Fig. 12 Influence of temperature and precipitation on tree-ring width data in each plot. Black solid lines represent the effect on TRW at the population level, dashed lines are the limits of 95% confidence intervals. Grey lines are the individual sensitivities to temperature and precipitation.

The same picture emerged also from the variance partitioning and partial RDA analyses (**Fig. 15**). Overall, the genetic structure explained a low proportion of variance (adjusted R^2 ranging from 0 to 0.13), and its effect was never statistically significant (**Fig. 15d**). On the contrary, the contribution of the spatial structure is much larger (adjusted R^2 up to 0.29) and its effect was statistically significant in nine cases out of 23 (**Fig. 15c**). A significant effect of the spatial structure was found on the intercepts (b_0) in the Italian plots, and on the growth-age relationship (b_A and $b_A{}^2$) in the German plots.

3.3.5 Fine-scale spatial arrangement of individual parameters

Spatial autocorrelograms revealed the existence of a clear departure from random spatial arrangements only for the intercepts of CAMH and CAME and the slope of the growth-age relationship of BAVH (**Fig. 16**). This picture was confirmed by the results of the kriging analysis (**Fig. 17**). In **Fig. 17** kriging results are presented only when variograms had a range parameter >3 m and a partial sill >0. A signal of spatial clumping was found for the intercepts of the Italian plots, for the growth-age relationship in the German plots and for the slope of the growth-temperature relationship in BAVH. Regarding the intercepts of the Italian plots, the intensity of spatial structuring (*i.e.* partial sill parameter) increased with altitude, with tree clusters' size (*i.e.* range parameter) varying from 12 m in CAMH to 16 m in CAME (**Fig. 17**). Spatial genetic structure was weak to negligible in all plots, with statistically significant Moran's I values found only in the first distance class in CAMH and BAVH (**Fig. 16**).

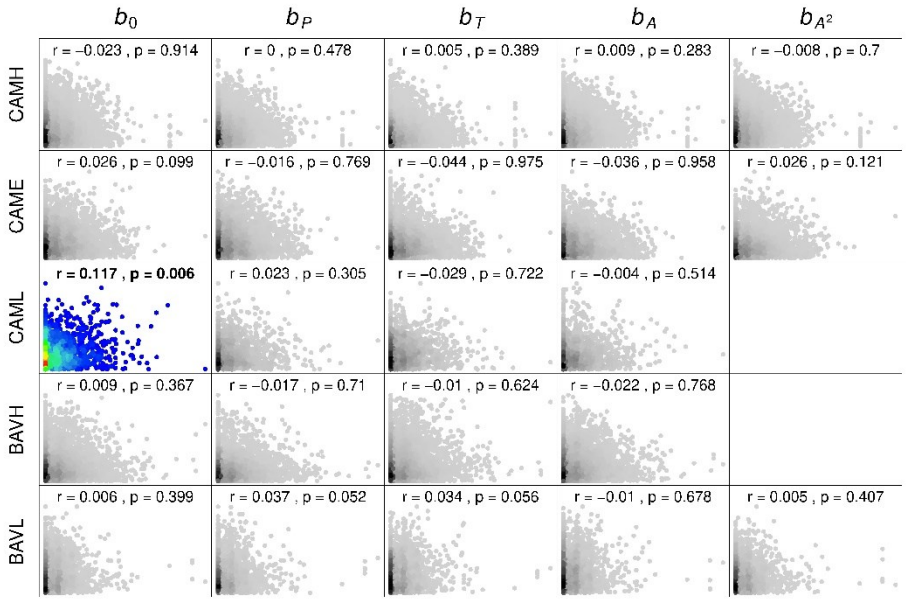

Fig. 13 Scatterplots of pairwise relatedness coefficients (on the x axis) *vs.* pairwise absolute differences of individual parameters (on the y axis). X axis values range from 0 to 1. Mantel test results (*i.e.* correlation coefficients and P-values) are reported for each combination of plot × individual parameter. The graph is coloured only when the Mantel test was significant, otherwise it is in greyscale. The R function *densCols* was used to colour points accordingly to their local densities in each area of the scatterplot, ranging from black/red (high density) to light grey/blue (low density).

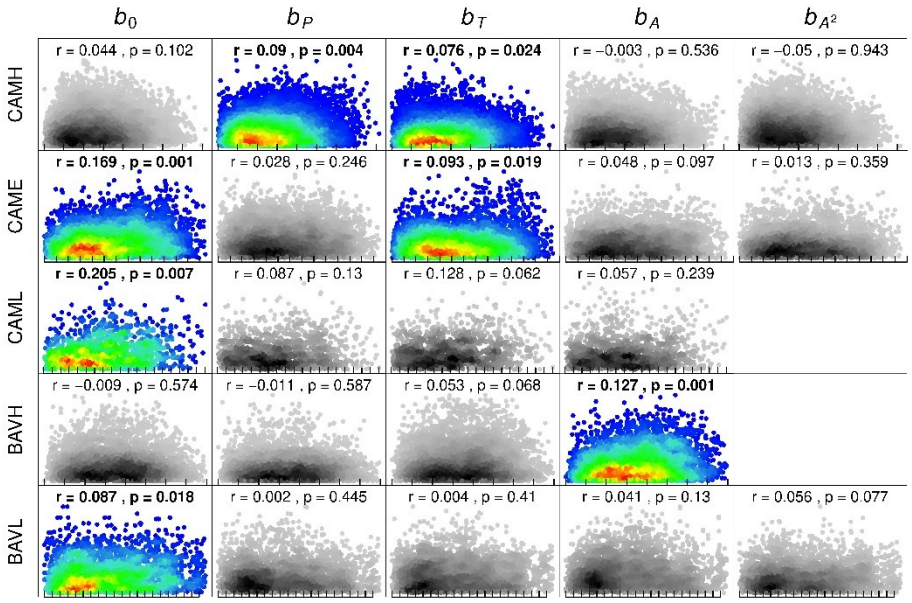

Fig. 14 Scatterplots of pairwise spatial distances (on the x axis) *vs.* pairwise absolute differences of individual parameters (on the y axis). Each tick on the x axis corresponds to 20 m of linear distance. Mantel test results (*i.e.* correlation coefficients and P-values) are reported for each combination of plot × individual parameter. The graph is coloured only when the Mantel test was significant, otherwise it is in greyscale. The R function *densCols* was used to colour points accordingly to their local densities in each area of the scatterplot, ranging from black/red (high density) to light grey/blue (low density).

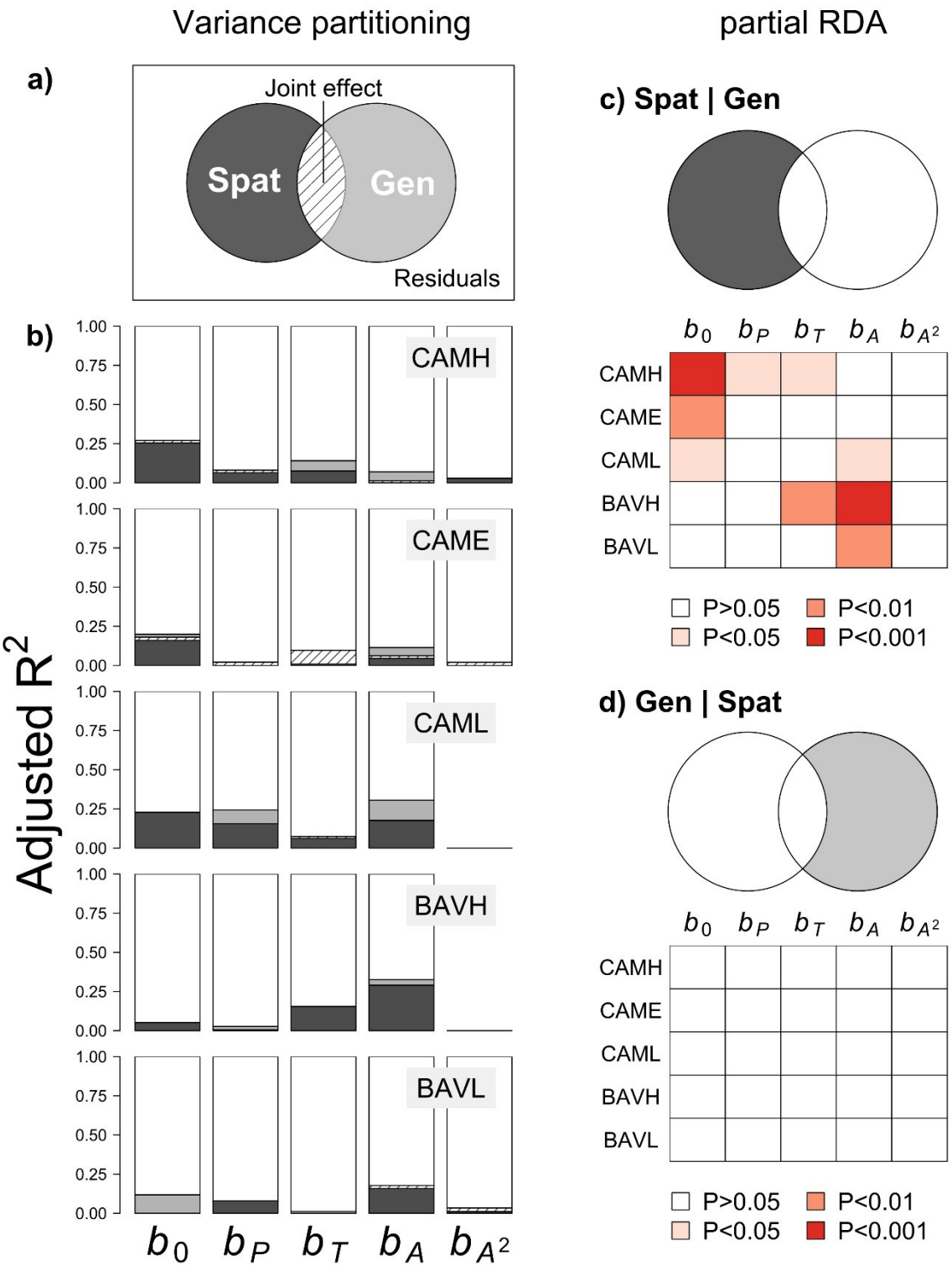

Fig. 15 Conceptual representation by Venn diagram (**a**) and plot-by-plot results (**b**) of variance partitioning on individual growth parameters. In the barplots, dark and light grey represent the portions of variance (adjusted R^2) uniquely explained by spatial (*Spat*) and genetic (*Gen*) structure, respectively. The portions of bars filled with striped lines represent the joint effect of spatial and genetic structure. The amount of unexplained variance (residuals) is represented in white. On the right side of the figure, the effect of spatial structure on individual parameters while controlling for genetic structure (**c**) and the effect of genetic structure while controlling for spatial structure (**d**) are represented. Statistical significance of the variance components, assessed through ANOVA like permutation tests for partial redundancy analysis (pRDA), is reported in the heat maps.

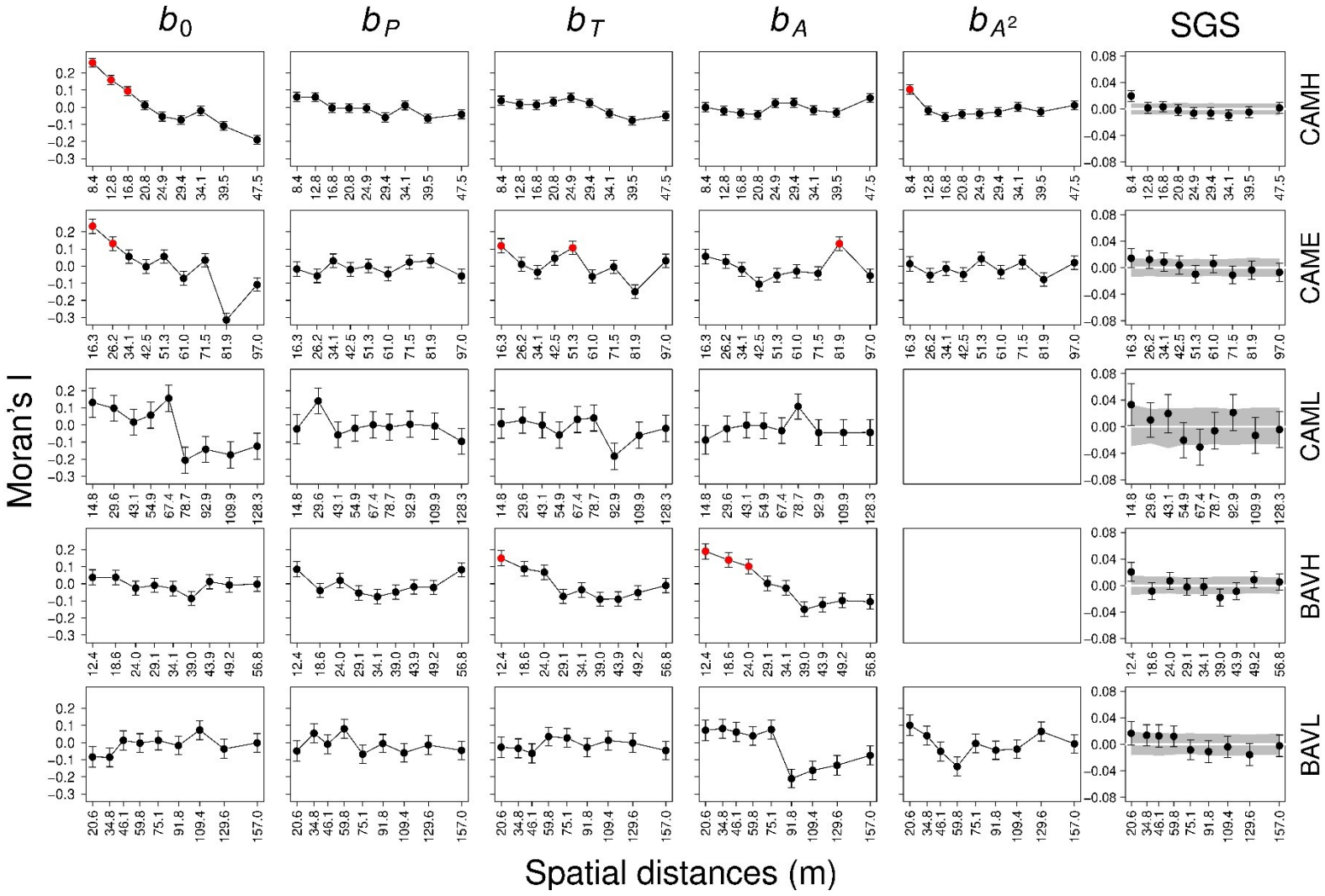

Fig. 16 Moran's I spatial correlograms on individual parameters (first to fifth column) and on pairwise relatedness coefficients indicating the spatial genetic structure (SGS, last column).

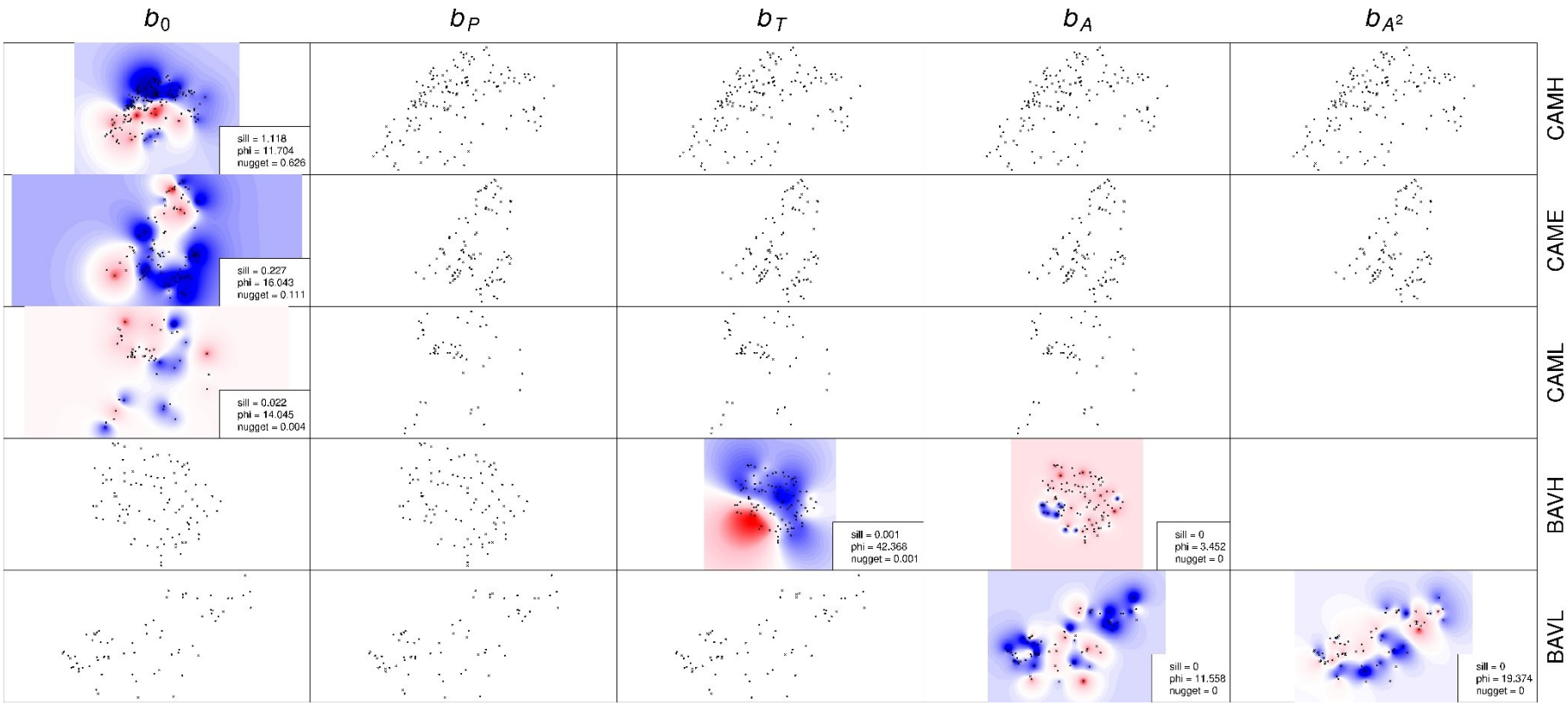

Fig. 17 Distribution maps from spatial interpolation (kriging) of individual parameters. Colors range from the highest values of within-plot parameters (red) to the lowest ones (blue). Partial sill (s^2), range (*phi*) and nugget size values used in the kriging are reported. These values were estimated by fitting a theoretical exponential curve on each variogram.

3.4 Discussion

3.4.1 Advantages of analysing individual dendrochronological data with a random slope model

Studying growth dynamics at the individual level is fundamental for understanding species dendroecology (Carrer, 2011; Galvan *et al.*, 2014; Primicia *et al.*, 2015; Rozas *et al.*, 2015; Redmond *et al.*, 2017). Inference of climate sensitivity might be inaccurate when based only on mean chronologies from few dominant trees (Cherubini *et al.*, 1998). Indeed, Carrer (2011) found that growth-climate correlations based on mean site chronologies are often above the 90th percentile of the distribution of individual growth-climate correlations. We observed a similar discrepancy when calculating growth-climate correlations at the plot level, with 11 values that are outliers as compared to the distribution of individual growth-climate correlations. These outliers were found in periods, such as spring of the previous year and summer of the current year, which are usually considered informative in dendrochronological studies. Altogether, such considerations highlight the importance of exploring individual growth dynamics and growth-climate correlations. To this aim, the main step forward provided by our work is using an individual-based modelling approach to distil all the information from an intensive sampling of inter-individual phenotypic variance in a natural setting. We downscaled the experimental set-up to a within-population level by sampling all adult trees within a circumscribed area. Such approach is inherently different from studying growth patterns of different populations in common garden experiments (as discussed in Heer *et al.*, 2018) and allowed us to correctly represent the whole spectrum of individual responses (Galvan *et al.*, 2014). Then, we estimated mean and individual sensitivities to precipitation, temperature and age through a random slope mixed-effects model. Among other promising features, this modelling strategy *i*) estimates the effect of every variable or their interactions ceteris paribus (*i.e.* holding other factors constant) allowing to remove the effect of tree age when estimating sensitivity to climate (Bowman *et al.*, 2013), and *ii*) provides individual parameters. In other words, all the information embedded in each time series is distilled into parameters that reflect individual growth responses to climate, after having removed the effects of the other factors. Such parameters describing individual sensitivities to climate can indeed represent a valuable addition to other recently introduced dendrophenotypic measures that characterized trees' responses to climate (Heer *et al.*, 2018). Such dendrophenotypes can be linked to other individual features ranging from detailed microenvironmental characteristics to genome-wide data. For

example, Heer *et al.* (2018) and Housset *et al.* (2018) showed how dendrophenotypes can be promisingly used in association genetic studies.

The random slope mixed-effects model used successfully captured most of the variance of TRW. We found that the variance explained by only fixed effects was rather small (marginal R^2 averaged over plots = 0.08) and lower than in other multi-site studies (marginal R^2 of 0.23 and 0.25 in Redmond *et al.* (2017) and Galvan *et al.* (2014), respectively). This can be partially attributed to the fact that analyses were run plot-by-plot. When the analysis was carried out on the whole dataset, including the plot as fixed effect, the marginal R^2 increased to 0.24 (results not shown). However, the variance explained by both fixed and random effects was much higher than considering fixed effects only. Except for CAML, the only plot where Norway spruce density is extremely low, conditional R^2 values ranged from 0.56 up to 0.94. This is a quite remarkable result, especially considering that we used as response variable a complex phenotypic trait such as TRW data, without applying any noise-removing technique (*e.g.* standardization, detrending). This finding highlights that most of the variance in growth is embedded in inter-individual differences. Although a large part of inter-individual variation is linked to unmeasured factors, such high conditional R^2 values confirm the relevance of an individual-based approach relying on the exhaustive sampling of phenotypic variance to comprehensively understand growth dynamics at the population level.

3.4.2 Effects of age and climate on tree ring width

The influence that ontogeny has on tree growth is well-known (Cook *et al.*, 1990), and our results coherently show the effect of cambial age on TRW is relevant and multi-faceted. The expected downward trend of TRW with increasing age (Esper *et al.*, 2002) was observed in all plots with distinctions that need to be discussed and can be partially interpreted in the light of stand history. For instance, CAMH is an area recently recolonized after high altitude pasture cessation and, thus, is the only Italian plot mainly made up of young individuals (109 out of 156 are younger than 50 years old). Such age distribution and the large number of samples collected in CAMH provided a higher accuracy when modelling the juvenile phase of tree lifetime (Bowman *et al.*, 2013). This allowed us to detect a short initial period when TRW moderately increases with age followed by a general decrease due to competition. Although the relationship between TRW and age is generally negative, an initial positive trend may appear when young cohorts are intensively sampled (*e.g.* Mencuccini *et al.*, 2005; Ivkovic *et al.*, 2013; Nehrbass-Ahles *et al.*, 2014; Primicia *et al.*, 2015). In BAVL, growth-age relationship decreases up to 100 years and then begins to increase but, interestingly, with

a much larger confidence interval, revealing a large inter-individual variation. This could reflect complex competition dynamics occurring in this plot with some old trees, reaching heights >55 m (Lars Opgenoorth, personal observation), which likely outcompeted remaining ones. Besides mean, stand-specific effects, it is worth noting that inter-individual variation of growth-age relationships is large in all plots. This suggests that ontogenetic trends are key to shed some light on the complex interaction among growth constrains, individual or local features (*e.g.* genotype and microtopography) and environmental variables (Rita *et al.*, 2016), and deserve increasing attention in dendroecological studies (Szeicz and MacDonald, 1994; Carrer and Urbinati, 2004; Bowman *et al.*, 2013; Carrer *et al.*, 2015). The use of random intercept models instead of classical dendrochronological analyses has been considered a step forward for separating the effects of different drivers on tree growth (Rita *et al.*, 2016; Redmond *et al.*, 2017). Our results highlight the further advantage of using random slope models to better account for inter-individual variation of growth responses.

In all plots, climatic variables showed a small effect size on TRW revealing a low sensitivity to temperature and precipitations, both at the population and individual levels. Interestingly, the use of random slope models allowed us to show that inter-individual variation associated to responses to climatic variables is substantially negligible (*i.e.* all individuals within the plot are similarly influenced by temperature and precipitations). The two most different individuals in terms of their growth response to a 100 mm Δ of precipitation exhibit a difference in radial increment of only 0.04 mm. Temperature has a slightly larger effect size, since the two individuals that are most contrasting in their growth response to a 1°C Δ of temperature show a difference in radial increment of only 0.17 mm. One possible reason of such low sensitivity to temperature and precipitation is the way climatic variables were used in the model (*i.e.* mean temperature and total precipitation of the vegetative season). However, this choice was supported by the absence of a clear and common pattern of growth-climate correlations among plots. This idiosyncratic behaviour confirms the large among-site variation in climate responses usually found in Norway spruce even at the regional scale (Makinen *et al.*, 2002; Levanič *et al.*, 2009). Another possible explanation for the low sensitivity to precipitation is that water availability is high at both sampling sites (Bässler, 2004; Crespi *et al.*, 2018) and, thus, it is likely not a limiting factor to growth. Nonetheless, spruce is often pictured as a highly drought-sensitive species in the montane belt of South-eastern Germany (Hartl-Meier *et al.*, 2014) and it is strongly dependent on summer water availability at low elevation in Central Europe (Wilson and Hopfmüller, 2001; Kolár *et al.*,

2017). However, these studies were based on mean chronologies over few dominant trees per site and comparisons with our results should be taken with caution.

3.4.3 Effects of spatial and genetic structure on individual parameters

The largest inter-individual variation of TRW is associated to the intercepts (b_0) of the model in all plots. The intercept represents how constantly each tree grows due to factors not explicitly considered in the model. An advantage of our individual-based modelling approach is that the intercept as well as other individual parameters can be *a posteriori* linked to individual-based features such as the genotype and microenvironmental conditions. A multitude of microenvironmental features spanning from light availability to soil characteristics create a mosaic of favourable or unfavourable niches for trees' survival and growth (Carrer *et al.*, 2013). Such complexity makes the microenvironment a multifaceted hyperspace difficult to characterize. However, sampling a large number of individuals in a limited area allowed us to use spatial position as a proxy of microenvironmental conditions, capturing their spatial heterogeneity. Using genotypic and spatial data we assessed whether similarity in growth performances summarized by individual model parameters is affected by sharing similar genetic characteristics and/or microenvironment. We found a generally larger effect of spatial structure than genetic structure on growth performances, regardless of the statistical approach used. Additionally, spatial analyses showed that model intercepts were spatially structured in the Italian plots, with an average radius of clusters equal to ~14 m. Thus far, few dendrochronological studies investigated whether growth traits are spatially structured. In Norway spruce, previous studies detected ~30 m-wide groups of trees with similar DBH irrespective of stand history (Lamedica *et al.*, 2011) and found a patchy distribution of regeneration age and adult mortality (Castagneri *et al.*, 2010; Carrer *et al.*, 2013). These studies concluded that the spatial aggregation of such traits should result from microenvironmental heterogeneity creating favourable niches for Norway spruce regeneration. Interestingly, the effect of spatial structure on individual model intercepts was nearly absent in German plots that are instead characterized by spatially structured growth-age relationships. Such discrepancy likely reflects the main differences between the two sites. German plots are generally less heterogeneous in terms of microenvironmental conditions than Italian plots, which are located on a steep and rocky sandstone slope (Chiarugi, 1936; Magini *et al.*, 1980).

The genetic structure did not have any influence on growth performances, in agreement with King *et al.* (2013). Norway spruce is a highly outcrossing species capable of long-distance pollen and seed dispersal (Xie and Knowles, 1994; Piotti *et al.*, 2009). At the local scale,

such features cause a strong reshuffle of genetic variation, the presence of few pairs of related individuals (Androsiuk *et al.*, 2013; King *et al.*, 2013), and weak to absent spatial genetic structure both within-populations and along altitudinal transects (Geburek, 1998; Unger *et al.*, 2011). This considered, it would be interesting to apply our experimental design and analytical approach on species with limited dispersal and strong spatial arrangement of genotypes. This would shed some light on how sharing a common coancestry may influence growth traits across a spectrum of dispersal syndromes.

3.4.4 Conclusions and outlook

The joint analysis of dendrochronological and genetic data has raised much interest in recent literature (Evans *et al.*, 2018). Potential applications span from individual-based association genetic studies in natural conditions (Heer *et al.*, 2018) to the study of local adaptation to climate (Housset *et al.*, 2018; Trujillo-Moya *et al.*, 2018). Fundamental prerequisites for assessing the genomic basis of dendrophenotypes is to identify potential drivers of inter-individual variation of growth traits (Heer *et al.*, 2018) and a correct definition of dendrophenotypic traits (Housset *et al.*, 2018). Here we have presented a statistical approach for modelling growth and estimating individual parameters which summarize key ecophysiological processes. By including individual trees as a random factor, we were able to capture a considerable portion of variance and to show that, in Norway spruce, influence of tree age on TRW is more relevant than that of climatic variables. We tested the relationship between individual parameters and spatial and genetic structure and found that sharing the same microenvironment is likely more relevant than genetic similarity to inducing similar growth patterns. On the other hand, it should be stressed that our investigation is based on neutral genetic markers and, thus, only allowed us to assess genetic similarity and relatedness among individuals. However, although jointly analysing phenotypic variation and genetic relatedness is a necessary and feasible first step for estimating heritability in situ (Ritland, 1996, 2000), our study demonstrates that a large proportion of phenotypic variance remained unexplained requesting further investigations. For instance, focusing on candidate genes for growth traits could increase our understanding of inter-individual variation. Rapid technical advances will allow, in next years, to make a detailed genomic and dendroanatomical characterization of hundreds of trees feasible. In the meanwhile, we demonstrated the advantages of individual modelling and the relevance of small-scale spatial processes for treating dendrochronological data. In addition, our statistical framework could have two straightforward applications: *i*) the screening of available dendrochronological datasets to quantify inter-individual variation of

dendrophenotypes across species, and *ii*) the quantitative assessment of the proportion of variance unexplained by neutral processes based on cost-effective genetic markers. The latter would reveal whether searching for signals of local adaptation by sophisticated genomic approaches could be lucrative. All these indications should be carefully taken into account in designing future association genetic studies in natural forest tree populations.

Results of this chapter have been published in a peer-review journal.

Avanzi, C., Piermattei, A., Piotti, A., Büntgen, U., Heer, K., Opgenoorth, L., Spanu, I., Urbinati, C., Vendramin, G.G., Leonardi, S., 2019. Disentangling the effects of spatial proximity and genetic similarity on individual growth performances in Norway spruce natural populations. Sci. Total Environ. 650, 493–504.

Chapter 4

Do dendrophenotypic traits influence individual reproductive success?

4.1 Introduction

Individual fitness can be defined in terms of reproductive success, as the actual number of surviving offspring produced by an individual. The distribution of within-population individual reproductive success ultimately affects next generations' allelic frequencies (González-Martínez *et al.*, 2006) and it is shaped by a complex interaction of local selection, gene flow and genetic drift (Klein *et al.*, 2008; Oddou-Muratorio *et al.*, 2018a). Understanding which individuals have a higher reproductive success and why are crucial issues in evolutionary research (Smouse *et al.*, 1999). In forest tree populations, the distribution of reproductive success is usually skewed, with few individuals that overwhelmingly contribute to the next generation (*e.g.* Kaufman *et al.*, 1998; Smouse *et al.*, 1999; Piotti *et al.*, 2012; Moran and Clark, 2012; Leonarduzzi *et al.*, 2016; Gerzabek *et al.*, 2017). Modelling and identifying the causes of such unequal reproductive success is still a challenging task (Klein *et al.*, 2008). In fact, reproductive success is the outcome of the complex interplay among *i*) individual tree features (*e.g.* phenotype, microsite conditions), *ii*) spatial processes, such as seed and pollen dispersal, as well as the relative arrangements of adult trees and sites favourable to offspring establishment *iii*) time-related processes, such as the flowering phenology (Smouse and Sork, 2004; Klein *et al.*, 2008; Oddou-Muratorio *et al.*, 2018a) and *iv*) pure random chance. Thus, research on this evolutionary process needs to comprehensively take into account all these aspects.

The development of highly polymorphic genetic markers has allowed plant biologists to move from quantifications of individual basic fecundity (*i.e.* the number of pollen grains and seeds produced) to more reliable estimates of individual reproductive success (Oddou-Muratorio *et al.*, 2018a). Reproductive success is indeed not a linear function of basic fecundity (Schoen and Stewart, 1986), even if the latter is commonly used as a proxy for the former (Davi *et al.*, 2016). Pre- or post-zygotic selection may decouple male basic fecundity and male reproductive success (Bernasconi, 2003). As well, trade-offs between seed number and quality as well as high mortality at the seed and seedling stages may decouple female

basic fecundity and female reproductive success (González-Martínez *et al.*, 2006; Moran and Clark, 2012). Combining genetic markers and modelling approaches to parentage analysis has represented a relevant advance for assessing reproductive success (Jones *et al.*, 2010). A modelling approach to parentage analysis permits to explicitly account for biologically meaningful phenomena such as dispersal process and inter-individual variation of fecundity (Oddou-Muratorio *et al.*, 2005; Burczyk *et al.*, 2006; Klein *et al.*, 2008; Moran and Clark, 2012) as well as for uncertainty in parentage assignments (Jones *et al.*, 2010) in the estimates of individual reproductive success.

Full-probability methods have been recently proposed to extend parentage analysis in a modelling framework and estimate, among others parameters, the effects of phenotypic variables on reproductive success (*e.g.* Burczyk *et al.*, 2006; Oddou-Muratorio and Klein, 2008; Chybicki and Burczyk, 2010). Such effects can be assessed through estimating selection gradients, defined as the slope of the regression of reproductive success on measures of individual phenotype (Morgan and Conner, 2001). Among phenotypic traits potentially linked to individual reproductive success, tree size is the most frequently investigated (*e.g.* Schnabel *et al.*, 1998; Kameyama *et al.*, 2001; González-Martínez *et al.*, 2006; Piotti *et al.*, 2009; Leonarduzzi *et al.*, 2016; Chybicki and Oleksa, 2018). In a recent review of 170 studies on individual fitness in herbs, shrubs and trees, Younginger *et al.* (2017) demonstrated that size is a reliable indirect measure of fitness. However, these authors also highlighted that using size to quantify fitness may be inappropriate in age-structured natural populations. In fact, tree size depends both on age and growth rate, and these two commingled components are not necessarily highly correlated. While the effects of age and growth rates on reproductive investments has been previously explored (*e.g.* Viglas *et al.*, 2013; Davi *et al.*, 2016), the combined effect of these two factors on individual reproductive success has been only rarely assessed in forest trees. González-Martínez *et al.* (2006) did not find any significant effect of age and growth rate on female reproductive success in a *Pinus pinaster* stand, while Moran and Clark (2012) showed a hump-shaped relationship between reproductive success and both age and growth rate in two populations of red oaks (*Quercus* spp). Such sporadic evidence might suggest a potential "senescence effect" (*i.e.* individuals tend to have a lower reproductive success beyond a certain age threshold) possibly due to a trade-off between investments in growth and reproduction. A similar trade-off between growth and resources allocated to reproductive structures has been often demonstrated (*e.g.* Pukkala *et al.*, 2010; Davi *et al.*, 2016).

Individual tree age and growth rate can be easily assessed through dendrochronological techniques, but the study of tree rings offers much more interesting opportunities. Tree rings

are natural archives of past environmental information and their morphological and anatomical properties are influenced by a multitude of environmental and climatic variables (Carrer *et al.*, 2015). By generating multi-decade to multi-century time series of individual annual growth, ring-width data are an exceptional resource to analyse trees' responses to climate and environmental stressors (Evans *et al.*, 2018). Indeed, dendrophenotypic traits (*i.e.* tree-ring-based phenotypes, *sensu* Heer *et al.*, 2018) have raised much interest in recent literature. They have been correlated to population genetic parameters calculated on neutral genetic markers (*e.g.* Avanzi *et al.*, 2019; Babushkina *et al.*, 2016; Housset *et al.*, 2016; King *et al.*, 2013; Latutrie *et al.*, 2015) and fruitfully used in genotype-phenotype association studies (Heer *et al.*, 2018; Housset *et al.*, 2018; Trujillo-Moya *et al.*, 2018). Whether a comprehensive set of dendrophenotypic traits may influence individual reproductive success has never been addressed, except for a couple of studies investigating single growth parameters (González-Martínez *et al.*, 2006; Moran and Clark, 2012).

The aim of this study was to assess the effects of a large set of dendrophenotypic traits on reproductive success within natural populations of Norway spruce. Following the approach proposed by Housset *et al.* (2018) my individual phenotyping was based on three classes of dendrophenotypic traits which describe *i*) individual absolute levels of growth, *ii*) individual sensitivity to climate and *iii*) individual growth reactions to extreme climatic events. Eleven variables were measured for 518 adult trees from five plots. A total of 604 established seedlings were collected to estimate the individual reproductive success of the local adult trees. A full probability method for parentage analysis fed by genotypes at 11 biparentally-inherited nuclear and three paternally-inherited chloroplast markers as well as spatial and phenotypic data was used to assess the influence of dendrophenotypes on individual fitness, disentangling the potential sex-specific effects on female and male reproductive success. Such relationships were tested both through selection gradients estimated within the neighbourhood model framework and by fitting a generalized linear model (GLM) on the most likely genealogies from the neighbourhood model run without selection gradient. The outcomes of these two methods were compared to evaluate the soundness of results.

4.2 Materials and methods

Study sites and datasets have been already presented in Chapter 2, sections 2.2, 2.3, 2.5. In the following paragraphs, I will describe the variables tested as potential determinants of reproductive success (4.2.1) and the methods used to assess such relationships (4.2.2).

4.2.1 Dendrophenotypic and ecological variables

A set of 11 dendrophenotypic and three ecological and spatial variables were measured for all adult trees (**Table 8**) to successively assess their effects on both female and male individual reproductive success.

Age and growth rate. Individual age and average basal area increment (BAI) were calculated for each tree. Individual age can be intended as a proxy of the number of reproductive seasons each tree have experienced throughout its lifetime. Average BAI is a long-term growth measure resulting from the intermingled effects of all growth determinants that have been acting in such lifespan.

Table 8 Dendrophenotypic and ecological variables investigated in this study as potential determinants of reproductive success and their abbreviations.

Variable	Definition	Female selection gradient	Male selection gradient
Age	Total tree age	γ_1	β_1
BAI	Average individual basal are increment	γ_2	β_2
$Prev_T$	Correlation between individual RWI time series and mean temperature of previous vegetative season	γ_3	β_3
$Wint_T$	Correlation between individual RWI time series and mean temperature of winter	γ_4	β_4
$Curr_T$	Correlation between individual RWI time series and mean temperature of current vegetative season	γ_5	β_5
$Prev_P$	Correlation between individual RWI time series and total precipitation of previous vegetative season	γ_6	β_6
$Wint_P$	Correlation between individual RWI time series and total precipitation of winter	γ_7	β_7
$Curr_P$	Correlation between individual RWI time series and total precipitation of current vegetative season	γ_8	β_8
Rt_{2003}	Resistance to 2003 summer drought, expressed as the ratio between drought and pre-drought growth	γ_9	β_9
Rc_{2003}	Recovery to 2003 summer drought, expressed as the ratio between post-drought and drought growth	γ_{10}	β_{10}
Rs_{2003}	Resilience to 2003 summer drought, expressed as the ratio between post-drought pre-drought growth	γ_{11}	β_{11}
Den_{10}	Number of conspecific adult trees in a neighbourhood of 10-m radius around each individual	γ_{12}	β_{12}
Den_{20}	Number of conspecific adult trees in a neighbourhood of 20-m radius around each individual	γ_{13}	β_{13}
Centr	Centrality index	γ_{14}	β_{14}

Sensitivity to climate. A growth-climate correlation analysis was performed using the climatic data described in section 2.6. Each RWI time series was correlated against mean temperature and total precipitation of *i*) previous vegetative season (from April to October of the previous year) ($Prev_T$, $Prev_P$), *ii*) winter (from November of the previous year to March

of the current year) ($Wint_T$, $Wint_P$) and *iii*) current vegetative season (from April to October of the current year) ($Curr_T$, $Curr_P$).

Growth reaction to extreme climatic conditions. In the ongoing climate change scenario, the predicted higher intensity and/or frequency of such extreme episodes will likely affect growth and survival of tree populations (Lloret *et al.*, 2011). Thus, dendrophenotypic traits describing individual growth reactions to extreme climatic events can be particularly fruitful to shed light on tree species potential to cope with such events. These reactions were expressed in terms of resistance, recovery and resilience (Lloret *et al*., 2011). In this framework, resistance (Rt) measures tree growth reduction during the extreme episode; recovery (Rc) measures tree growth increase after the extreme episode; resilience (Rs) measures the capacity of the tree to reach pre-episode growth levels. Since spruce growth is highly influenced by the summer water deficit of the current growing season (Lebourgeois, 2007), all these indices (Rt_{2003}, Rc_{2003}, Rs_{2003}) were calculated on BAI time series for year 2003, when Europe experienced one of the hottest and driest summer over the last centuries (Fink *et al.*, 2004). Such extreme climatic conditions occurred also in my study sites, where summer temperatures were, on average, 3°C above the mean values calculated for the 1901-2013 period, while precipitations 37% below (**Fig. 18a** and **Fig. 18b**, respectively). All indices were calculated with the *res.comp* function of the R package *pointRes* (van der Maaten-Theunissen *et al.*, 2015) using a "reference period" of four years before and after the 2003 extreme climatic event (**Fig. 18c**).

Local density. By using spatial positions, conspecific local density was calculated as the number of adult trees found in a 10 and 20 m-radius neighbourhood around each adult individual (Den_{10} and Den_{20}, respectively). A centrality index (Centr) was also calculated to take into account a potential "edge-effect", i.e. trees may exhibit lower densities at the borders because individuals outside the plot were not sampled. Such index was expressed as the lowest distance between each tree and the borders of the polygon representing the convex hull (drawn using *chull* function in R) of the set of tree locations in each plot.

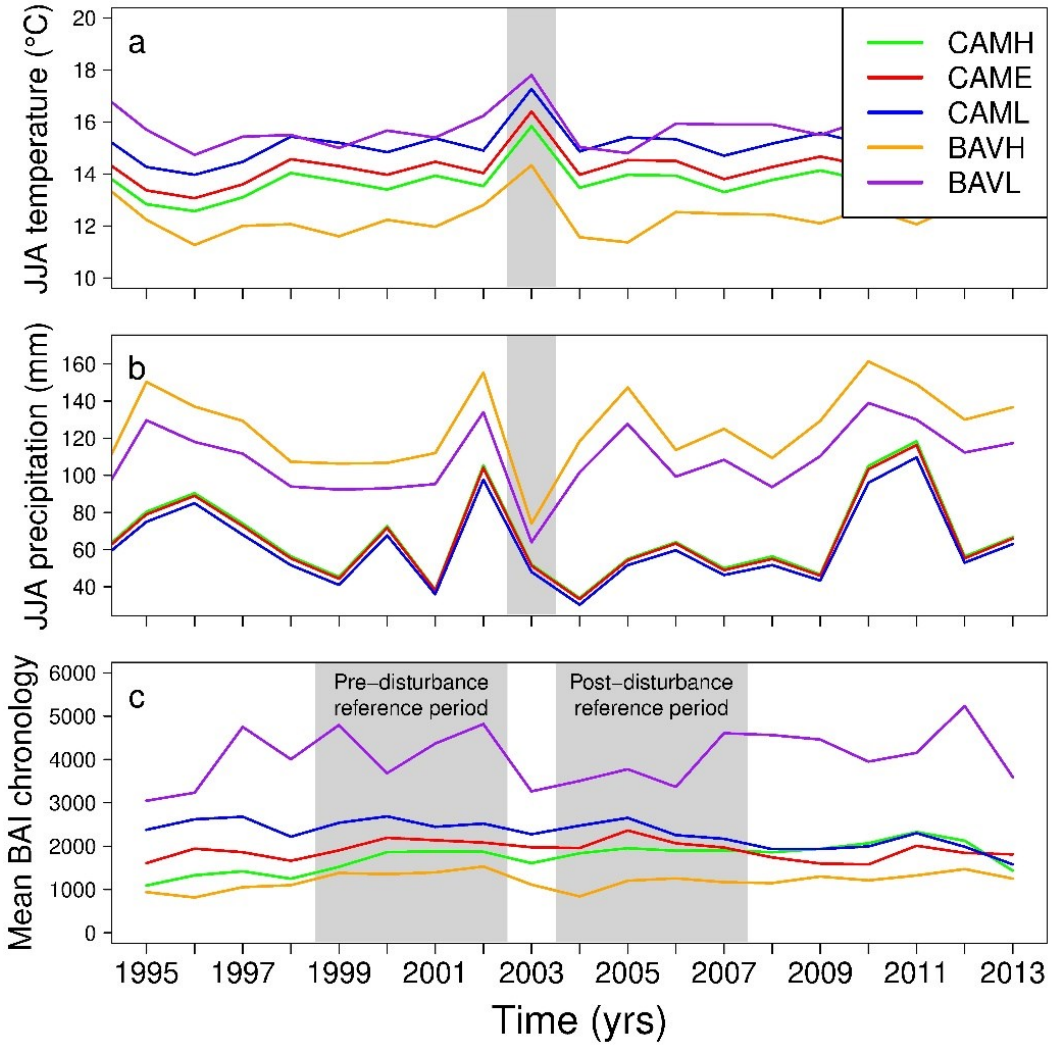

Fig. 18 Climatic and growth fluctuations of the last twenty years in sampled *Picea abies* plots. (**a**) Mean temperature and (**b**) mean precipitation of the summer period (June-July-August; JJA). (**c**) Mean basal area increment (BAI) chronologies calculated at the plot level. A 4-year reference period before and after the 2003 extreme climatic event was used to calculate the indices describing growth reactions to extreme climatic conditions (*i.e.* resistance, recovery, resilience).

4.2.2 Determinants of female and male individual reproductive success

Two different methods were used to assess the effect of dendrophenotypic ad ecological variables on both female and male individual reproductive success. First, it was tested through selection gradients estimated within the neighbourhood model framework. Secondly, female and male individual reproductive success, calculated from the most likely genealogies from the neighbourhood model run without selection gradients, were modelled as a function of dendrophenotypic and ecological variables by fitting a GLM. Both methods have advantages and drawbacks. The neighbourhood model allows to estimate selection gradients simultaneously with all other model parameters (Burczyk *et al.*, 2006) and, thus, limits the propagation of error possibly linked to a categorical parentage assignment. However, being the neighbourhood model based on a maximum-likelihood estimation of

parameters, it might fail to converge when it has to estimate a high number of parameters. To model the effects of phenotypic traits on reproductive success, neighbourhood model performs a soft-max regression analysis, which is an efficient approach to multinomial logistic regression. It is worth mentioning that soft-max regression uses exponential function for all explanatory variables, that, thus, are assumed to have a multiplicative effect on reproductive success (Smouse *et al.*, 1999). On the contrary, GLM has the major advantage of modelling the shape of the relationship between reproductive success and phenotypic traits more flexibly, *e.g.* by using the link function that describes the error distribution more properly, or by implementing model averaging strategies. In addition, it allows to account for interaction terms, whether there are enough degrees of freedom to increase the number of fitted parameters.

Neighbourhood model. The neighbourhood model is one of the possible methods to reconstruct offspring genealogies given the genetic data of a sample of putative parents and offspring (Jones *et al.*, 2010). It represents an elegant and efficient method to estimate parameters related to reproductive success while accounting for uncertainty about parentage assignments (Chybicki, 2018). It is a spatially explicit modelling approach that uses multilocus genotypes and spatial positions of both offspring and putative parents to simultaneously estimate offspring genealogies as well as seed and pollen immigration rates, self-pollination rate, genotyping errors, parameters of pollen and seed dispersal kernels and selection gradients (Adams and Birkes, 1991; Oddou-Muratorio *et al.*, 2005; Burczyk *et al.*, 2006; Klein *et al.*, 2008; Chybicki and Burczyk, 2010; Chybicki, 2018). Selection gradients are the slopes of the linear regression analysis between reproductive success and the phenotypic traits of putative parents (Morgan and Conner, 2001). The neighbourhood model advantageously allows to estimate selection gradients of phenotypic traits in both female and male parents, making possible to evaluate their importance on both female and male individual reproductive success (Burczyk *et al.*, 2006). In this study, neighbourhood model was used as implemented in NMπ software (Chybicki, 2018). In such a framework, the probability of observing the *i*-th offspring with genotype o_i is modelled as the sum of probabilities of alternative events, that is:

$$Pr(o_i) = \omega_i m_s Pr(o_i|u \times u) + (1 - \omega_i m_s) \sum_j^J \psi_{ij} \left[s\, Pr\left(o_i \middle| p_j \times p_j\right) + m_p\, Pr\left(o_i \middle| p_j \times u\right) + \left(1 - s - m_p\right) \sum_{k \neq j}^J \varphi_{jk} \Pr(o_i|p_j \times p_k) \right], \quad (6)$$

where m_s and m_p are the seed and pollen immigration rates from outside the neighbourhood, respectively; s is the self-pollination rate; ω_i is a binary variable that indicates whether offspring are *dispersed* or not (in this study, it was equal to 1 because we analysed established seedlings); ψ_{ij} and φ_{jk} are the female and male reproductive success of the j-th and k-th putative parents, respectively; p_j is the genotype of the j-th putative parent and u is the genotype of an unsampled putative parent located outside the neighbourhood. Pr($o_i|u \times u$), Pr($o_i|p_j \times p_j$), Pr($o_i|p_j \times u$), and Pr($o_i|p_j \times p_k$) are the Mendelian transition probabilities that the observed o_i genotype of the i-th offspring originated outside the neighbourhood or from a local mother that is self-pollinated, pollinated by a unknown father outside its neighbourhood or by a local father. Transition probabilities are computed as a function of genotypes and mistyping error rates (ε). Here, allele frequencies of the background population located outside the neighbourhood were assumed to be equal to local allele frequencies (as suggested by Burczyk and Chybicki, 2004). Reproductive success (ψ_{ij}, φ_{jk}) is assumed to be a function of reproductive success covariates, such as relative spatial positions of individuals as well as phenotypic traits. They are expressed as:

$$\psi_{ij} = \mu_j \pi_{ij}^{s} \lambda_j^{f} \; / \; \sum_k^J \mu_k \pi_{ik}^{s} \lambda_k^{f}, \qquad (7)$$

$$\varphi_{jk} = (1-\mu_k)\pi_{jk}^{p} \lambda_{jk}^{m} \; / \; \sum_l^J (1-\mu_l)\pi_{jl}^{p} \lambda_{jl}^{m}, \qquad (8)$$

where J is the number of putative parents; μ_j indicates the gender of the j-th putative parent (in this study, it was always equal to 0.5 because Norway spruce is a hermaphrodite species); π_{ij}^{s} is the effect of the i-th offspring position relatively to the j-th putative parent position; π_{jk}^{p} is the effect of the j-th putative parent position relatively to the k-th putative parent position; λ_j^{f} and λ_{jk}^{m} are the effects of the measured phenotypic traits on female and male individual reproductive success, respectively. π_{ij}^{s} and π_{jk}^{p} are assumed to equal the probability of seed and pollen dispersal, respectively. In this study, such probabilities were modelled using an exponential-power distribution, that is:

$$\pi_{ij} = c \exp\left[-\left(\frac{d_{ij}}{a}\right)^{b}\right], \qquad (9)$$

where d_{ij} is the Euclidean distance between the i-th and j-th individual; a and b are the scale and shape parameters of dispersal kernel, respectively. λ_j^{f} and λ_{jk}^{m} are exponential functions of form:

$$\lambda_j^{f} = \exp\left(\sum_n^N \gamma_n z_{jn}\right), \qquad (10)$$

$$\lambda_{jk}^{m} = \exp\left(\sum_n^N \beta_n z_{kn}\right), \qquad (11)$$

where N is the number of measured phenotypic traits; z_{jn} is the n-th phenotypic traits measured for the j-th putative parent; γ_n and β_n are the slope coefficients mirroring the effects of the n-th phenotypic character on female and male reproductive success, respectively.

Analyses were performed on the entire dataset, setting the neighbourhood size to 215 m (*i.e.* the maximum within-plot pairwise spatial distance between individuals) to model the dispersal process at the neighbourhood level. First, neighbourhood model was run estimating all parameters, including selection gradients (14 γ parameters and 14 β parameters for female and male effects, respectively; **Table 8**). Before model fitting, dendrophenotypic and ecological variables were scaled to compare the relative strength of selection gradients (as suggested by Chybicki, 2018). Different models were sequentially run to find the optimal fitting. A first series of 28 models was run including only one selection gradient at a time. This step aimed at ranking female and male selection gradients based on their fits in terms of the Akaike Information Criterion (AIC) of the model. Based on such ranking, a second and a third series of models were run adding sequentially female and male selection gradients, respectively. Each selection gradient was retained in the model when it improved the model fitting, which was evaluated by a Likelihood-ratio test on nested models. A final model including all the retained female and male selection gradients was run to get the final estimates of all model parameters.

Secondly, neighbourhood model was run estimating all parameters (*i.e.* immigration and self-pollination rates, genotyping errors and pollen and seed dispersal kernel parameters) but no selection gradients. The resulting most likely genealogies were used to calculate female and male individual reproductive success, expressed as the sum of gametes assigned to each mother and father tree, respectively. Such estimates were successively tested against dendrophenotypic and ecological variables by fitting a GLM, as described in the following paragraph.

Generalized Linear Model. Using parentage assignments, female and male individual reproductive success (ψ and φ, respectively) were calculated as the sum of gametes produced by each mother and father tree, respectively. Such reproductive success estimates were then modelled as a function of dendrophenotypic and ecological variables fitting a GLM with negative binomial error distribution to account for overdispersion. The starting models were the following:

$$\psi, \varphi \sim Plot + Age + Age^2 + BAI + BAI^2 + Rt_{2003} + Rc_{2003} + Rs_{2003} + Prev_T + Wint_T + Curr_T + Prev_P + Wint_P + Curr_P + Den_{10} + Den_{20} + Centr + \varepsilon, \quad (12)$$

where plot was considered as a categorical variable, whereas all the other variables as quantitative covariates. A quadratic term for both tree age (Age^2) and average BAI (BAI^2) was included in the model to test for an age-related decline of reproductive success and a trade-off between reproductive success and growth, respectively. All explanatory variables were centred and scaled. Analyses were performed by using the *glm.nb* function of the R package *MASS* (Venables and Ripley, 2002) in the R suite. To avoid collinearity problems, the variance inflation index (VIF) was calculated for each variable of (12) using the R package *car* (Fox and Weisberg, 2011). The variable with the highest VIF was sequentially dropped from the model until all variables had VIF values <3 (Zuur *et al.*, 2010). This procedure led to the exclusion of Rs_{2003} and Den_{20} from both models of female and male reproductive success. After this first step, model averaging with Bayesian information criterion (BIC) was performed to account for model uncertainty and to reduce parameter estimation bias (Burnham and Anderson, 2002) through the R package *MuMIn* (Barton, 2018). To this aim, alternative models with all possible combinations of the considered variables were built using the *dredge* function. The site variable (Plot) was arbitrarily forced to be always included in each alternative model. Model comparison was made using BIC, by selecting models with Δ_{BIC} <10 (Aho *et al.*, 2014). On this subset of models, model averaging based on model weights was performed using the *model.avg* to obtain averaged standardized conditional coefficients.

4.3 Results

4.3.1 Dendrophenotypic traits

The five plots were characterized by different age structures (**Fig. 8**; **Fig. 19a**). In CAMH and CAML, 81% and 64% of the trees were younger than 60 years, with a median age of 42 and 53 years, respectively. In the other three plots, the percentage of trees < 60 years was markedly lower (CAME: 16%; BAVH: 3%; BAVL: 20%) and the median age ≥100.

The distribution of individual average BAI was quite similar among plots, except for BAVL which was much more variable and had three times the standard deviation of other plots (**Fig. 19b**). Growth-climate correlations were globally low, with mean correlation values of 0.014 and 0.018 for temperature and precipitation responses, respectively (**Fig. 19c-h**). Correlation values showed a wide range of individual responses to temperature and precipitation, ranging from highly negative (-0.774) to highly positive (0.552) values.

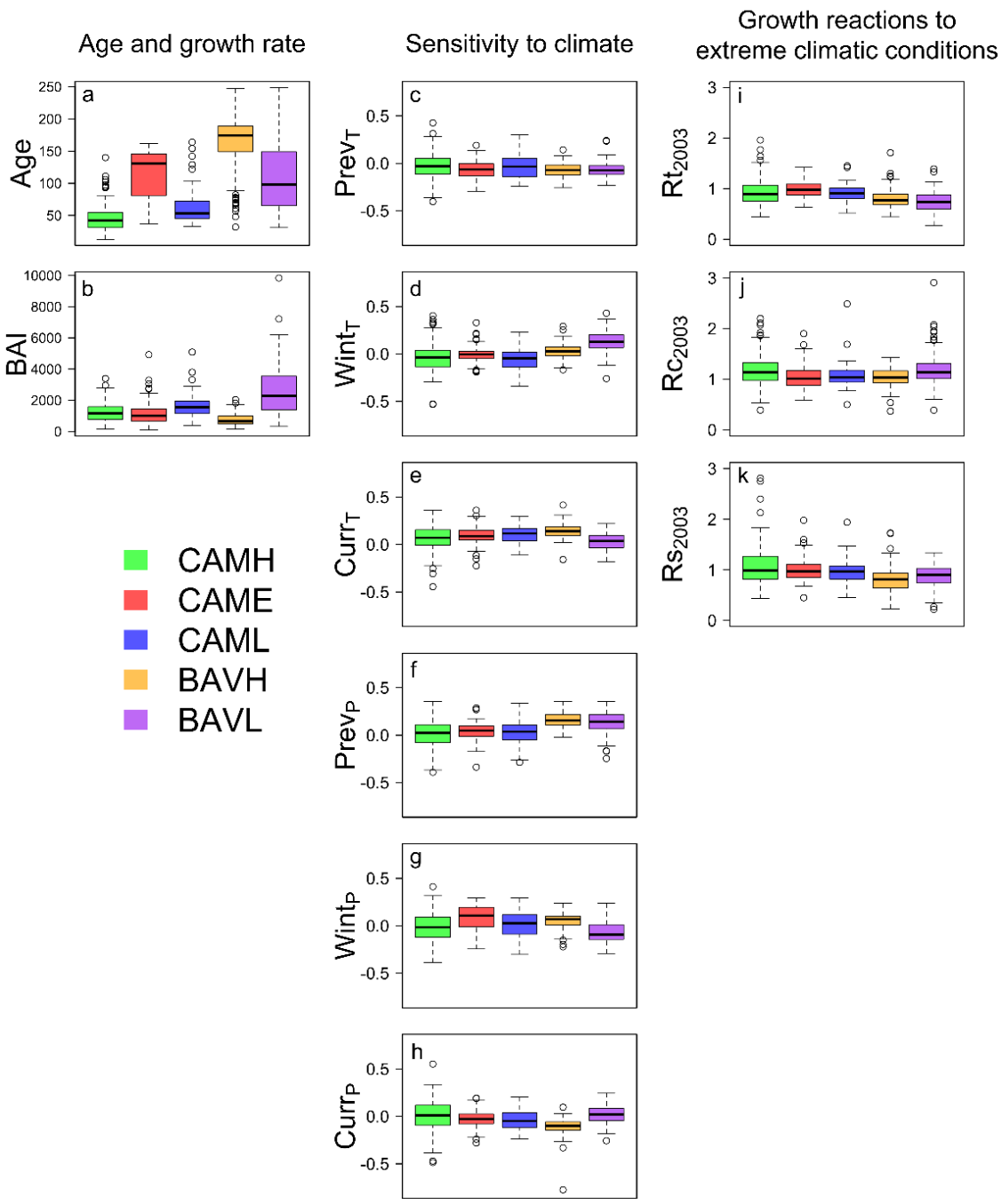

Fig. 19 Dendrophenotypic traits for each plot. Dendrophenotypic traits are grouped based on the three classes of phenotypic measures defined according to Housset *et al.* (2018).

Mean values of the indices describing growth reactions to extreme climatic conditions are reported in **Table 9**. Once again, it is worth mentioning the large inter-individual variation associated to such indices, with individuals showing opposite growth reactions (**Fig. 19i-k**). By analysing resistance and resilience values, it emerged that trees from the German site were more affected by the 2003 summer drought with respect to trees from the Italian one. In fact, almost all trees from the German site showed a growth decline (89% and 91% of

trees with Rt <1 in BAVH and BAVL, respectively) while the ones from the Italian site were less affected (54%, 61% and 67% of trees with Rt <1 in CAME, CAML and CAMH, respectively) (**Fig. 19i**). Similarly, in the four years following the 2003 summer drought, German trees grew less, on average, with respect to the pre-drought period (**Fig. 19k**; **Table 9**).

Table 9 Mean values of resistance, recovery and resilience to 2003 summer drought calculated for each plot. Standard deviations are reported in brackets.

	CAMH	CAME	CAML	BAVH	BAVL
Rt_{2003}	0.94 (±0.26)	0.99 (±0.18)	0.92 (±0.18)	0.80 (±0.19)	0.75 (±0.21)
Rc_{2003}	1.17 (±0.30)	1.03 (±0.22)	1.09 (±0.28)	1.03 (±0.20)	1.22 (0.39)
Rs_{2003}	1.08 (±0.38)	1.01 (±0.24)	0.98 (±0.23)	0.82 (±0.25)	0.88 (±0.24)

4.3.2 Individual reproductive success

For each seedling, the *a posteriori* probabilities of the first most likely and the second most likely genealogies were determined. The probabilities of the most likely genealogy were generally much higher than those of the second one (**Fig. 20**), with an average value of 0.80 (±0.19). Mother trees could be identified for 296 (49%) of the total 604 sampled seedlings, while father trees only for 79 (13%) seedlings. Seedlings with both parents, one parent and no parents inside the plot were 79 (13%), 217 (36%) and 308 (51%), respectively. As expected, within-plot distribution of individual reproductive success was skewed. The percentages of trees producing >2 gametes were 5% in CAMH and BAVH, 9% in CAML, 13% in CAME and BAVL (**Fig. 21**).

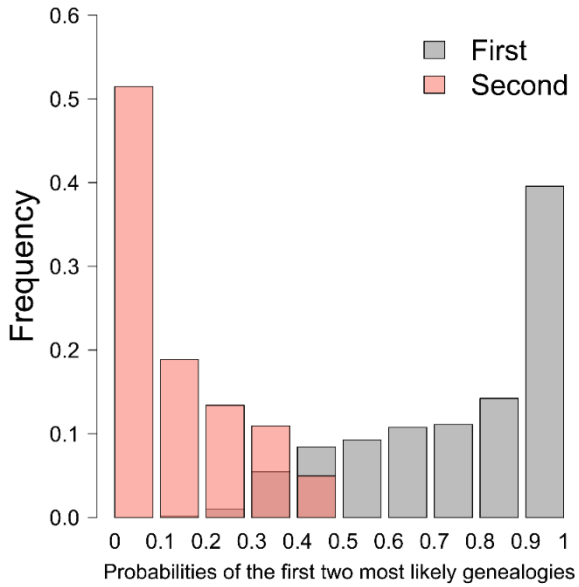

Fig. 20 Distribution of the *a posteriori* probabilities of the first most likely (gray bars) and the second most likely (pink bars) genealogies determined by NMπ for each seedling.

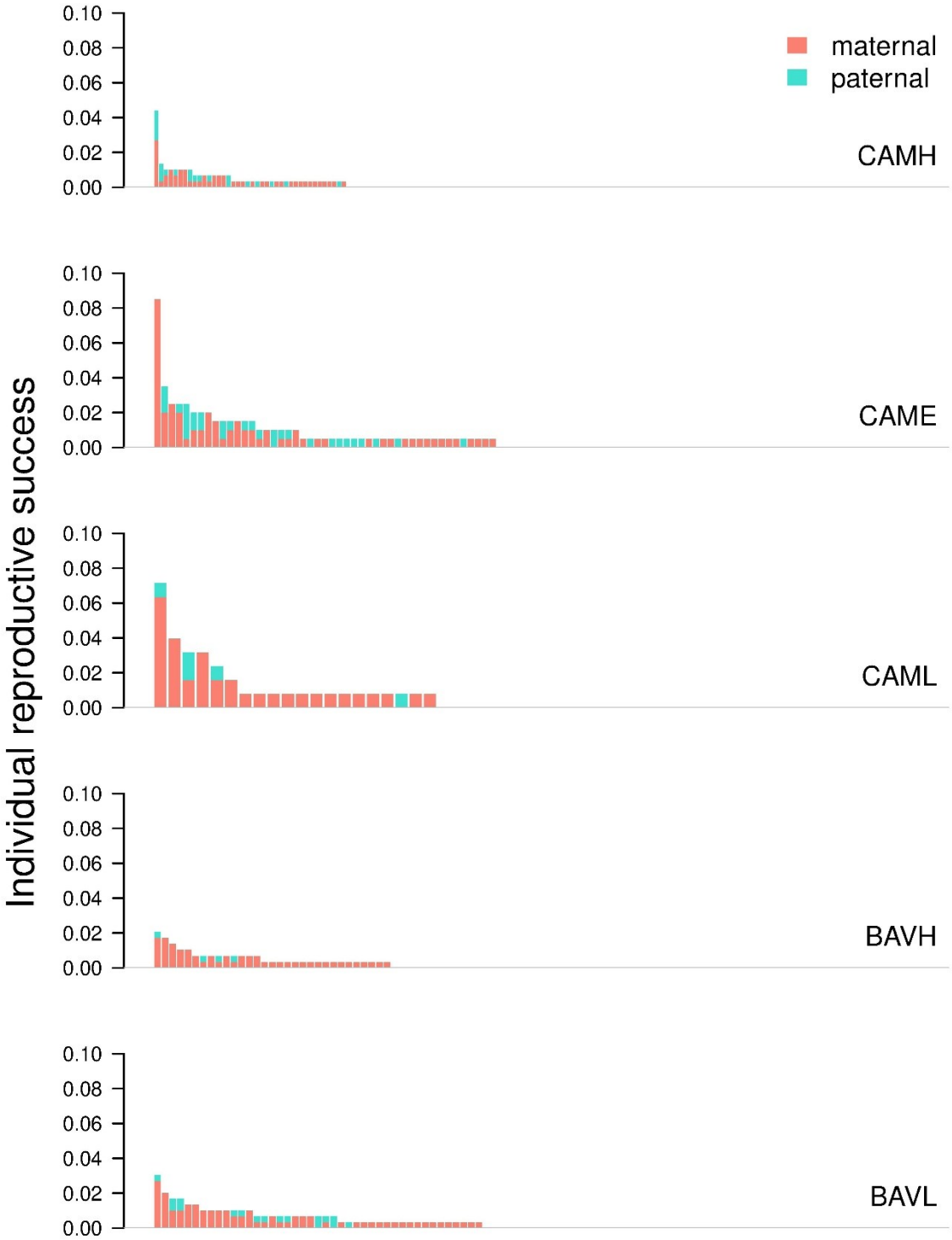

Fig. 21 Distribution of individual reproductive success. Each bar corresponds to an adult individual. Pink bars represent the number of gametes produced by maternal function, while light blue bars the ones produced by paternal function. The total number of gametes produced by each tree are divided by the total number of gametes sampled within each plot.

4.3.3 Determinants of female and male individual reproductive success

Neighbourhood model. Since neighbourhood model parameters estimated with no selection gradients very highly consistent with those of the model run including selection gradients, only the latter were shown (**Table 10**). Seed and pollen immigration rates were equal to 0.461 (± 0.025) and 0.755 (±0.029), respectively. Estimates of genotyping error rates ranged from zero to 0.085, with an average value of 0.040. Self-pollination rate was not statistically higher than zero, and it was treated as a fixed parameter, using the default value in NMπ (*s* = 0.01). The scale parameter of the seed dispersal function ($1/\delta_s$) was equal to 0.026 (± 0.002) and, therefore the estimated mean seed dispersal distance was 37.5 m. The scale parameter of the pollen dispersal function ($1/\delta_p$) did not significantly differ from zero, and it was treated as a fixed parameter ($1/\delta_p = 0$). This means that the estimated mean pollen dispersal distance was equal to ∞. Shape parameters of both seed and pollen dispersal functions were not statistically different from 1, and were treated as fixed parameters (b_s = 1, b_p = 1). When shape parameter of an exponential-power function is equal to 1, the curve is reduced to an exponential function. When $b_p = 1$ and mean pollen dispersal distance equal to ∞, the pollen dispersal function becomes basically a flat curve.

Table 10 Final estimates of model parameters obtained by running the neighbourhood model including all parameters. Here, immigration and self-pollination rates (m_s, m_p, s) pollen and seed dispersal parameters ($1/\delta_s$, $1/\delta_p$, b_s, b_p) as well as genotyping errors (ε_1- ε_{11}) are reported. Selection gradients are reported separately in **Table 11**.

Description	Parameter	Estimate	s.e.	95 % CI
Probability of seed immigration	m_s	0.461	0.025	0.410, 0.486
Probability of pollen immigration	m_p	0.755	0.029	0.699, 0.811
Probability of self-pollination	s	0.01		
Scale parameter of seed dispersal	$1/\delta_s$	0.026	0.002	0.022, 0.031
Scale parameter of pollen dispersal	$1/\delta_p$	0		
Shape parameter of seed dispersal	b_s	1		
Shape parameter of pollen dispersal	b_p	1		
Genotyping error rates:				
WS0092.A19	ε_1	0.049	0.010	0.029, 0.068
Pa28	ε_2	0.051	0.012	0.029, 0.074
Pa05	ε_3	0		
WS0022.B15	ε_4	0.043	0.010	0.024, 0.062
WS0016.O09	ε_5	0.022	0.008	0.007, 0.038
Pa44	ε_6	0.031	0.009	0.014, 0.048
EATC1E03	ε_7	0.026	0.007	0.013, 0.039
EATC2G05	ε_8	0.085	0.012	0.062, 0.108
WS0111.K13	ε_9	0.047	0.010	0.027, 0.067
WS0023.B03	ε_{10}	0.058	0.011	0.037,0 .079
SpaGG03	ε_{11}	0.032	0.008	0.016, 0.048

Female reproductive success was significantly, positively influenced by age (γ_1 = 0.312), average BAI (γ_2 = 0.231) and growth-climate correlations with temperatures of the previous vegetative season (γ_6 = 0.207), while it was negatively influenced by resilience (γ_5 = -0.364) (**Fig. 22**; **Table 11**). Male reproductive success was significantly, positively influenced by age (β_1 = 0.792), growth-climate correlations with precipitation of the previous vegetative season (β_9 = 0.637) and average BAI (β_2 = 0.416) (**Fig. 22**; **Table 10**).

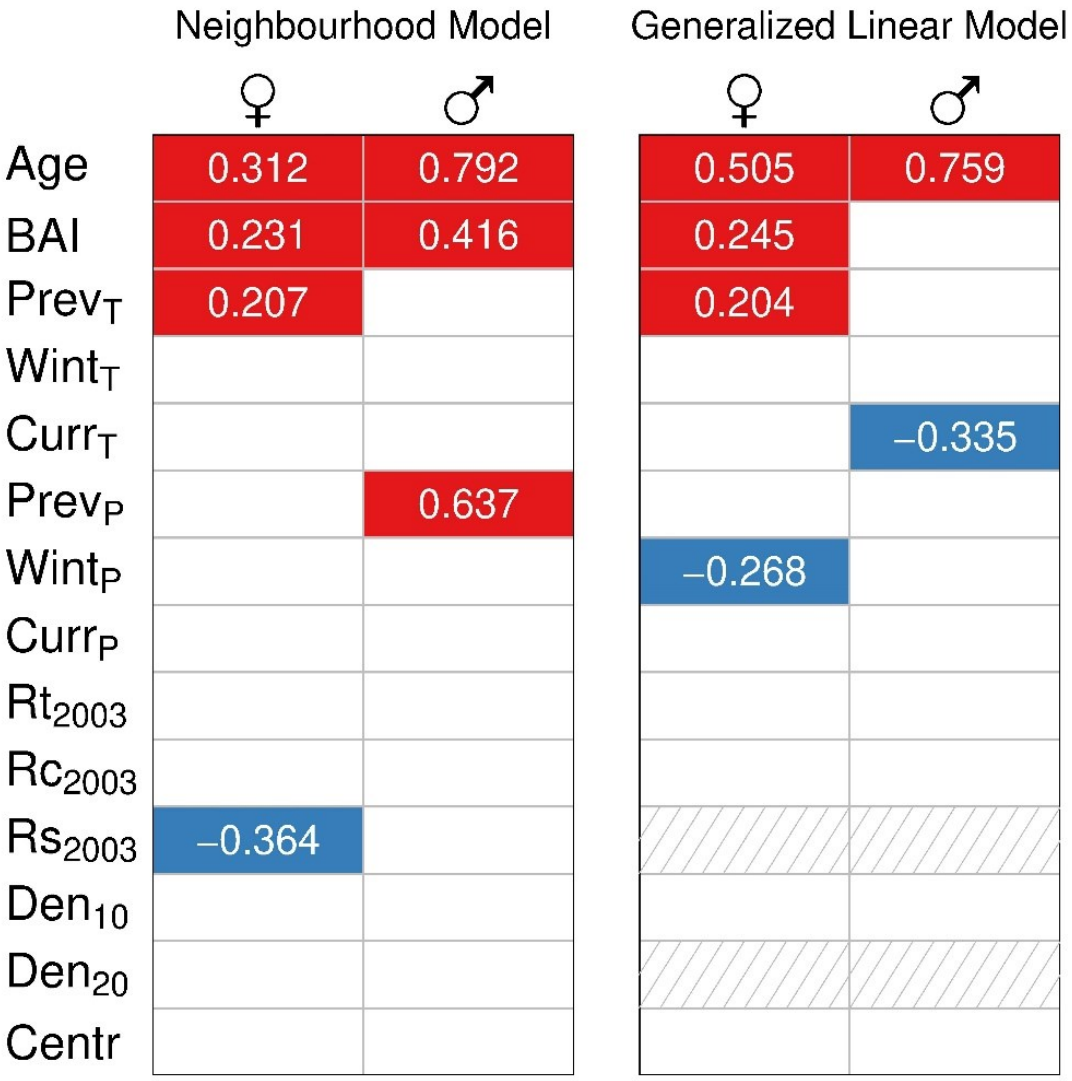

Fig. 22 Comparison of the results of the two methods applied to assess the effects of dendrophenotypic and ecological variables on both female and male reproductive success. Red boxes indicate that the variable has a significant and positive effect, while blue boxes that it has a significant and negative effect. The magnitude of all significant variables is reported, and it is expressed in terms of selection gradient for the neighbourhood model and averaged coefficients for GLM. All reported coefficients are in standard deviation units, so they are comparable within method. Striped boxes indicate the variables which were removed from the model because of collinearity (VIF >3; Zuur *et al.*, 2010).

Generalized Linear Model. Averaged standardized coefficients predicting the effects of dendrophenotypic and ecological variables on both female and male individual reproductive success are reported in **Table 12**. Female individual reproductive success was strongly positively associated to age, both for the linear term (β = 0.505) and the quadratic one (β = -0.319), to average BAI (β = 0.245) and to growth-climate correlations with the mean temperature of the previous vegetative season (β = 0.204) while it was negatively associated to growth-climate correlations with winter precipitation (β = -0.268) (**Fig. 22**). Male individual reproductive success was positively associated to age (β = 0.759), while it was negatively associated to growth-climate correlations with temperatures of the current vegetative season (β = -0.335). (**Fig. 22**). BAI had only a marginal effect on male reproductive success (β = -0.335; $P < 0.10$). The plot factor was statistically significant in both models, meaning that there were differences among plots in the mean female and male individual reproductive success. Since BAVH was the reference level, plot-specific estimates were calculated by comparing BAVH with the other plots (**Table 12**).

Table 11 Slopes of the regression of phenotypic traits against female and male individual reproductive success (shortened to FRS and MRS, respectively). Only selection gradients that were statistically significant in the final run of the neighbourhood model were reported.

Variable	Description	Parameter	Estimate	s.e.	95 % CI
Age	Effect of tree age on FRS	γ_1	0.312	0.098	0.119, 0.505
BAI	Effect of tree average BAI on FRS	γ_2	0.231	0.054	0.126, 0.337
Rs_{2003}	Effect of tree resilience on FRS	γ_5	-0.364	0.111	-0.582, -0.146
$Prev_T$	Effect of correlation with temperatures of the previous vegetative season on FRS	γ_6	0.207	0.079	0.052, 0.363
Age	Effect of tree age on MRS	β_1	0.792	0.236	0.329, 1.255
BAI	Effect of tree average BAI on MRS	β_2	0.416	0.127	0.166, 0.665
$Prev_P$	Effect of correlation with precipitation of the previous vegetative season on MRS	β_9	0.637	0.200	0.245, 1.028

Table 12 Averaged standardized coefficients predicting the effect of dendrophenotypic, ecological and plot variables on both female and male individual reproductive success. Coefficients are in boldface if the 95% confidence interval (95% CI) does not overlap zero.

	Female Reproductive Success				**Male Reproductive Success**			
Variable	**Estimate**	**s.e.**	**95% CI**	**Z**	**Estimate**	**s.e.**	**95% CI**	**z**
Intercept	**-1.084**	0.336	-1.743, -0.424	3.215	**-3.985**	0.720	-5.396, -2.575	5.528
Age	**0.505**	0.150	0.211, 0.799	3.355	**0.759**	0.238	0.293, 1.224	3.186
Age^2	**-0.319**	0.124	-0.562, -0.076	2.573	-0.212	0.208	-0.620, 0.196	1.020
BAI	**0.245**	0.099	0.051, 0.439	2.464	0.259	0.156	-0.046, 0.564	1.659
BAI^2	0.028	0.025	-0.021, 0.077	1.099	0.004	0.054	-0.102, 0.110	0.065
$Prev_T$	**0.204**	0.099	0.01, 0.397	2.056	-0.160	0.162	-0.478, 0.159	0.980
$Wint_T$	-0.125	0.115	-0.351, 0.101	1.079	0.231	0.179	-0.12, 0.582	1.286
$Curr_T$	0.124	0.110	-0.092, 0.341	1.122	**-0.335**	0.157	-0.643, -0.028	2.131
$Prev_P$	0.031	0.121	-0.206, 0.269	0.259	0.171	0.179	-0.179, 0.522	0.955
$Wint_P$	**-0.268**	0.108	-0.48, -0.056	2.469	0.030	0.171	-0.306, 0.366	0.175
$Curr_P$	0.142	0.113	-0.081, 0.364	1.245	-0.042	0.175	-0.385, 0.3	0.243
Rt_{2003}	-0.134	0.117	-0.363, 0.095	1.141	-0.147	0.195	-0.529, 0.235	0.752
Rc_{2003}	-0.004	0.098	-0.196, 0.188	0.041	0.046	0.155	-0.258, 0.35	0.296
Rs_{2003}								
Den_{10}	-0.080	0.159	-0.392, 0.232	0.502	0.306	0.230	-0.144, 0.757	1.330
Den_{20}								
Centr	0.090	0.103	-0.111, 0.291	0.874	0.090	0.166	-0.236, 0.417	0.542
$Plot_{CAMH}$	0.509	0.464	-0.402, 1.419	1.094	**1.846**	0.726	0.422, 3.269	2.535
$Plot_{CAME}$	**0.677**	0.342	0.007, 1.347	1.977	**2.483**	0.671	1.168, 3.798	3.692
$Plot_{CAML}$	0.360	0.506	-0.632, 1.352	0.709	**2.510**	0.989	0.572, 4.448	2.535
$Plot_{BAVL}$	0.678	0.503	-0.307, 1.664	1.347	1.857	0.957	-0.018, 3.733	1.937

4.4 Discussion

Quantifying individual reproductive success and its determinants are crucial topics in evolutionary research because of the major consequences that the transmission of genetic variation across generations has on populations' adaptive potential (Oddou-Muratorio *et al.*, 2018a). In this study, I investigated such reproductive dynamics within five Norway spruce natural populations to identify which trees had the highest reproductive success and why. Reproductive success was highly heterogeneous within plots, with generally few individuals overwhelmingly contributing to the next generation. A skewed distributions of reproductive success is usually found in parentage-based studies on conifers (*e.g.* González-Martinez *et al.*, 2006; Lian *et al.*, 2008; Piotti *et al.*, 2009; Steinitz *et al.*, 2011; Leonarduzzi *et al.*, 2016), broad-leaves species (*e.g.* Aldrich and Hamrick, 1998; Schnabel *et al.*, 1998; Moran and Clark, 2012; Gerzabek *et al.*, 2017; Oddou-Muratorio *et al.*, 2018a) and also herbaceous plants (*e.g.* Meagher and Thompson, 1987). Apart from this finding that was somehow expected, the main step forward offered by my work is a detailed investigation of the potential phenotypic determinants of both male and female reproductive success.

To my knowledge, in *Picea abies* the relationship between reproductive success and potential phenotypic determinants was investigated only by Piotti *et al.* (2009), that found no correlation between tree size and reproductive success in a population at the tree-line. Few others paternity-based studies were made on this species but they aimed only at estimating pollen immigration rates from external sources in seed orchards (Paule *et al.*, 1993; Pakkanen *et al.*, 2000; Burczyk *et al.*, 2004). Here, I assessed the sex-specific effects of a large set of dendrophenotypic traits on individual reproductive success. Age, average BAI and growth-climate correlations with mean temperature of the previous vegetative season were found to be consistently associated with reproductive success. I decided to focus the discussion on findings which were consistent between the two statistical approaches used, while overlooking other results that were method-dependent.

4.4.1 Beyond diameter as a phenotypic determinant of reproductive success

Most parentage-based studies aimed at assessing the determinants of reproductive success used tree diameter as phenotypic trait to be correlated with individual fitness (*e.g.*; Oddou-Muratorio *et al.*, 2005, 2008; Klein *et al.*, 2008; Chybicki and Oleksa, 2018). Diameter is a soft trait that can be easily measured (Hodgson *et al.*, 1999), but it is also a very rough representation of how a tree copes with its environment. Diameter results from the interplay of a multitude of intrinsic and extrinsic factors, and it is mainly determined by age and growth rate of a tree (indeed, it is basically their product) (Chybicki and Oleska, 2018). For these reasons, carefully selecting the phenotypic variables to be correlated with reproductive success is crucial not to confound the effects of different processes, such as aging and tree annual productivity. Quantifying both the effects of age and growth rate on individual reproductive success is particularly relevant for long-lived species forming age-structured natural populations, such as forest trees, for which mere measures of tree size are considered potentially misleading proxies of fitness (Younginger *et al.*, 2017). Through dendrochronological techniques it is indeed possible to simultaneously assess trees' age and growth rate. Growth rate is usually calculated in terms of average TRW or average BAI. Describing growth rate through BAI instead of TRW has some advantages. BAI better represents the absolute growth rate of stemwood biomass (Hember *et al.*, 2015) and it is less influenced by geometric constraints due to the age-related increase of stem circumference (Biondi and Quedan, 2008) with respect to linear measurements such as TRW. Therefore, BAI is usually recommended to evaluate growth differences among years (Biondi and Quedan, 2008). BAI is characterized by an age-related sigmoid trend: comparing average BAI of trees of different ages may be misleading. In this study, I took advantage of a

modelling approach to disentangle the effects of both age and average BAI. Such approach allowed me to i) evaluate the effect of a single variable *ceteris paribus* (*i.e.* isolating the relative contribution of each variable while holding constant the effects of the others) and *ii*) to check for potential collinearity between variables.

4.4.2 Age and growth rate effects on reproductive success

The joint effects of age and growth rate on reproductive success have been rarely investigated in forest tree species (González-Martínez *et al.*, 2006; Moran and Clark, 2012). To my knowledge, this is the first multi-site parentage-based study aimed at disentangling such effects in conifers. A previous study evaluated the effects of tree size, age and growth on female reproductive success in a single *Pinus pinaster* population (González-Martínez *et al.*, 2006). These authors found that reproductive success was neither associated to tree age nor to diameter increment in the 10 years before sampling, while it was highly, positively influenced by diameter and size of cone crop. In red oaks, Moran and Clark (2012) found a hump-shaped relationship between female reproductive success and both age and growth rate. However, their statistical inferences were based on a small subsample of trees for which these phenotypic traits were scored (34/51 out of 317 for age and growth, respectively). This implies, for example, that the hump-shaped relationship between female reproductive success and age founded in their study might be driven by the only very old sampled tree (approx. 170 yrs) which had a low number of assigned seedlings. In fact, the relationship between age and reproductive success seemed to increase linearly at least in the age interval for which heteroscedasticity was not problematic (between 70 yrs and 110 yrs). An advantage of the large number of individuals sampled and phenotyped for my work (518 trees from five plots) was the low heteroscedasticity due to the scarce sampling of extreme values of covariates.

Consistently across methods, average BAI had a positive effect on both female and male reproductive success. This means that faster growing trees have produced a larger number of surviving offspring, both through the male and female function. Such finding excluded a possible trade-off between growth rate and reproductive success, as previously hypothesized by Moran and Clark (2012) in red oaks. Although a negative correlation between radial growth rates in previous years and cone production has been found in conifers (*e.g.* Pukkala, 1987; Davi *et al.*, 2016), my results suggested that, at least in Norway spruce, those trees that had been able to invest a larger amount of resources in growth (with respect to the population average) have had an advantage in terms of lifetime fitness. A positive and significant effect of tree size on reproductive success has been often found in conifers (*e.g.*

Picea glauca, Schoen and Stewart (1986); *Pinus pinaster*, González-Martínez *et al.*, (2006); *Abies sachalinensis*, Lian *et al.* (2008); *Abies alba*, Leonarduzzi *et al.* (2016); *Taxus baccata*, Chybicki and Oleska (2018)) but not accounting for the effect of age might have misguided the interpretation of such relationship, as explained earlier. The focus of my study on the effect of individual growth rate given the effect of other predictors (in particular, age) changed the perspective on the relationship between growth and reproductive investment with respect to population-level researches (Obeso, 2002). At the population level, reproduction is costly and reduces vegetative growth, at least for a limited period of time (*e.g.* Pukkala, 1987; Obeso, 2002; Petit and Hampe, 2006; Davi *et al.*, 2016). For example, low radial growth rates in previous years were associated to higher cone production in silver fir (Davi *et al.*, 2016), whereas masting years determined a 15-20% reduction of diameter growth in Norway spruce (Pukkala, 1987). When this relationship was analysed at the individual level, as in my case, a positive effect of growth rate on reproductive success was shown. The positive effect is extended to the entire tree lifetime and it might determine a higher fitness in evolutionary terms on the long-term (*i.e.* a higher genomic heritage in the next generation). For instance, these individuals may better compensate costs of reproduction by increasing their resource intake and/or developing other compensatory mechanisms (Tuomi *et al.*, 1983; Obeso, 2002). It should be stressed that my study was not aimed at tracking the costs of reproduction at specific years or masting events. Not knowing when the seeds that originated the sampled seedlings were produced, I could not calculate trade-offs between costs and gains of reproduction in single reproductive seasons. On the contrary I could quantify individual lifetime fitness by providing a snapshot relative to the time period covered by the sampled seedling cohort. However, the indications emerging from my study showed that a higher reproductive success was associated to a larger lifetime growth rate, despite the possible reproductive costs in terms of growth that trees might experience.

Age had a positive effect on reproductive success as well. The shape of this relationship was different among sexes: there was a quadratic dependency with downward concavity for female reproductive success, whereas the relationship was linear for male reproductive success. On the "father" hand, this age-related increase in reproductive success was likely determined by the higher number of reproductive seasons that each tree experienced throughout its lifetime. This explanation was previously proposed by Schnabel *et al.* (1998) that, using diameter as a proxy for age, found a positive effect on female reproductive success of *Gleditsia triacanthos*. However, diameter is not necessarily a good proxy of tree age. For example, Blum (1961) and Gibbs (1963) reported a large age variation between

trees of the same diameter in hardwood trees. In Norway spruce, diameter and age can be weakly related because of the period of slow growth during juvenile life stages under the dense shade of adult tree canopies (Piussi, 1979) or because of peculiar ecological conditions (*e.g.* at the upper forest limit, as reported by Piotti *et al.*, 2009). On the "mother" hand, the quadratic term for age included in the GLM was significant indicating that there was an age-related decrease in reproductive success at ~ 160 years (**Fig. 23**). Such senescence effect was found also by Moran and Clark (2012) that showed how female reproductive success declined after ~ 100 years in red oaks. Signatures of reproductive senescence were reported by Silvertown *et al.* (2001) which found an age-related decline of reproductive value in 6 of the 65 iteroparous perennial plant species analysed. Female reproductive senescence may be due to a reduced seed production with increasing age, coupled with the advancement of established seedlings out of the seedling cohort that may increase the local number of conspecific competitors (Moran and Clark, 2012).

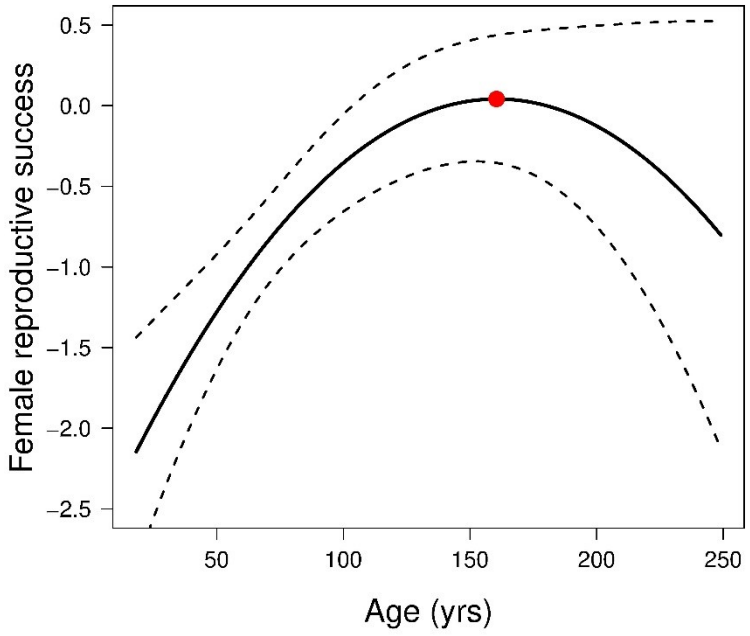

Fig. 23 The black solid line represent the effect of age on individual female reproductive success, dashed lines are the limits of the 95% confidence interval. The red point points to the age (~ 160 years) beyond which reproductive success started to decrease.

4.4.3 The influence of climate sensitivity on reproductive success

Among the dendrophenotypic traits related to climate sensitivity, PrevT was the only one that positively influenced female reproductive success consistently across methods. In a context in which sampled trees showed an average slightly negative value of PrevT, such positive relationship between reproductive success and PrevT means that those trees that

responded more positively (or less negatively) to mean temperature of the previous vegetative season produced more offspring. Although Norway spruce has a very large among-site variation in its climate responses (Makinen *et al.*, 2002; Lebourgeois, 2007), an average negative climate-growth correlation with temperature of the previous summer has been often documented (*e.g.* Miina 2000; Makinen *et al.*, 2002; Carrer *et al.*, 2012). Such negative correlation can be partly explained by the fact that, in boreal trees, high temperature during the latter part of the previous summer promotes flowering during next summer (Tirén, 1935; Lindgren *et al.*, 1977; Pukkala *et al.*, 2010) and that significant growth reduction can be associated to these masting years (*e.g.* Chalupka *et al.*, 1975; Pukkala, 1987). However, it is essential to highlight that growth-climate correlations were generally calculated at the population level, thus preventing to depict the entire range of individual climate responses (Carrer, 2011). When such climate responses were investigated at the individual level, a large inter-individual variation was found (Carrer, 2011; Avanzi *et al.*, 2019). Among this wide spectrum of climate responses, my results pointed out that trees which better handle potential growth limitations due to the temperature of the previous vegetative season were the most successful in terms of lifetime fitness. As explained before, this might represent a mechanism to compensate the costs of reproduction (Tuomi *et al.*, 1983; Obeso, 2002) in Norway spruce.

4.4.4. Sex-specific strategies for increasing reproductive success

Differential effects of phenotypic traits on reproductive success between sexes have been rarely investigated in studies based on genetic markers, most of which aimed at assessing only male reproductive success by paternity analysis. Moreover, even in parentage-based studies high pollen immigration rates may strongly reduce the sample size of gametes assigned to local fathers thus impeding a thorough analysis of male selection gradients (*e.g.* González-Martínez *et al.*, 2006). A recent study evaluated the ecological determinants of male *vs*. female individual fecundities in three *F. sylvatica* stands by applying a Bayesian framework to paternity and parentage analyses (Oddou-Muratorio *et al.*, 2018a). These authors found that both female and male fecundities increased with tree size and decreased with density, but that the details of these effects were sex-specific. In fact, male fecundity was positively associated to the sum of diameters of stems of individual genets, while female fecundity to the diameter of the largest stem, suggesting that larger fecundities were achieved by sex-specific strategies. In particular, gains in male fecundity were achieved by incrementing tree crown (*i.e.* several small stems) to likely increase flower production and/or maximize pollen dispersal. By contrast, gains in female fecundity could require a larger

investment in both aerial and underground biomass (*i.e.* a bigger main stem) to increase resources for seed production.

In my study, I found that average BAI influence female and male reproductive success in a similar manner (*i.e.* with a similar slope, whatever the approach). On the other hand, the effect of age was sex-specific. There was a quadratic dependency with downward concavity for female reproductive success, whereas the relationship was linear and positive for male reproductive success. Although cone production does not decline with age in other conifers (*e.g.* Viglas *et al.*, 2013; Davi *et al.*, 2016), a similar senescence effect on reproductive success associated to the female function was interpreted in oaks as an age-related reduction of the seed crop (Moran and Clark, 2010), possibly due to the higher unit costs of seed *vs.* pollen production (Sato, 2004). Indeed, possible larger costs of seed production were also highlighted by the already discussed positive effect of PrevT on female reproductive success only. As seed production requires a substantial investment of resources, those mother trees that managed to develop a larger aerial and underground biomass, regardless potential growth limitations, might be the most successful in terms of lifetime fitness (Oddou-Muratorio *et al.*, 2018a).

4.4.5. Conclusions and outlook

Understanding the phenotypic basis of reproductive success is a crucial topic in evolutionary research. To this aim, combining parentage analysis with a dendrophenotypic characterization of putative parents offers the unique opportunity of linking forest trees' growth performances and their evolutionary gains. In order that results can be generalized at least at the regional scale, such approach has requirements that strongly limits its practical implementation. First, the experimental set-up is resource- and time-consuming and the low number of offspring assigned to local parents often limits further analyses on reproductive success (Younginger *et al.*, 2017). Secondly, if it is not properly replicated, it can only provide idiosyncratic evidence. A handful of multi-site studies aimed at elucidating phenotypic and ecological determinants of reproductive success were performed in broad-leaves (Moran and Clark, 2012; Piotti *et al.*, 2012; Bontemps *et al.*, 2013; Gauzere *et al.*, 2013; Gerber *et al.*, 2014; Oddou-Muratorio *et al.*, 2018a) and in conifers (Leonarduzzi *et al.*, 2016). Most well-replicated studies were focused on *F. sylvatica*, which is probably one of the most intensively studied species when dealing with reproductive dynamics in natural settings (Piotti *et al.*, 2012; Bontemps *et al.*, 2013; Gauzere *et al.*, 2013; Oddou-Muratorio *et al.*, 2018a). Such studies led to a thorough and generally coherent description of the species reproductive dynamics. Gathering results on replicated sites is the only way to move

from case-study evidence towards a generalization at the species level. Here, I have presented a detailed investigation of potential determinants of reproductive success in five natural populations of Norway spruce. By embracing the change in perspective suggested by recent dendrochronological literature to switch from a classical population-based approach to a deep individual-based exploration of growth dynamics (Carrer, 2011; Galvan *et al.*, 2014; Büntgen, 2019), a large set of dendrophenotypic traits were tested against reproductive success in order to *i*) decouple the effects of aging and tree growth rate and *ii*) evaluate the effects of climate sensitivity on reproductive success. The main findings of my work coherently suggest that, regardless the number of reproductive seasons they have been through, individuals with the highest lifetime fitness are those keeping general high growth rates and, in particular, when temperature of the previous vegetative season might be limiting. My study itself suffers from several limitations. The main one is that the five plots were not replicates in a statistical sense. Future investigations would certainly benefit from a careful selection of highly comparable sites (or altitudinal transects). Moreover, several factors that can shape dispersal dynamics were not considered (*e.g.* tree height, density of other species, intensity of competition, flowering phenology) thus leaving open questions about how they could interact with the phenotypic and ecological variables tested in this study. It should be noted that enlarging the number of covariates also requires a substantial increase of the sample size in order to ensure sufficient statistical power. Despite such potential refinements of the experimental set-up presented here, I deem that combining marker-based measures of fitness and a comprehensive set of dendrophenotypic traits is a fruitful strategy to gain deeper insights on reproductive dynamics of forest tree natural populations, thus increasing knowledge about the transmission of genetic information across generations in Norway spruce.

This Chapter resulted in a draft that we will soon submit to New Phythologist.

Chapter 5

Do SNP loci putatively under selection have an influence on individual reproductive success?

5.1 Introduction

Local adaptation plays a key role in driving populations toward phenotypic and genetic *optima* in response to local environmental conditions (Savolainen *et al.*, 2007). A population is indeed considered locally adapted whether it has a higher fitness in its own site than non-local populations originating from different sites (Clausen *et al.*, 1948; Kawecki and Ebert, 2004). Investigating whether and how natural populations are adapted to their habitats and predicting their potential to cope with future environmental changes are nowadays crucial issues, especially in the context of the ongoing climate change. Gathering this information is particularly urgent for forest tree species because of their key role in natural systems and for the ecosystem services they provide (Bonan, 2008; Allen *et al.*, 2010). In addition, being sessile, long-lived organisms with overlapping generations, they are potentially more vulnerable to shifts in ecological conditions (Kremer *et al.*, 2012). In fact, although there is strong evidence that forest tree populations are generally adapted to local climate (*e.g.* Savolainen *et al.*, 2007), their ability to timely respond to future climatic conditions is still debated (*e.g.* Jump and Peñuelas, 2005; Aitken *et al.*, 2008) as well as the genetic and physiological mechanisms involved in their responses to climate are still largely unknown (Aubin *et al.*, 2016; Housset *et al.* 2018).

The genetic signature of local adaptation can be identified by applying a variety of statistical methods (Vitti *et al.*, 2013). A first class of methods is represented by F_{ST}-based outlier detection tests. The rationale of such methods is that loci under divergent (or homogenizing) selection show larger (or lower) variation in allele frequencies among populations than neutral genomic regions (Lewontin and Krakauer, 1973). Therefore, potentially adaptive loci exhibiting larger or lower F_{ST} values than neutral expectations may be indicative of local adaptation. However, F_{ST}-based methods do not provide any clue about the selective pressures that may drive selection (Schoville *et al.*, 2012). For this purpose, environmental association analysis (EAA) has been proposed as a fruitful class of methods aimed at identifying genetic variants associated with environmental variables (reviewed in Rellstab

et al., 2015). By explicitly integrating environmental information into the analysis of genomic datasets, such methods have the potential for detecting even subtle adaptive patterns that may be not discovered by traditional F_{ST} -based tests (De Mita *et al.*, 2013; Rellstab *et al.*, 2015). Therefore, F_{ST}-based tests and EAA are considered complementary methods for the detection of genomic regions potentially under selection (De Mita *et al.*, 2013; de Villemereuil *et al.*, 2014). These two classes of methods have been widely used for the study of local adaptation in forest tree species, both separately (*e.g.* Sork *et al.*, 2010; Grivet *et al.*, 2011; Pluess *et al.*, 2016; Rellstab *et al.*, 2016) and in combination (*e.g.* Jump *et al.*, 2006; Eckert *et al.*, 2010; Brousseau *et al.*, 2016; Sork *et al.*, 2016; Cuervo-Alarcon *et al.*, 2018; Ruiz Daniels *et al.*, 2018).

Once loci putatively under selection have been identified, the subsequent step for elucidating their effective relevance in adaptive responses to climate change is their experimental validation (Barrett and Hoekstra, 2011; Savolainen *et al.*, 2013). In a pivotal study aimed at carrying out such validation approach in forest trees, Jaramillo-Correa *et al.* (2015) undertook these two steps (*i.e.* identifying molecular markers associated with climate in natural populations and testing their effect on fitness in controlled and/or natural conditions). To validate the 18 SNP loci found to be associated with climate in *Pinus pinaster* natural populations, they set up a common garden experiment at the hot and dry limit of the species ecological niche. They showed that the frequency of locally advantageous alleles was highly correlated to survival rates at the population level. Another promising approach to validate markers potentially under selection is studying temporal changes of genotypic frequencies, *i.e.* changes in allele frequencies in subsequent life stages (Cuervo-Alarcon *et al.*, 2018; Robledo-Arnuncio and Unger, 2018). In this context, parentage-based methods can offer the unique advantage of precisely reconstructing the genealogy of specific markers in their transmission across generations. This may provide additional insights with respect to mere comparison of individuals which are randomly sampled in subsequent age cohorts.

In this study, patterns of allele frequencies were explored across two study sites to detect signals of local adaptation in Norway spruce. In each site, both adult trees and seedlings were sampled at distinct elevations (*i.e.* low and high altitude in Germany; low, intermediate and high altitude in Italy) (**Table 1**). Such experimental design intercepts a large heterogeneity in environmental conditions, including differences in temperature and precipitation which influence Norway spruce growth performances (Miina, 2000; Lebourgeois, 2007; Carrer *et al.*, 2012). All individuals were genotyped with a set of 135 SNP loci that were putatively located in candidate genes involved in wood formation, growth and phenology (Chen *et al.*, 2012b; Pavy *et al.*, 2013; reviewed and selected by Heer *et al.*,

2016) (**Table 3**). My first aim was to identify candidate SNP loci potentially involved in adaptive responses both in adults and seedlings. To this purpose, an integrated approach based on two F_{ST}-based tests (BayeScan, Foll and Gaggiotti, 2008; *pcadapt*, Luu *et al.*, 2017) and one EAA method (Bayenv2, Coop *et al.*, 2010) was used to detect potential signatures of selection. SNP loci were considered potentially under selection when detected by at least two out of the three methods used. Then, my second and main aim was to assess whether these potential outlier SNP loci have any influence on individual fitness. To this purpose, individual reproductive success estimated through the analyses described in Chapter 4 was regressed against SNP genotypes through a GLM fitting.

5.2 Materials and methods

Study sites and datasets have been already presented in Chapter 2, sections 2.2, 2.3, 2.4. In the following paragraphs, I will describe the environmental variables used for EAA (5.2.1) and the three methods used to detect signatures of local adaptation (5.2.2). After that, the influence of SNP genotypes on reproductive success was assessed. Such evaluation was made both at *i*) single SNP level by modelling reproductive success as a function of locus that were found to be potentially under selection (5.2.3) and *ii*) at the dataset level by applying a variance partitioning approach to evaluate the relative contribution of the entire set of SNP loci on individual reproductive success (5.2.4).

5.2.1 Environmental variables

Climatic data for the reference period 1901-2013 were used as proxies for the selective pressures imposed by climate on adult trees, whereas climatic data for the reference period 1980-2013 were used for the seedlings. The environmental variables included latitude, longitude and altitude, as well as annual and growing season total precipitation, and annual and growing season mean, maximum and minimum temperature (**Table 13**). Spearman's rank correlation between all pairs of environmental variables were calculated.

5.2.2 Signatures of local adaptation at SNP loci

Both F_{ST} outlier tests and EAA were used to detect SNP loci that may be putatively under selection. All methods that will be described here were applied on adults and seedlings separately. Individuals that resulted admixed from the STRUCTURE analysis on SSR genotypes (*i.e.* q_1 >0.2 and <0.8) (**Fig. 5**) were removed from the dataset, that was made up of 369 adults and 454 seedlings (**Table 2**).

Table 13. Summary of the environmental variables used for environmental association analysis (EAA).

Abbreviation	Description
Lat	Latitude
Lon	Longitude
Alt	Altitude
MeanAT	Mean annual temperature (°C)
MaxAT	Maximum annual temperature (°C)
MinAT	Minimum annual temperature (°C)
MeanGST	Mean temperature of the growing season[a] (°C)
MaxGST	Maximum temperature of the growing season (°C)
MinGST	Minimum temperature of the growing season (°C)
TotAP	Total annual precipitation (mm)
TotGSP	Total precipitation of the growing season (mm)

[a]From April to October

Two different methods were applied for the detection of F_{ST} outlier SNP loci, one based on a Bayesian approach and the other on a principal component analysis (PCA). The first method is implemented in the BayeScan v2.1 software (Foll and Gaggiotti, 2008). It assumes an island model where each population diverged from an ancestral gene pool from which it shows a certain degree of genetic differentiation, measured by a F_{ST} coefficient. The method decouples the F_{ST} coefficients into a population-specific effect (β), shared by all loci, and a locus-specific effect (α), shared by all populations. The presence of selection is inferred if the locus-specific effect is necessary to explain the observed divergence. Positive and negative values of α suggest diversifying and balancing selection, respectively. BayeScan implements these two alternative models (with and without selection, that is with or without α, respectively) within a Bayesian framework, using a reversible-jump MCMC algorithm to estimate the posterior probabilities of both models. Here, MCMC was made up of 20 pilot runs of 1×10^4 iterations each, followed by a burn-in of 5×10^4, a sample size 5×10^4 and a thinning of 10 and 20 for adults and seedlings, respectively. Prior odd was set to 10, indicating that the neutral model is 10 times more likely than the model with selection. A value of 10 is considered reasonable for the identification of candidate loci within a few hundreds of markers, according to manual instructions. SNP loci were considered outlier whether they showed a significant effect of α under a false discovery rate (FDR) threshold of 0.05.

The second method used for the detection of F_{ST} outliers is implemented in the R package *pcadapt* (Luu *et al.*, 2017). It accounts for population structure through PCA, which is particularly advantageous when there is evidence of gene flow across populations like in forest tree species (De Mita *et al.*, 2013). The rationale behind *pcadapt* is that differences in

allele frequencies among populations, caused by positive selection, are mirrored in differences in PCA loadings contributed by different loci. Preliminarily, the number of principal component (PC) to be retained (K) was defined by running a PCA with a large number of PCs (20 in our case). The best K was chosen as the one showing most of the cumulative explained variance, by plotting the percentage of variance explained by each PC in decreasing order (*i.e.* scree plot). Such choice was confirmed by plotting individuals on the first two PCs (*i.e.* score plot) to verify if the grouping is consistent with the chosen K. After this preliminary steps, PCA was run setting the number of PCs to the optimal K value. Alleles with minor allele frequency (MAF) <5% were removed from the analysis. The Mahalanobis distance was used to detect outlier SNPs. A FDR of 0.05 was applied to avoid false positives, by using the R package *qvalue* (Storey *et al.*, 2015).

For EAA, the correlation between environmental variables and allelic frequencies at SNP loci was evaluated using the Bayesian method implemented in the software Bayenv2 (Coop *et al.*, 2010; Gunther and Coop, 2013). This method tests for associations, while explicitly integrating a covariance matrix of allele frequencies in the model. This allows to explicitly take into account the among-population allele frequency correlations due to neutral processes. Here, the covariance matrix was calculated as the mean of 20 covariance matrices estimated from 20 independent runs of 2×10^6 iterations each. The correlation between such covariance matrix and that of pairwise F_{ST} was calculated to check whether the covariance matrix well represented the true variance of allele frequencies across populations. Bayes factors (BF) were calculated for each SNP against each environmental variable using 1×10^5 iterations and the covariance matrix as null model. This approach was repeated five times to account for instability between runs (Blair *et al.*, 2014). The cut-off for significant BF was set to the 99th percentile of the BF distribution. All SNPs with BF greater than such threshold were considered significantly associated with the corresponding environmental variable. The strength of such associations was evaluated by applying the Jeffreys' scale of evidence for BF (*i.e.* 3≤ BF ≤10 = substantial selection; 10≤ BF ≤30 = strong selection; 30≤ BF ≤100 = very strong selection; BF >100 = decisive selection) (Jeffreys, 1961).

Results of the three methods (BayeScan, *pcadapt*, Bayenv2) were compared across methods and generations. methods with different demographic assumptions can be used and compared, so that common loci detected in consensus are more likely to be real target of selection (Li *et al.*, 2012). Here, SNPs that were detected by at least two methods out of the three used were considered as likely candidates of loci under selection. For these SNPs, genotype frequencies at the plot level were calculated to investigate whether there were similar patterns across or within study sites.

5.2.3 The effect of SNP loci potentially under selection on reproductive success

Individual reproductive success was calculated from the parentage assignments obtained by the final run of the neighbourhood model (see 4.2.2). The parameters included in this final model were genotyping errors, seed and pollen immigration rates, scale parameter of the seed dispersal kernel (**Table 10**) as well as some selection gradients (**Table 11**). SNPs detected by at least two of the methods described in 5.2.2 were investigated as potential determinants of individual total (ω), maternal (ψ) and paternal (φ) reproductive success. This relationship was assessed by fitting a GLM with negative binomial error distribution to account for overdispersion. The starting models were the following:

$$\omega, \psi, \varphi \sim Age + (SNP * Plot) + SNP^2 + \varepsilon. \qquad (13)$$

Different types of selection (*e.g.* directional, balancing or diverging) were modelled by including both a linear and a quadratic term of the individual genotype at the given candidate locus (SNP and SNP^2), expressed in terms of allelic doses. Tree age was added to take into account the number of reproductive opportunities that each tree had throughout its lifetime, while plot to account for differences among plots. An interaction term between the candidate locus and the plot (SNP:plot) was included to assess if genotypes had different effects across plots. Analyses were performed by using the *glm.nb* function of the R package *MASS* (Venables and Ripley, 2002) in the R suite. To avoid collinearity problems, the variance inflation index (VIF) was calculated for each variable of (13) using the R package *car* (Fox and Weisberg, 2011). The variable with the highest VIF was sequentially dropped from the starting model until all variables had VIF values <5 (Zuur *et al.*, 2010). The optimal model was selected using the *Anova* function of the R package *car*. Variables were dropped whether the Likelihood Ratio Test on nested models indicated that a simpler model structure was more parsimonious.

5.2.4 Relative contribution of the entire set of SNP loci on reproductive success

A variance partitioning approach (Legendre and Legendre, 2012) was used to evaluate whether the entire set of SNP loci had an overall influence on individual total, maternal and paternal reproductive success. The rationale of such approach is to assess the relative contribution of different sets of explanatory variables on a response data table. Here, three sets of explanatory variables were considered, that is *i*) genetic structure (*Gen*), *ii*) spatial structure (*Spat*) and *iii*) phenotypic characteristics (*Phen*) (**Fig. 24**). Genetic structure was included through a PCA on SNP genotypes, using the *dudi.pca* function of the R package *adegenet* (Jombart and Ahmed, 2011). In each plot, only PCs accounting for >70% of the

variance in genotypes were used. Spatial structure was modelled by a distance-based Moran's eigenvectors map (dbMEM, Dray *et al.*, 2006), which has been proposed as a powerful and informative method of spatial analysis by Legendre *et al.* (2015). In each plot, only the statistically significant eigenfunctions modelling positive spatial autocorrelation, as estimated by the *mem* function of the R package *adespatial* (Dray *et al.*, 2018), were retained. Phenotypic characteristics were modelled by using tree age and average BAI, which were the most relevant dendrophenotypic features influencing reproductive success according to the results of the previous chapter. The relative contribution of genetic and spatial structure as well as phenotypic characteristics in explaining the variance of individual reproductive success was assessed using the *varpart* function of the R package *vegan* (Oksanen *et al.*, 2018), following the procedure described in Borcard *et al.* (2011). Such relative contributions were expressed in terms of adjusted R^2 according to Ezekiel's formula (Ezekiel, 1930), which is:

$$R^2_{adj} = 1 - \frac{(n-1)}{(n-m-1)}(1 - R^2) \qquad (14)$$

where n is the number of observations and m is the number of explanatory variables (*i.e.* the degrees of freedom of the model). Ezekiel's adjustment can be used as long as n is much larger than m (Borcard *et al.*, 2011). When $m > n/2$ this adjustment may be excessively conservative and the R^2 value not reliable. Significance of the variance components was calculated through ANOVA-like permutation test for redundancy analysis (RDA) and partial redundancy analysis pRDA based on 1×10^4 permutations (Legendre and Legendre, 2012).

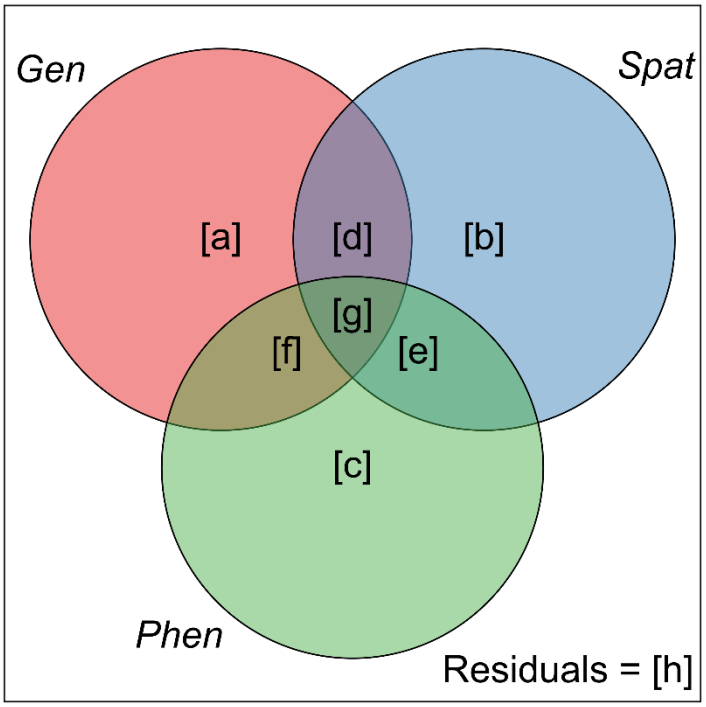

Fig. 24 Conceptual representation by Venn diagram of the variance partitioning of a response table by three sets of explanatory variables (*Gen*: genetic structure; *Spat*: spatial structure; *Phen*: phenotypic characteristics). The relative contribution of each of these three sets of explanatory variables are represented by [a], [b] and [c] fractions, respectively. [d], [e], [f] fractions represent the amount of variation explained jointly by two sets of variables, while [g] the one explained by all three sets. The amount of unexplained variance (Residuals) is represented by [h].

5.3 Results

5.3.1 Relationships between environmental variables

Spearman's rank correlation coefficients between environmental variables calculated on the two reference periods (1901-2013 and 1980-2013) were strongly consistent (**Fig. 25**).

Annual and growing season total precipitation were significantly positively correlated to each other. In addition, they were significantly negatively correlated with longitude and latitude, while positively with altitude. The annual mean, maximum and minimum temperatures were strongly correlated with those of the growing season.

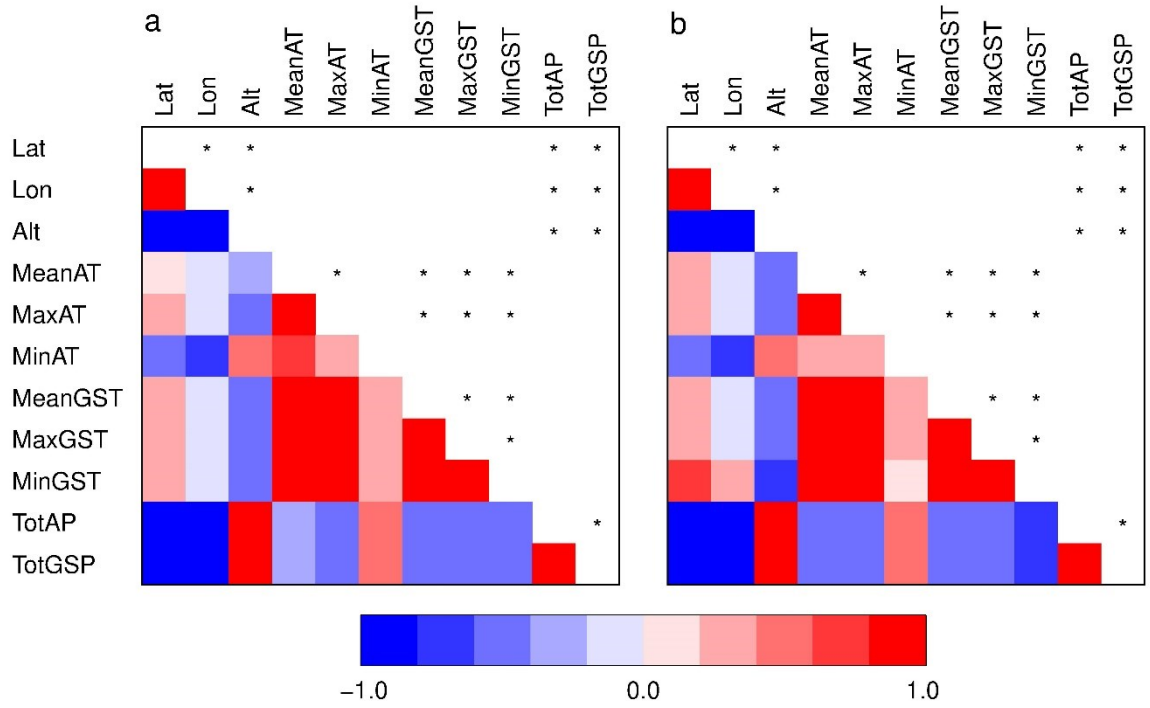

Fig. 25 Spearman's rank correlation coefficient matrices for environmental variables for the reference periods 1901-2013 (**a**) and 1980-2013 (**b**). Correlation coefficients are reported below the diagonal, while the corresponding P values that were <0.05 are reported above and indicated with an asterisk (*).

5.3.2 Signatures of local adaptation at SNP loci

Three and four outlier SNP loci were identified by BayeScan for adults and seedlings, respectively. (**Fig. 26**). For all these seven loci, α values were positives, thus indicating diversifying selection (**Table 14**).

Table 14 Summary statistics of the outlier SNP loci identified by BayeScan.

Stage	ID	SNP	$\log_{10}$PO	prob	*q* value	alpha
Adults	36	GQ02805.H15.1.75	1.000	1.000	0.000	1.631
	52	GQ03209.H09.1.774	0.978	1.656	0.011	1.271
	109	SB18.686	0.884	0.882	0.046	1.272
Seedlings	29	GQ0046.B3.E02.1.777	0.881	0.868	0.044	1.181
	36	GQ02805.H15.1.75	1.000	1.000	0.000	1.615
	52	GQ03209.H09.1.774	0.966	1.456	0.019	1.226
	62	GQ03702.D08.1.1408	0.976	1.617	0.012	1.306

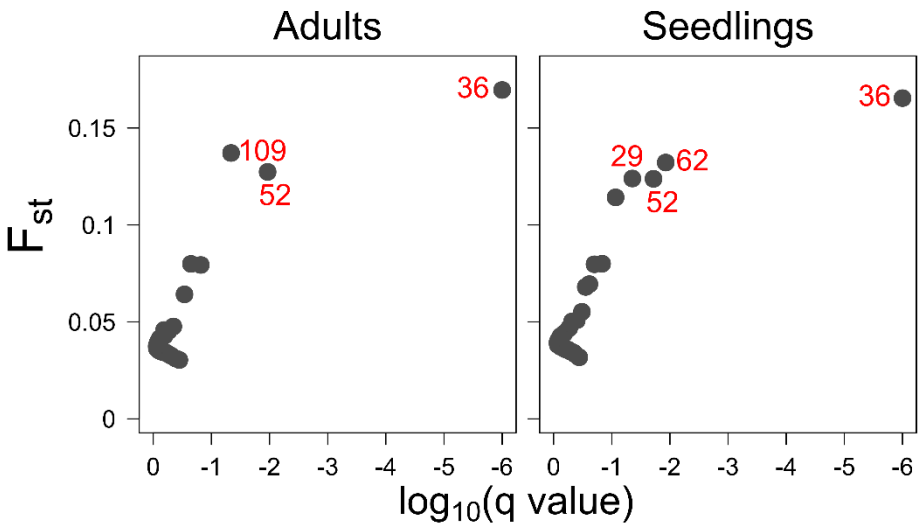

Fig. 26 Results of the outlier detection made by BayeScan. Outlier SNP loci are reported in red. SNP loci were considered outlier whether they showed a significant effect of α under a false discovery rate (FDR) threshold of 0.05.

Three and 16 outlier SNP loci were identified by *pcadapt* for adults and seedlings, respectively (**Fig. 27c**; **Table 15**). Even if scree and score plots indicated K=1 and K=2 as the grouping explaining most of the variation of adult and seedling genotypes, respectively (**Fig. 27a**,**b**), K was set to 2 for both adults and seedlings to account for the results of the Bayesian clustering that showed an optimal grouping at K=2 (**Fig. 5**).

Table 15 Summary statistics of the outlier SNP loci identified by *pcadapt*.

Stage	ID	SNP	P value
Adults	22	FCL1947Contig1.1181	6.1×10^{-6}
	52	GQ03209.H09.1.774	8.0×10^{-17}
	68	GQ03912.E20.1.589	1.2×10^{-10}
Seedlings	2	08Pg04341e.2	1.3×10^{-8}
	8	c89584.g2.i1.197	1.2×10^{-6}
	22	FCL1947Contig1.1181	4.6×10^{-8}
	23	FCL2232Contig1.745	1.7×10^{-7}
	32	GQ01312.B05.2.453	1.3×10^{-5}
	36	GQ02805.H15.1.75	1.4×10^{-4}
	41	GQ02907.H19.1.164	1.5×10^{-7}
	43	GQ03104.H16.1.718	8.3×10^{-6}
	51	GQ03201.F12.1.693	2.2×10^{-3}
	52	GQ03209.H09.1.774	4.8×10^{-11}
	68	GQ03912.E20.1.589	8.4×10^{-3}
	88	P3747.3	6.9×10^{-3}
	95	paP08075.2	7.0×10^{-8}
	98	PBB.PF02309.12.1	7.0×10^{-3}
	103	PGLM2.0624	4.7×10^{-4}
	108	SB18.506	5.8×10^{-6}

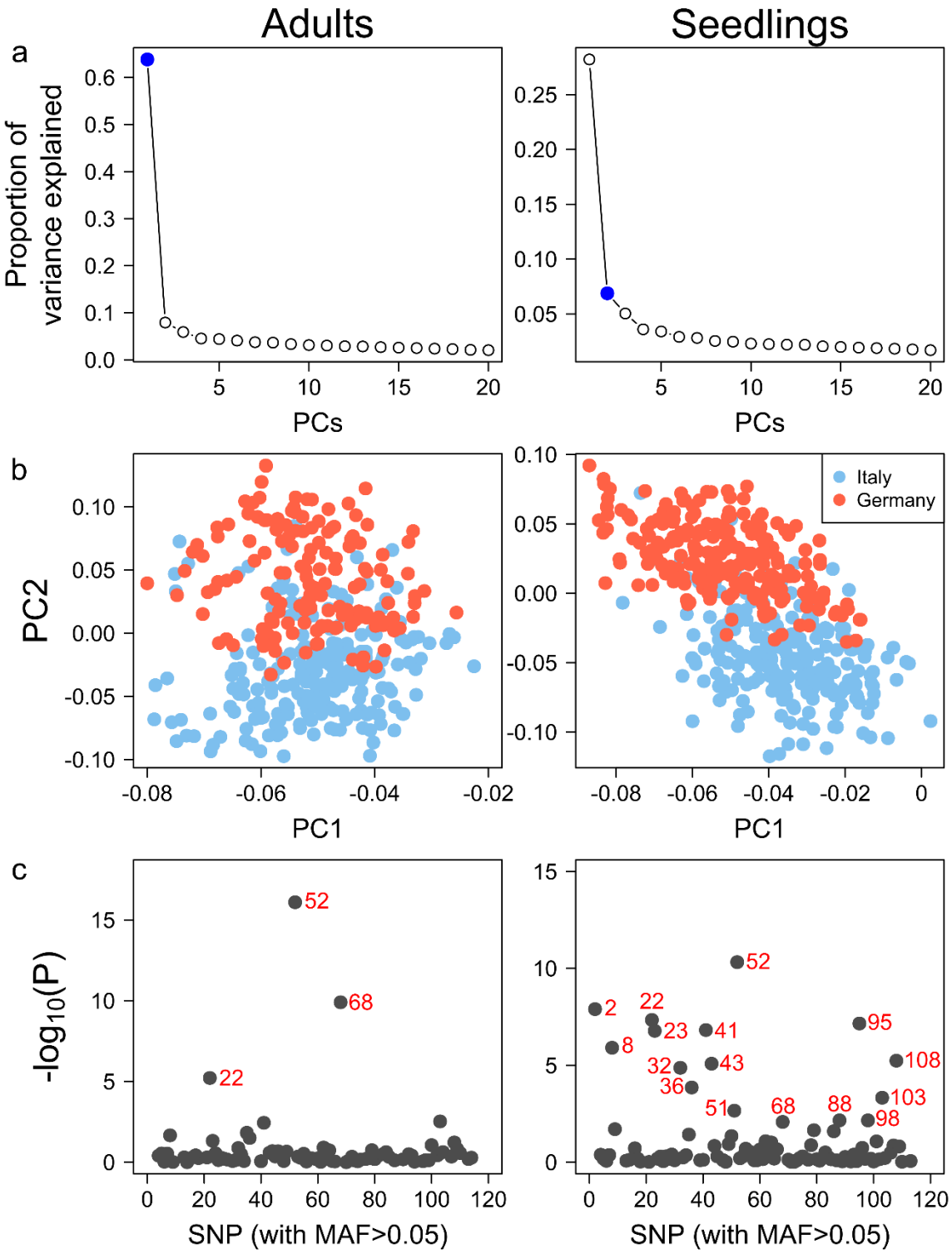

Fig. 27 (**a**) Scree plots showing the percentage of variance explained by each of the 20 PCs tested. (**b**) Score plots showing the projection of the individuals onto the first two PCs. Individuals are colour-coded according to the study site (Italy: light blue; Germany: salmon). (**c**) Manhattan plots showing which SNP loci were considered outlier after applying a FDR of 0.05.

The correlation between the covariance matrix calculated by BayEnv2 and that of pairwise F_{ST} was equal to -0.90 (P <0.001) and to -0.91 (P <0.001) for adults and seedlings, respectively. Such high correlation coefficients proved that both covariance matrices well

represented the true variance of allele frequencies across populations. The 99th percentile of the BF distribution gave me a cut-off value of BF equal to 4.91 and 3.54 for adults and seedlings, respectively. Based on such thresholds, a total of 26 statistically significant SNP-environmental variable associations were identified (**Table 16**), for a total of seven SNPs involved. Annual and growing season total precipitation (TotAP, TotGSP) and minimum annual temperature (MinAT) were found in several of these 26 significant associations. The other significant associations concerned latitude, longitude and altitude, which were highly correlated with TotAP, TotGSP and MinAT (**Fig. 25**).

Table 16 SNP-environmental variable significant associations identified by Bayenv2.

Stage	ID	SNP	Variable	BF	Jeffreys' scale
Adults	36	GQ02805.H15.1.75	Lat	13.67	Strong
			Lon	13.41	Strong
			Alt	8.61	Substantial
			TotAP	14.08	Strong
			TotGSP	13.67	Strong
	52	GQ03209.H09.1.774	Lat	6.48	Substantial
			Lon	6.59	Substantial
			MinAT	5.52	Substantial
			TotAP	5.39	Substantial
	104	PGLM2.0690	MinAT	5.01	Substantial
	109	SB18.686	Alt	6.67	Substantial
			TotAP	5.83	Substantial
			TotGSP	6.82	Substantial
Seedling	29	GQ0046.B3.E02.1.777	Lat	3.60	Substantial
	36	GQ02805.H15.1.75	Lat	10.38	Strong
			Lon	10.35	Strong
			Alt	5.09	Substantial
			TotAP	9.75	Substantial
			TotGSP	8.17	Substantial
	52	GQ03209.H09.1.774	Lat	4.42	Substantial
			Lon	4.39	Substantial
			TotAP	3.85	Substantial
	62	GQ03702.D08.1.1408	Lat	4.31	Substantial
			Lon	4.39	Substantial
			MinAT	6.67	Substantial
	115	WS00841.F23.1.82	Lon	3.54	Substantial

Comparing the results from *pcadapt*, BayeScan and Bayenv2 (**Fig. 28**), three and four SNPs were identified as potential loci under selection by at least two methods in adults and seedlings, respectively (**Table 17**). Of these SNPs, two loci were consistently identified both

in adults and seedlings (SNP36, SNP52). Genotype frequencies at the plot level were represented in **Fig.29**.

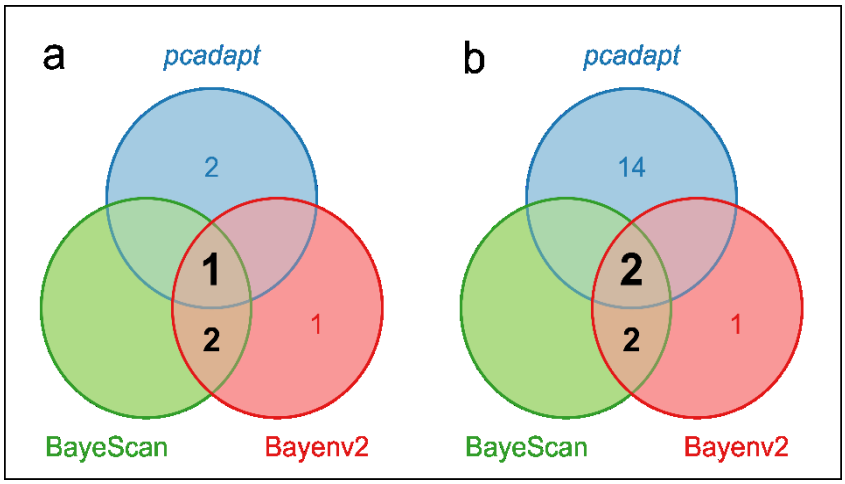

Fig. 28 Number of SNP loci that were found to be likely under selection in (**a**) adults and (**b**) seedlings, according to the results of the three methods used. The representation through Venn diagram allowed to highlight how many SNP loci were in common across methods.

Table 17 SNP loci that were found to be likely under selection with at least two of the three methods used to investigate signatures of local adaptation.

Stage	ID	SNP	Method
Adults	52	GQ03209.H09.1.774	*pcadapt*, BayeScan, Bayenv2
	36	GQ02805.H15.1.75	BayeScan, Bayenv2
	109	SB18.686	BayeScan, Bayenv2
Seedlings	36	GQ02805.H15.1.75	*pcadapt*, BayeScan, Bayenv2
	52	GQ03209.H09.1.774	*pcadapt*, BayeScan, Bayenv2
	29	GQ0046.B3.E02.1.777	BayeScan, Bayenv2
	62	GQ03702.D08.1.1408	BayeScan, Bayenv2

5.2.3 The effect of SNP loci potentially under selection on reproductive success

None of the three SNPs that were found to be likely under selection in adults (SNP52, SNP36, SNP109; **Table 17**) had a significant effect on total, maternal and paternal reproductive success. In all cases, the best model included only age and plot variables.

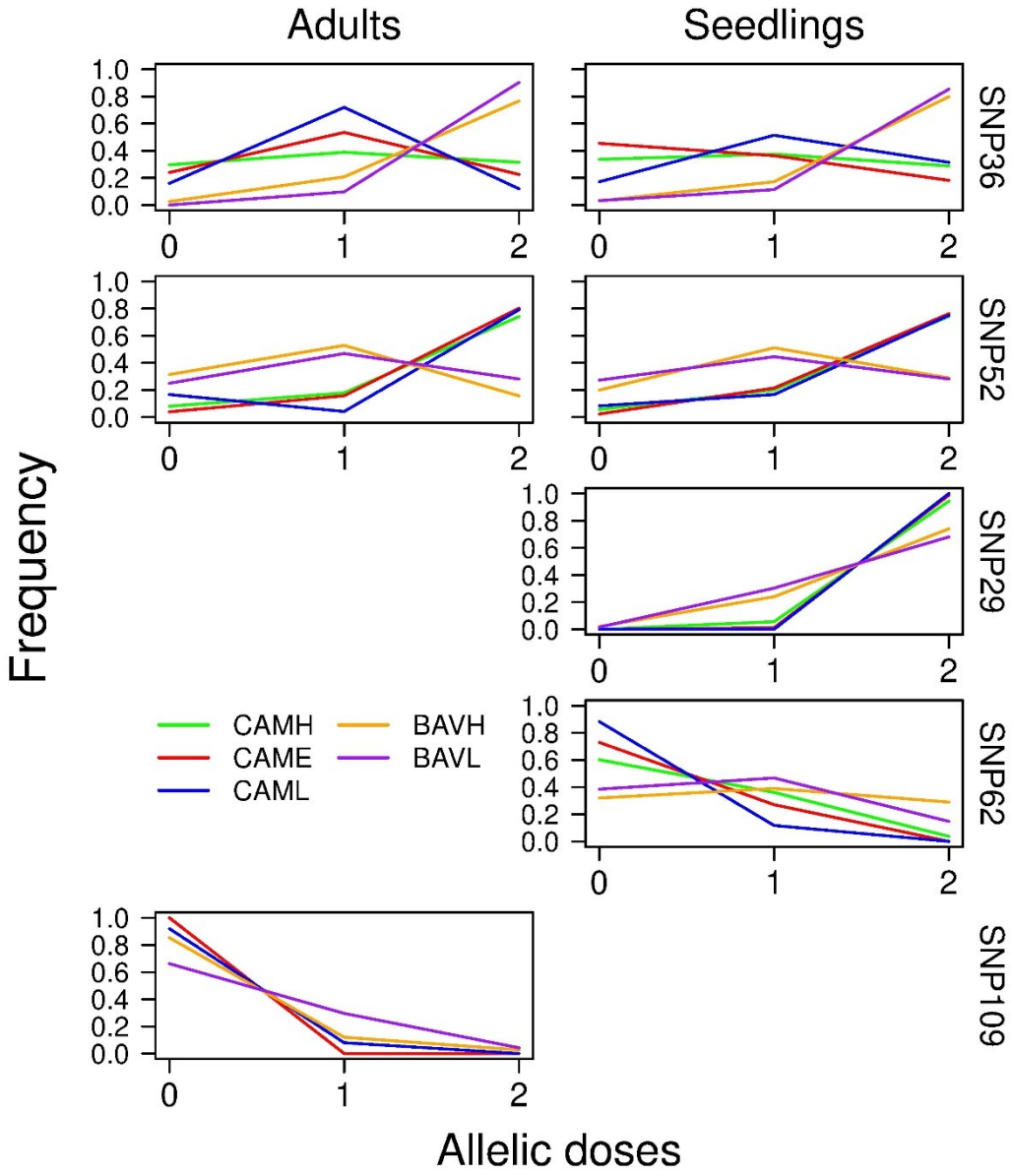

Fig. 29 Genotypic frequencies of the SNP loci putatively under selection in the five plots. SNP36 and SPN52 were detected in both adults and seedlings, while the other three loci only in one of the two life stages.

5.2.4 Relative contribution of the entire set of SNP loci on reproductive success

Overall, the genetic structure at SNP loci explained a low proportion of the variance of individual reproductive success (adjusted R^2 ranging from -0.18 to 0.16; **Table 19**), and its effect was never statistically significant (**Fig. 30a**). Similarly, the contribution of spatial structure was also quite low (adjusted R^2 ranging from -0.06 to 0.18; **Table 19**) but statistically significant ($P < 0.05$) in four cases out of 15 and marginally significant ($P < 0.1$) in one case (**Fig. 30b**). On the contrary, the most relevant contribution is that of phenotypic characteristics (adjusted R^2 up to 0.55; **Table 19**), whose effect was statistically significant ($P < 0.05$) in six cases out of 15 and marginally significant ($P < 0.1$) in 3 cases (**Fig. 30c**).

Table 19 Adjusted R^2 values estimated through a variance partitioning approach. These values represent the relative contribution of genetic and spatial structure as well as phenotypic characteristics in explaining the variance of total, maternal and paternal reproductive success (RS).

Individual fractions	Plot	*n*	*m*	*m* > *n*/2?[a]	Adjusted R^2 for total RS	Adjusted R^2 for maternal RS	Adjusted R^2 for paternal RS
[a]	CAMH	113	30	yes	0.06031	0.06772	-0.17833
[b]			8	yes	0.02156	0.06461	-0.05804
[c]			2	yes	0.03834	0.03472	0.01437
[d]			0		-0.03588	-0.03864	0.00033
[e]			0		-0.01984	-0.01188	-0.00967
[f]			0		-0.04543	-0.03850	-0.03192
[g]			0		0.03135	0.01607	0.01886
[h]					0.94959	0.90590	1.24440
[a]	CAME	77	23	yes	-0.04827	-0.03373	-0.03640
[b]			6	yes	0.15442	0.18154	0.11541
[c]			2	yes	0.33685	0.41114	0.12983
[d]			0		0.06712	0.06930	-0.00126
[e]			0		-0.09499	-0.19163	0.00493
[f]			0		-0.06529	-0.14728	0.02520
[g]			0		-0.03540	0.01842	-0.03987
[h]					0.68556	0.69223	0.80216
[a]	CAML	25	12	no	-0.04592	-0.07338	-0.07687
[b]			4	yes	0.02173	0.00108	0.07258
[c]			2	yes	0.49883	0.54902	-0.07171
[d]			0		0.10617	0.10810	-0.00037
[e]			0		0.31417	0.26045	0.40297
[f]			0		-0.18349	-0.23913	0.20265
[g]			0		-0.37456	-0.31879	-0.42843
[h]					0.66305	0.71266	0.89918
[a]	BAVH	77	27	yes	-0.00419	0.01688	0.07313
[b]			5	yes	-0.00038	0.00992	-0.06367
[c]			2	yes	0.16609	0.14135	0.10320
[d]			0		0.07506	0.07295	0.04707
[e]			0		-0.00974	-0.01300	0.01488
[f]			0		-0.10849	-0.11065	0.02380
[g]			0		0.01568	0.02062	-0.01251
[h]					0.86597	0.86194	0.81410
[a]	BAVL	53	19	yes	0.06429	0.05768	0.15870
[b]			4	yes	0.15591	0.08964	0.13912
[c]			2	yes	-0.02588	-0.02408	-0.01599
[d]			0		0.02343	0.08336	-0.11754
[e]			0		0.08753	0.05069	0.13702
[f]			0		0.01492	0.00959	-0.00554
[g]			0		-0.01987	-0.00190	-0.08688
[h]					0.69967	0.73503	0.79111

[a]Ezekiel's formula (Ezekiel 1930) for "adjusting" the R^2 can be used as long as the degrees of freedom of the model (*m*) are much smaller with respect to the number of observations (*n*). Here, I reported whether our data follow the rule of thumb reported in Borcard *et al.* (2011), that is that *m* should not exceed *n*/2.

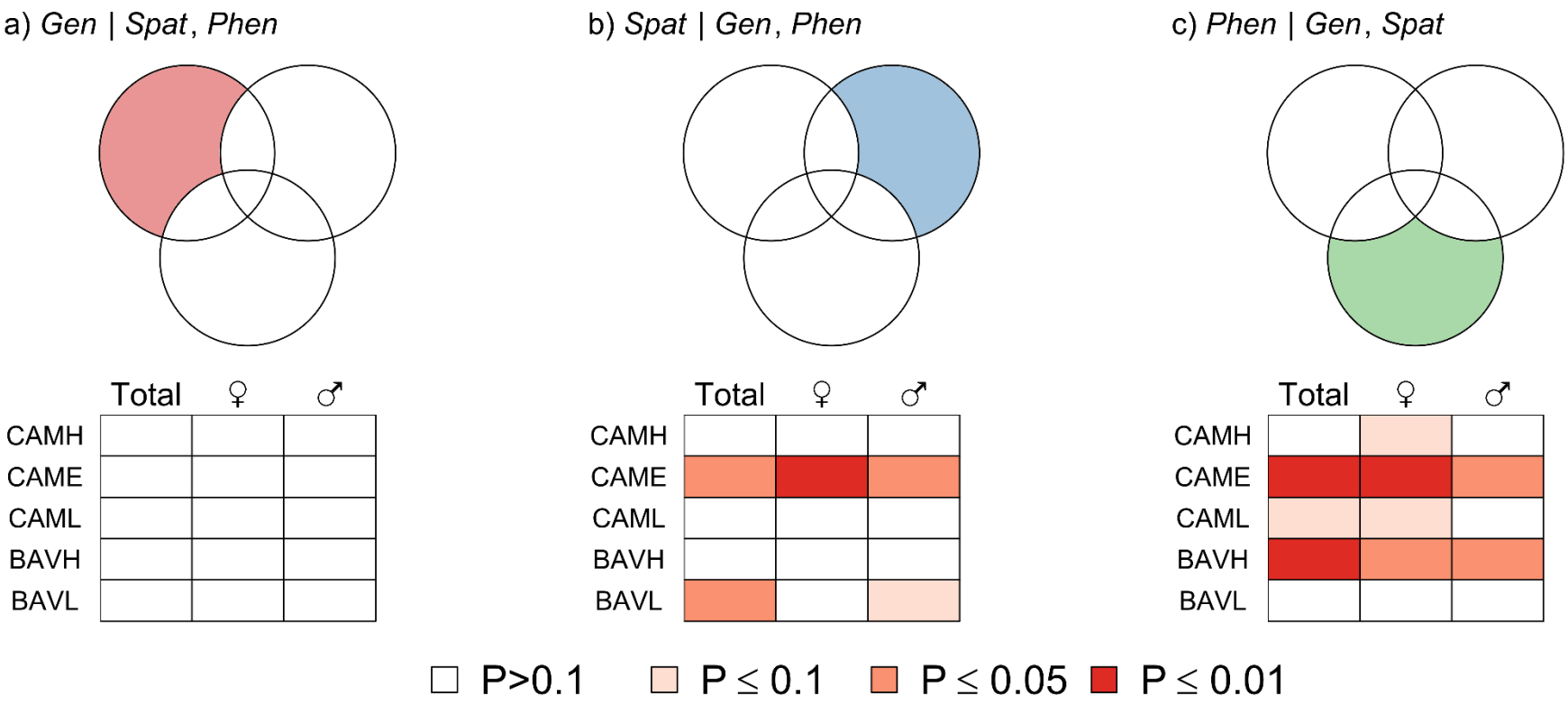

Fig. 30 (**a**) Effect of genetic structure (*Gen*) on total, maternal and paternal reproductive success while controlling for spatial structure (*Spat*) and phenotypic characteristics (*Phen*). (**b**) Effect of spatial structure (*Spat*) while controlling for genetic structure (*Gen*) and phenotypic characteristics (*Phen*). (**c**) Effect of phenotypic characteristics (*Phen*) while controlling for genetic (*Gen*) and spatial structure (*Spat*). Statistical significance of the variance components, assessed through ANOVA like permutation tests for partial redundancy analysis (pRDA), is reported in the heat maps.

5.4 Discussion

In the present chapter, I investigated the adaptive genetic variation of Norway spruce natural populations in order to detect genomic regions potentially under selection. The three methods used to detect signals of local adaptation (*e.g.* two F_{ST}-based tests and one EAA) identified different sets of outlier SNPs, but partly overlapping. In particular, three and four SNPs were detected as putative loci under selection in adults and seedlings, respectively. Two SNPs were consistently identified as markers putatively under selection both in adults and seedlings. Along with such a handful of SNP loci, I identified the environmental variables that are potentially driving the adaptive process, *i.e.* annual and vegetative season total precipitation and minimum annual temperature. Finally, I regressed individual reproductive success against the genotypes at these SNP loci that were likely under selection. No significant relationship between such SNP loci and individual reproductive success was found.

Forest tree species have recently received extensive attention regarding local adaptation and landscape genomics. In conifers, there are several studies aimed at identifying loci which are likely involved in adaptive responses to environmental selective pressures (*e.g.* Namroud *et al.*, 2008; Eckert *et al.*, 2009, 2010; Grivet *et al.*, 2011; Mosca *et al.*, 2012, 2014; Prunier *et al.*, 2012; Brousseau *et al.*, 2016; Ruiz Daniels *et al.*, 2018). Among them, some focused their investigations precisely on the adaptive genetic variation of Norway spruce (Chen *et al.*, 2012, 2016; Karlgren *et al.*, 2013; Kallman *et al.*, 2014; Scalfi *et al.*, 2014; Di Pierro *et al.*, 2016). For instance, Scalfi *et al.* (2014) genotyped 27 Norway spruce populations located in central and south-east Europe with a set of 384 SNPs. At such spatial scale and by integrating F_{ST}-based tests and environmental associations, these authors identified six SNPs as putatively under selection markers and confirmed previous evidence that temperature is a relevant variable in driving the selective process in conifers (Eckert *et al.*, 2010; Wang *et al.*, 2010; Alberto *et al.*, 2013). The same set of SNPs of Scalfi *et al.* (2014) was also used by Di Pierro *et al.* (2016), who genotyped 24 natural populations across the Italian part of the species range. In this work, 13 SNPs were overall detected as potentially under selection loci, three of which have already been found by Scalfi *et al.* (2014) at a broader spatial scale. In this second study, precipitation was significantly associated to population genotype frequencies, thus emerging as a relevant variable in shaping Norway spruce adaptive responses. In my study, I genotyped five Norway spruce populations from central and south-east Europe with an initial set of 135 SNPs. Although the number of populations was much lower with respect to the above-mentioned studies, it should be noted that the number of individuals per population were generally higher in my study (N ranging from 25 to 123),

leading to overall comparable sample sizes. None of the SNPs that I found to be likely under selection has been reported as putative outlier in previous studies performed in Norway spruce. However, the SNP datasets used in this kind of studies often poorly overlapped, preventing correct comparisons of the results. Nevertheless, I found that genotype frequencies were mainly associated to annual and growing season total precipitation (TotAP, TotGSP) and minimum annual temperature (MinAT). TotAP and TotGSP were themselves highly correlated, meaning that the genotype-environment correlations probably intercepted the same signal. On the contrary, MinAT was weakly related to both TotAP and TotGSP. Such evidence suggested that both temperature and precipitations were relevant in shaping Norway spruce adaptive responses. This might be linked to the fact that the species is sensitive to soil water supply (Sutinen *et al.*, 2002) and to early spring temperatures regulating bud burst (Partanen *et al.*, 1998).

Of the five SNPs detected as putatively under selection loci, only SNP29 and SNP62 were successfully found to be in annotated genes. Such information was derived from Heer *et al.* (2016) that analysed 3257 SNPs selected from various SNP resources and annotated them using *P. abies* reference genome (Nystedt *et al.*, 2013). SNP62 (GQ03702.D08.1.1408) was found to be in the gene sequence MA.10228148g00100, which encodes for a transcriptional regulator factor (TRAF). In mammals, TRAF proteins are involved in protein processing and ubiquitination and in immune activation and responses to stresses as well (Zapata *et al.*, 2007) while their biological roles are poorly defined in plants. In *Arabidopsis thaliana*, Huang *et al.* (2016) identified two TRAF proteins (MUSE13 and MUSE14) that took part in regulating a complex molecular pathway involved in pathogen resistance, autoimmunity and homeostasis maintenance. On the other hand, SNP29 (GQ0046.B3.E02.1.777) was found within the gene sequence MA.10426168g0010, that encodes for an AA2 protein (PlantCAZyme; Ekstrom *et al.*, 2014). This family of proteins contains lignin-modifying peroxidases that catalyses a large number of oxidative reactions. Although the molecular mechanisms are still poorly uderstood, there is some evidence that this protein family may increase the expression of defensive mechanisms against pathogens in plants (Stintzi *et al.*, 1993; Karthikeyan *et al.*, 2005).

Although selected among candidate genes putatively involved in wood formation, growth and phenology (Chen *et al.*, 2012b; Pavy *et al.*, 2013; Heer *et al.*, 2016), the number of genetic markers tested in this work was low (135 SNPs). However, it should be noted that the genomic resources available were quite limited for conifers. For instance, the first conifer genome assemblies were published only recently (Norway spruce: Nystedt *et al.*, 2013; white spruce: Birol *et al.*, 2013; loblolly pine: Zimin *et al.*, 2014), because of their enormous

genome sizes (20-30 Gb) and high number of repetitive sequences. The road toward fully assembled and annotated conifer genomes still presents significant technological challenges (De La Torre *et al.*, 2014). Another limitation of this study was the fact that the five plots were not true replicates in a statistical sense. Future investigations would certainly benefit from a careful selection of highly comparable altitudinal transects, involving a higher number of population replicated across a broad spatial scale. As an example, Brosseaux *et al.* (2016) fruitfully investigated patterns of local adaptation to altitude in silver fir by analysing nine populations pairs (low *vs.* high elevation) along the southern edge of the species range.

Despite these limitations, the most relevant aspect of this work lies in the opportunity of testing putatively under selection loci against individual reproductive success. Both GLM fitting and variance partitioning consistently showed that reproductive success was strongly associated with the phenotypic features included in the analyses (*i.e.* age and average BAI), confirming the results of Chapter 4. Also micro-environmental variation had a marginal influence, at least in some stands, partially confirming the results of Chapter 3. On the contrary, there is no evidence that any SNP loci influenced individual reproductive success. This lack of statistical evidence may be partially due to the fact that genotype frequency data at SNP loci may suffer from heteroscedasticity, due to the generally low frequency of the minor allele. To this purpose, sample size should be larger to get greater statistical power. Here, I lost part of this power because many individuals were discarded after the filtering procedure or because they were considered genetically admixed and, as such, excluded from the analysis. Nonetheless, reconstructing the genealogy of specific markers in their transmission across generations and directly evaluating their effects on reproductive success might be a straightforward strategy to validate the results from classical approaches to the study of local adaptation.

Chapter 6

Conclusions and future insights

In this PhD thesis, I presented a comprehensive framework to jointly analyse dendrochronological and genetic data. The combination of selected approaches contributed to elucidate the tight link between growth and reproductive dynamics within Norway spruce natural populations.

The analytical framework developed in Chapter 3, aimed at assessing the relative importance of potential growth determinants, successfully captured a large amount of the variance in growth, which was mainly due to inter-individual differences. This first result highlighted how commonly used dendrochronological procedures aimed at removing inter-individual variation (*e.g.* standardization, averaging individual data to obtain site chronologies) might be risky when the focus of the study is understanding the effect of growth determinants and quantifying responses to climate. In this regard, individual-based modelling approaches are particularly suitable for taking into account such inter-individual variation, which lies at the basis of evolutionary processes. Inter-individual variance in response to climate is indeed relevant in determining the fate of forest tree species in the ongoing global change scenarios. The other main finding of this chapter is that microenvironmental features are more relevant than genetic similarity in determining similar growth patterns. However, a large proportion of phenotypic variance remained unexplained requesting further investigations. For instance, focusing on candidate genes for growth could increase our understanding of such large inter-individual variation and its relationship with spatial processes.

Investigating the phenotypic basis of reproductive success shed some light on the evolutionary constraints acting on Norway spruce life history traits. Indeed, the main findings of Chapter 4 consistently suggested that, regardless the number of reproductive seasons they have been through, individuals with the higher lifetime fitness had higher growth rates, in particular when temperature of the previous vegetative season is potentially limiting. This means that individuals which grew more throughout their entire lifetime had, on the long-term, a higher fitness in evolutionary terms, because they may better compensate reproductive costs by increasing their resource intake and/or through other compensatory mechanisms. It seems straightforward to identify competition as the ecological process that translates the higher average lifetime growth rates into a larger reproductive success. In the

future, the effects of other phenotypic (*e.g.* tree height, flowering phenology, wood anatomical features) and ecological (*e.g.* competition, drought and other extreme climatic events) determinants of reproductive success, as well as their interactions, should be integrated to better characterize the intricate network of processes shaping the individual evolutionary outcome of forest trees.

The investigation of the adaptive genetic variation of Norway spruce natural populations provided new insights on genes that may be involved in processes leading to local adaptation. A total of five SNPs were found to be likely under selection in both adult and seedling cohorts. The most relevant aspect emerging from this chapter was the methodological approach to test whether such loci influence individual reproductive success. Although no evidence of such an influence was found, I showed how evaluating the effect of SNP loci on reproductive success might be a straightforward strategy to validate results from classical approaches to the study of local adaptation. Further investigations based on a larger number of SNPs and a larger sample size will be necessary to gain sounder results. In addition, genotype–phenotype association analysis might be applied to identify genomic regions that are potentially involved in the architecture of adaptive traits.

In general, future investigations aimed at elucidating the link between growth and reproductive dynamics would certainly benefit from a careful selection of highly comparable sites. Gathering results on well-replicated sites is the only way to move from case-study evidence towards generalizations at the species level. However, it should be noted that such experimental set-up is resource- and time-consuming and that replicates would require a significant further effort. Besides these potential refinements, I deem that combining genetic and dendrochronological data within a parentage analysis framework is fruitful to gain deeper insights on growth and reproductive dynamics of natural populations and to shed new light on the transmission of potentially adaptive genetic variation across generations.

References

Adams, W.T., Birkes, D.S., 1991. Estimating mating patterns in forest tree populations, in: Fineschi, S., Malvolti, M.E., Cannata, F., Hattemer, H.H., (Eds.), Biochemical markers in the population genetics of forest trees. SPB Academic Publishing, The Hague, pp 157–172.

Aho, K., Derryberry, D., Peterson, T., 2014. Model selection for ecologists: the worldviews of AIC and BIC. Ecology 95, 631–636.

Aitken, S.N., Whitlock, M.C., 2013. Assisted gene flow to facilitate local adaptation to climate change. Annu. Rev. Ecol. Evol. Syst. 44, 367–388.

Aitken, S.N., Yeaman, S., Holliday, J.A., Wang, T., Curtis-Mclane, S., 2008. Adaptation, migration or extirpation: climate change outcomes for tree populations. Evol. Appl. 1, 95–111.

Albert, C.H., Grassein, F., Schurr, F.M., Vieilledent, G., Violle, C., 2011. When and how should intraspecific variability be considered in trait-based plant ecology? Perspect. Plant Ecol. Evol. Syst. 13, 217–225.

Alberto, F.J., Aitken, S.N., Alía, R., González-Martínez, S.C., Hänninen, H., Kremer, A., Lefèvre, F., Lenormand, T., Yeaman, S., Whetten, R., *et al.*, 2013. Potential for evolutionary responses to climate change - evidence from tree populations. Glob. Chang. Biol. 19, 1645–1661.

Aldrich, P.R., Hamrick, J.L., 1998. Reproductive dominance of pasture trees in a fragmented tropical forest mosaic. Science 281, 103–105.

Allen, C.D., Macalady, A.K., Chenchouni, H., Bachelet, D., Mcdowell, N., Vennetier, M., Kitzberger, T., Rigling, A., Breshears, D.D., Hogg, E.H.T., *et al.*, 2010. A global overview of drought and heat-induced tree mortality reveals emerging climate change risks for forests. For. Ecol. Manage. 259, 660–684.

Amm, A., Pichot, C., Dreyfus, P., Davi, H., Fady, B., 2012. Improving the estimation of landscape scale seed dispersal by integrating seedling recruitment. Ann. For. Sci. 69, 845–856.

Androsiuk, P., Shimono, A., Westin, J., Lindgren, D., Fries, A., Wang, X.R., 2013. Genetic status of Norway spruce (*Picea abies*) breeding populations for Northern Sweden. Silvae Genet. 62, 127–136.

Araus, J.L., Cairns, J.E., 2014. Field high-throughput phenotyping: the new crop breeding frontier. Trends Plant Sci. 19, 52–61.

Avanzi, C., Piermattei, A., Piotti, A., Büntgen, U., Heer, K., Opgenoorth, L., Spanu, I., Urbinati, C., Vendramin, G.G., Leonardi, S., 2019. Disentangling the effects of spatial proximity and genetic similarity on individual growth performances in Norway spruce natural populations. Sci. Total Environ. 650, 493–504.

Aubin, I., Munson, A., Cardou, F., Burton, P.J., Isabel, N., Pedlar, J., Paquette, A., Taylor, A., Delagrange, S., Kebli, H., *et al.*, 2016. Traits to stay, traits to move: a review of functional traits to assess sensitivity and adaptive capacity of temperate and boreal trees to climate change. Environ. Rev. 24, 1–23.

Augspurger, C.K., 1983. Offspring recruitment around tropical trees: changes in cohort distance with time. Oikos 40, 189–196.

Babushkina, E.A., Vaganov, E.A., Grachev, A.M., Oreshkova, N. V, Belokopytova, L. V, Kostyakova, T. V, Krutovsky, K. V, 2016. The effect of individual genetic heterozygosity on general homeostasis, heterosis and resilience in Siberian larch (*Larix sibirica* Ledeb.) using dendrochronology and microsatellite loci genotyping. Dendrochronologia 38, 26–37.

Barrett, R.D.H., Hoekstra, H.E., 2011. Molecular spandrels: tests of adaptation at the genetic level. Nat. Rev. Genet. 12, 767–780.

Barton, K. 2018. MuMIn: Multi-Model Inference. R package version 1.40.4. https://CRAN.R-project.org/package=MuMIn

Bässler, C., 2004. Das Klima im Nationalpark Bayerischer Wald – Darstellung, Entwicklung und Auswirkung. Nationalparkverwaltung Bayerischer Wald, Grafenau, Germany.

Bernasconi, G., 2003. Seed paternity in flowering plants: an evolutionary perspective. Perspect. Plant Ecol. Evol. Syst. 6, 149–158.

Biondi, F., Qeadan, F., 2008. A theory-driven approach to tree-ring standardization: defining the biological trend from expected basal area increment. Tree-Ring Res. 64, 81–96.

Birol, I., Raymond, A., Jackman, S.D., Pleasance, S., Coope, R., Taylor, G.A., Yuen, M.M. Saint, Keeling, C.I., Brand, D., *et al.*, 2013. Assembling the 20 Gb white spruce (*Picea glauca*) genome from whole-genome shotgun sequencing data. Bioinformatics 29, 1492–1497.

Bivand, R., Piras, G., 2015. Comparing implementations of estimation methods for spatial econometrics. J Statistical Software 63,1–36.

Blair, L.M., Granka, J.M., Feldman, M.W., 2014. On the stability of the Bayenv method in assessing human SNP-environment associations. Hum. Genomics 8, 1.

Blum, B.M., 1961. Age-size relationships in all-aged northern hardwoods. For. Res. Notes 125, 1–3.

Bolker, B.M., Brooks, M.E., Clark, C.J., Geange, S.W., Poulsen, J.R., Stevens, M.H.H., White, J.S., 2008. Generalized linear mixed models: a practical guide for ecology and evolution. Trends Ecol. Evol. 24, 127–135.

Bonan, G.B., 2008. Forests and climate change: forcings, feedbacks, and the climate benefits of forests. Science 320, 1444–1449.

Bontemps, A., Lefèvre, F., Davi, H., Oddou-Muratorio, S., 2016. In situ marker-based assessment of leaf trait evolutionary potential in a marginal European beech population. J. Evol. Biol. 29, 514–527.

Bontemps, A., Klein, E.K., Oddou-Muratorio, S., 2013. Shift of spatial patterns during early recruitment in *Fagus sylvatica*: evidence from seed dispersal estimates based on genotypic data. For. Ecol. Manage. 305, 67–76.

Borcard, D., Gillet, F., Legendre, P., 2011. Numerical ecology with R. Springer, New York.

Bosela, M., Popa, I., Gömöry, D., Longauer, R., Tobin, B., Kyncl, J., Kyncl, T., Nechita, C., Petráš, R., Sidor, C.G., *et al.*, 2016. Effects of post-glacial phylogeny and genetic diversity on the growth variability and climate sensitivity of European silver fir. J. Ecol. 104, 716–724.

Bowman, D.M.J.S., Brienen, R.J.W., Gloor, E., Phillips, O.L., Prior, L.D., 2013. Detecting trends in tree growth: not so simple. Trends Plant Sci. 18, 11–17.

Brousseau, L., Postolache, D., Lascoux, M., Drouzas, A.D., Källman, T., Leonarduzzi, C., Liepelt, S., Piotti, A., Popescu, F., Roschanski, A.M., *et al*., 2016. Local adaptation in European firs assessed through extensive sampling across altitudinal gradients in Southern Europe. PLoS One 11, e0158216.

Bucci, G., Vendramin, G.G., 2000. Delineation of genetic zones in the European Norway spruce natural range: preliminary evidence. Mol. Ecol. 9, 923–934.

Bunn, A.G., 2008. A dendrochronology program library in R (dplR). Dendrochronologia 26, 115–124.

Büntgen, U., 2019. Re-thinking the boundaries of dendrochronology. Dendrochronologia 53, 1–4.

Burczyk, J., Adams, W.T., Birkes, D.S., Chybicki, I.J., 2006. Using genetic markers to directly estimate gene flow and reproductive parameters in plants on the basis of naturally regenerated seedlings. Genetics 173, 363–372.

Burczyk, J., Chybicki, I.J., 2004. Cautions on direct gene flow estimation in plant populations. Evolution 58, 956–963.

Burczyk, J., Lewandowski, A., Chalupka, W., 2004. Local pollen dispersal and distant gene flow in Norway spruce (*Picea abies* [L.] Karst.). For. Ecol. Manage. 197, 39–48.

Burczyk, J., Prat, D., 1997. Male reproductive success in *Pseudotsuga menziesii* (Mirb.) Franco: the effects of spatial structure and flowering characteristics. Heredity 79, 638–647.

Burnham, K.P., Anderson, D.R., 2002. Model selection and multimodel inference: a practical information-theoretic approach, 2nd edn. Springer-Verlag, Berlin.

Busov, V.B., Brunner, A.M., Strauss S.H., 2008. Genes for control of plant stature and form. New Phytol. 177, 589–607.

Carrer, M., Von Arx, G., Castagneri, D., Petit, G., 2015. Distilling allometric and environmental information from time series of conduit size: the standardization issue and its relationship to tree hydraulic architecture. Tree Physiol. 35, 27–33.

Carrer, M., Soraruf, L., Lingua, E., 2013. Convergent space-time tree regeneration patterns along an elevation gradient at high altitude in the Alps. For. Ecol. Manage. 304, 1–9.

Carrer, M., Motta, R., Nola, P., 2012. Significant mean and extreme climate sensitivity of Norway spruce and silver fir at mid-elevation mesic sites in the Alps. PLoS One 7, e50755.

Carrer, M., 2011. Individualistic and time-varying tree-ring growth to climate sensitivity. PLoS One 6.

Carrer, M., Urbinati, C., 2004. Age-dependent tree-ring growth responses to climate in *Larix decidua* and *Pinus cembra*. Ecology 85, 730–740.

Castagneri, D., Lingua, E., Vacchiano, G., Nola, P., Motta, R., 2010. Diachronic analysis of individual-tree mortality in a Norway spruce stand in the eastern Italian Alps. Ann. For. Sci. 67, 304–304.

Castellanos, M.C., González-Martínez, S.C., Pausas, J.G., 2015. Field heritability of a plant adaptation to fire in heterogeneous landscapes. Mol. Ecol. 24, 5633–5642.

Chalupka, W., Giertych, M., Krolikowski, Z., 1975. The effect of cone crops on growth of Norway spruce (*Picea abies* (L.) Karst.). Arboretum Kornickie 20, 201–212.

Chen, J., Källman, T., Ma, X.-F., Zaina, G., Morgante, M., Lascoux, M., 2016. Identifying genetic signatures of natural selection using pooled population sequencing in *Picea abies*. Genes|Genomes|Genetics 6, 1979–1989.

Chen, J., Gyllenstrand, N., Zaina, G., Morgante, M., Bousquet, J., Eckert, A., Wegrzyn, J., Neale, D., Lagercrantz, U., Lascoux, M., 2012a. Disentangling the roles of history and local selection in shaping clinal variation of allele frequencies and gene expression in Norway spruce (*Picea abies*). Genetics 191, 865–881.

Chen, J., Uebbing, S., Gyllenstrand, N., Lagercrantz, U., Lascoux, M., Källman, T., 2012b. Sequencing of the needle transcriptome from Norway spruce (*Picea abie*s Karst L.) reveals lower substitution rates, but similar selective constraints in gymnosperms and angiosperms. BMC Genomics 13, 589.

Chen, I., Hill, J.K., Ohlemüller, R., Roy, D.B., Thomas, C.D., 2011. Rapid range shifts of species. Science 333, 1024–1026.

Chen, J., Källman, T., Gyllenstrand, N., Lascoux, M., 2010. New insights on the speciation history and nucleotide diversity of three boreal spruce species and a Tertiary relict. Heredity 104, 3–14.

Cherubini, P., Dobbertin, M., Innes, J.L., 1998. Potential sampling bias in long-term forest growth trends reconstructed from tree rings: a case study from the Italian Alps. For. Ecol. Manag. 109, 103–118.

Chiarugi, A., 1936. L'indigenato della "*Picea excelsa*" nell'Appennino Etrusco. Nuovo G. Bot. Ital. XLIII, 131–166.

Chybicki, I.J., 2018. NMπ—improved re-implementation of NM+, a software for estimating gene dispersal and mating patterns. Mol. Ecol. Resour. 18, 159–168.

Chybicki, I.J., Oleksa, A., 2018. Seed and pollen gene dispersal in *Taxus baccata*, a dioecious conifer in the face of strong population fragmentation. Ann. Bot. 122, 409–421.

Chybicki, I.J., Burczyk, J., 2010. Realized gene flow within mixed stands of *Quercus robur* L. and *Q. petraea* (Matt.) L. revealed at the stage of naturally established seedling. Mol. Ecol. 19, 2137–2151.

Clausen, J., Keck, D.D., Hiesey, W.M., 1948. Experimental studies on the nature of species. III. Environmental responses of climatic races of *Achillea*. Carnegie Inst. Wash. Publ. 581, 1–189.

Cook, E.R., Briffa, K., Shiyatov, S., Mazepa, V., 1990. Tree-ring standardization and growth-trend estimation, in: Cook, E.R., Kairiukstis, L.A. (Eds.), Methods of Dendrochronology: Applications in the Environmental Sciences. Kluwer Academic Publisher, Dordrecht, pp. 104–123.

Cook, E.R., Kairiukstis, L.A., 1990. Methods of dendrochronology: applications in the environmental sciences. Kluwer Academic Publishers, Dondrecht.

Cook, E.R., 1985. Time series analysis approach to tree-ring standardization. PhD thesis, University of Arizona.

Coop, G., Witonsky, D., Di Rienzo, A., Pritchard, J.K., 2010. Using environmental correlations to identify loci underlying local adaptation. Genetics 185, 1411–1423.

Corlett, R.T., Westcott, D.A., 2013. Will plant movements keep up with climate change? Trends Ecol. Evol. 28, 482–488.

Cornelius, J., 1994. Heritabilities and additive genetic coefficients of variation in forest trees. Can. J. For. Res. 24, 372–379.

Crespi, A., Brunetti, M., Lentini, G., Maugeri, M., 2018. 1961-1990 high-resolution monthly precipitation climatologies for Italy. Int. J. Climatol. 38, 878–895.

Cuervo-Alarcon, L., Arend, M., Müller, M., Sperisen, C., Finkeldey, R., Krutovsky, K. V., 2018. Genetic variation and signatures of natural selection in populations of European beech (*Fagus sylvatica* L.) along precipitation gradients. Tree Genet. Genomes 14, 84.

Davi, H., Cailleret, M., Restoux, G., Amm, A., Pichot, C., Fady, B., 2016. Disentangling the factors driving tree reproduction. Ecosphere 7, 01389.

Davis, M.B., Shaw, R.G., 2001. Range shifts and adaptive responses to quaternary climate change. Science 292, 673–679.

De La Torre, A.R., Birol, I., Bousquet, J., Ingvarsson, P.K., Jansson, S., Jones, S.J.M., Keeling, C.I., MacKay, J., Nilsson, O., Ritland, K., *et al.*, 2014. Insights into conifer giga-genomes. Plant Physiol. 166, 1724–1732.

De Mita, S., Thuillet, A.-C., Gay, L., Ahmadi, N., Manel, S., Ronfort, J., Vigouroux, Y., 2013. Detecting selection along environmental gradients: analysis of eight methods and their effectiveness for outbreeding and selfing populations. Mol. Ecol. 22, 1383–1399.

Di Pierro, E.A., Mosca, E., Rocchini, D., Binelli, G., Neale, D.B., La Porta, N., 2016. Climate-related adaptive genetic variation and population structure in natural stands of Norway spruce in the South-Eastern Alps. Tree Genet. Genomes 12.

Dray, S., Blanchet G., Borcard, D., Clappe, S., Guenard, G., Jombart, T., Larocque, G., Legendre, P., Madi, N., Wagner, H.H., 2018. *adespatial*: multivariate multiscale spatial analysis. R package version 0.1-1. https://CRAN.R-project.org/package=adespatial

Dray, S., Legendre, P., Peres-Neto, P.R., 2006. Spatial modelling: a comprehensive framework for principal coordinate analysis of neighbour matrices (PCNM). Ecol. Modell. 196, 483–493.

Earl, D.A., VonHoldt, B.M., 2012. STRUCTURE HARVESTER: a website and program for visualizing STRUCTURE output and implementing the Evanno method. Conserv. Genet. Resour. 4, 359–361.

Eckert, A.J., van Heerwaarden, J., Wegrzyn, J.L., Nelson, C.D., Ross-Ibarra, J., González-Martínez, S.C., Neale, D.B., 2010. Patterns of population structure and environmental associations to aridity across the range of loblolly pine (*Pinus taeda* L., Pinaceae). Genetics 185, 969–982.

Eckert, A.J., Wegrzyn, J.L., Pande, B., Jermstad, K.D., Lee, J.M., Liechty, J.D., Tearse, B.R., Krutovsky, K. V., Neale, D.B., 2009. Multilocus patterns of nucleotide diversity and divergence reveal positive selection at candidate genes related to cold hardiness in coastal Douglas fir (*Pseudotsuga menziesii* var. *menziesii*). Genetics 183, 289–298.

Ekstrom, A., Taujale, R., McGinn, N., Yin, Y., 2014. PlantCAZyme: a database for plant carbohydrate-active enzymes. Database 2014, bau079.

Esper, J., Cook, E.R., Schweingruber, F.H., 2002. Low-frequency signals in long tree-ring chronologies for reconstructing past temperature variability. Science 295, 2250–2253.

Evanno, G., Regnaut, S., Goudet, J., 2005. Detecting the number of clusters of individuals using the software STRUCTURE: a simulation study. Mol. Ecol. 14, 2611–2620.

Evans, M.E.K., Gugger, P.F., Lynch, A.M., Guiterman, C.H., Fowler, J.C., Klesse, S., Riordan, E.C., 2018. Dendroecology meets genomics in the common garden: new insights into climate adaptation. New Phytol. 218, 401–403.

Ezekiel, M., 1930. Methods of correlational analysis. Wiley, New York.

Falconer, D.S., Mackay, T.F.C., 1996. Introduction to quantitative genetics, fourth ed. Longman, Harlow.

Fink, A.H., Brucher, T., Kruger, A., Leckebusch, G.C., Pinto, J.G., Ulbrich, U., 2004. The 2003 European summer heat waves and drought- synoptic diagnosis and impact. Weather 59, 209–216.

Fiorani, F., Schurr, U., 2013. Future scenarios for plant phenotyping. Annu. Rev. Plant Biol. 64, 267–291.

Fluch, S., Burg, A., Kopecky, D., Homolka, A., Spiess, N., Vendramin, G.G., 2011. Characterization of variable EST SSR markers for Norway spruce (*Picea abies* L.). BMC Res. Notes 4, 401.

Foll, M., Gaggiotti, O., 2008. A genome-scan method to identify selected loci appropriate for both dominant and codominant markers: a Bayesian perspective. Genetics 180, 977–993.

Fox, J., Weisberg, S., 2011. An R Companion to Applied Regression, second ed. Sage, Thousand Oaks.

Franks, S.J., Weber, J.J., Aitken, S.N., 2014. Evolutionary and plastic responses to climate change in terrestrial plant populations. Evol. Appl. 7, 123–139.

Fritts, H.C., 1976. Tree rings and Climate. Academic Press, London.

Furbank, R.T., Tester, M., 2011. Phenomics - technologies to relieve the phenotyping bottleneck. Trends Plant Sci. 16, 635–644.

Galván, J.D., Camarero, J.J., Gutiérrez, E., 2014. Seeing the trees for the forest: drivers of individual growth responses to climate in *Pinus uncinata* mountain forests. J. Ecol. 102, 1244–1257.

Gauzere, J., Klein, E.K., Oddou-Muratorio, S., 2013. Ecological determinants of mating system within and between three *Fagus sylvatica* populations along an elevational gradient. Mol. Ecol. 22, 5001–5015.

Geburek, T., 1998. Genetic variation of Norway spruce (*Picea abies* K.) populations in Austria. For. Genet. 5, 221–230.

Gerber, S., Chadœuf, J., Gugerli, F., Lascoux, M., Buiteveld, J., Cottrell, J., Dounavi, A., Fineschi, S., Forrest, L.L., Fogelqvist, J., *et al.*, 2014. High rates of gene flow by pollen and seed in oak populations across Europe. PLoS One 9, e85130.

Gerzabek, G., Oddou-Muratorio, S., Hampe, A., 2017. Temporal change and determinants of maternal reproductive success in an expanding oak forest stand. J. Ecol. 105, 39–48.

Gibbs, C.B., 1963. Tree diameter a poor indicator of age in West Virginia hardwoods. For. Res. Notes, 1–4.

Giesecke, T., Bennett, K.D., 2004. The Holocene spread of *Picea abies* (L.) Karst. in Fennoscandia and adjacent areas. J. Biogeogr. 31, 1523–1548.

González-Martínez, S.C., Burczyk, J., Nathan, R., Nanos, N., Gil, L., Alía, R., 2006. Effective gene dispersal and female reproductive success in Mediterranean maritime pine (*Pinus pinaster* Aiton). Mol. Ecol. 15, 4577–4588.

Grattapaglia, D., Plomion, C., Kirst, M., Sederoff, R.R., 2009. Genomics of growth traits in forest trees. Curr. Opin. Plant Biol. 12, 148–156.

Grivet, D., Sebastiani, F., Alia, R., Bataillon, T., Torre, S., Zabal-Aguirre, M., Vendramin, G.G., González-Martínez, S.C., 2011. Molecular footprints of local adaptation in two mediterranean conifers. Mol. Biol. Evol. 28, 101–116.

Gunther, T., Coop, G., 2013. Robust identification of local adaptation from allele frequencies. Genetics 195, 205–220.

Hamann, A., Wang, T., Spittlehouse, D.L., Murdock, T.Q., 2013. A comprehensive, high-resolution database of historical and projected climate surfaces for western North America. Bull. Am. Meteorol. Soc. 94, 1307–1309.

Hampe, A., Petit, R.J., 2005. Conserving biodiversity under climate change: the rear edge matters. Ecol. Lett. 8, 461–467.

Hamrick, J.., 2004. Response of forest trees to global environmental changes. For. Ecol. Manage. 197, 323–335.

Hannrup, B., Cahalan, C., Chantre, G., Grabner, M., Karlsson, B., Le Bayon, I., Jones, G.L., Müller, U., Pereira, H., Rodrigues, J.C., *et al.*, 2004. Genetic parameters of growth and wood quality traits in *Picea abies*. Scand. J. For. Res. 19, 14–29.

Hardy, O.J., 2003. Estimation of pairwise relatedness between individuals and characterization of isolation-by-distance processes using dominant genetic markers. Mol. Ecol. 12, 1577–1588.

Hardy, O.J., Vekemans, X., 2002. SPAGeDi: a versatile computer program to analyse spatial genetic structure at the individual or population levels. Mol. Ecol. Notes 2, 618–620.

Harper, J.L., 1977. Population biology of plants. Academic Press, London.

Harris, I., Jones, P.D., Osborn, T.J., Lister, D.H., 2014. Updated high-resolution grids of monthly climatic observations - the CRU TS3.10 Dataset. Int. J. Climatol. 34, 623–642.

Hartl-Meier, C., Dittmar, C., Zang, C., Rothe, A., 2014. Mountain forest growth response to climate change in the Northern Limestone Alps. Trees 28, 819–829.

Hedrick, P.W., 2005. A standardized genetic differentiation measure. Evolution 59, 1633-1638.

Heer, K., Behringer, D., Piermattei, A., Bässler, C., Brandl, R., Fady, B., Jehl, H., Liepelt, S., Lorch, S., Piotti, A., *et al.*, 2018. Linking dendroecology and association genetics in natural

populations: stress responses archived in tree rings associate with SNP genotypes in silver fir (*Abies alba* Mill.). Mol. Ecol. 27, 1428–1438.

Heer, K., Ullrich, K.K., Liepelt, S., Rensing, S.A., Zhou, J., Ziegenhagen, B., Opgenoorth, L., 2016. Detection of SNPs based on transcriptome sequencing in Norway spruce (*Picea abies* (L.) Karst). Conserv. Genet. Resour. 8, 105–107.

Hember, R.A., Kurz, W.A., Metsaranta, J.M., 2015. Ideas and perspectives: use of tree-ring width as an indicator of tree growth. Biogeosciences Discuss. 12, 8341–8352.

Hereş, A.M., Martínez-Vilalta, J., López, B.C., 2012. Growth patterns in relation to drought-induced mortality at two Scots pine (*Pinus sylvestris* L.) sites in NE Iberian Peninsula. Trees 26, 621–630.

Heuertz, M., De Paoli, E., Kallman, T., Larsson, H., Jurman, I., Morgante, M., Lascoux, M., Gyllenstrand, N., 2006. Multilocus patterns of nucleotide diversity, linkage disequilibrium and demographic history of Norway spruce [*Picea abies* (L.) Karst]. Genetics 174, 2095–2105.

Hodgson, J.G., Wilson, P.J., Hunt, R., Grime, J.P., Thompson, K., 1999. Allocating C-S-R plant functional types: a soft approach to a hard problem. Oikos 85, 282–294.

Holmes, R.L., 1983. Computer-assisted quality control in tree- ring dating and measurement. Tree-ring Bull. 43, 69–78.

Housset, J.M., Nadeau, S., Isabel, N., Depardieu, C., Duchesne, I., Lenz, P., Girardin, M.P., 2018. Tree rings provide a new class of phenotypes for genetic associations that foster insights into adaptation of conifers to climate change. New Phytol. 218, 630–645.

Housset, J.M., Carcaillet, C., Girardin, M.P., Xu, H., Tremblay, F., Bergeron, Y., 2016. In situ comparison of tree-ring responses to climate and population genetics: the need to control for local climate and site variables. Front. Ecol. Evol. 4, 123.

Huang, S., Chen, X., Zhong, X., Li, M., Ao, K., Huang, J., Li, X., 2016. Plant TRAF Proteins Regulate NLR Immune Receptor Turnover. Cell Host Microbe 19, 204–215.

IPCC, 2013. Climate change 2013: the physical science basis. Contribution of Working Group I to the Fifth Assessment Report of the IPCC. Cambridge, UK: Cambridge University Press.

Ivković, M., Gapare, W., Wu, H., Espinoza, S., Rozenberg, P., 2013. Influence of cambial age and climate on ring width and wood density in *Pinus radiata* families. Ann. For. Sci. 70, 525–534.

Jaramillo-Correa, J.P., Rodríguez-Quilón, I., Grivet, D., Lepoittevin, C., Sebastiani, F., Heuertz, M., Garnier-Géré, P.H., Alía, R., Plomion, C., Vendramin, G.G., *et al.*, 2015. Molecular proxies for climate maladaptation in a long-lived tree (*Pinus pinaster* Aiton, Pinaceae). Genetics 199, 793–807.

Jeffreys, H., 1961. Theory of probability. 3rd ed Oxford University Press, Oxford.

Jombart, T., Ahmed, I., 2011. *adegenet* 1.3-1: new tools for the analysis of genome-wide SNP data. Bioinformatics 27, 3070–3071.

Jones, A.G., Small, C.M., Paczolt, K.A., Ratterman, N.L., 2010. A practical guide to methods of parentage analysis. Mol. Ecol. Resour. 10, 6–30.

Jones, P.D., Osborn, T.J., Briffa, K.R., 2001. The evolution of climate over the last millennium. Science 292, 662–667.

Jump, A.S., Hunt, J.M., Martínez-Izquierdo, J.A., Peñuelas, J., 2006. Natural selection and climate change: temperature-linked spatial and temporal trends in gene frequency in *Fagus sylvatica*. Mol. Ecol. 15, 3469–3480.

Jump, A.S., Penuelas, J., 2005. Running to stand still: adaptation and the response of plants to rapid climate change. Ecol. Lett. 8, 1010–1020.

Kalinowski, S., 2005. HP-RARE 1. 0: a computer program for performing rarefaction on measures of allelic richness. Mol. Ecol. Notes 5, 187–189.

Källman, T., De Mita, S., Larsson, H., Gyllenstrand, N., Heuertz, M., Parducci, L., Suyama, Y., Lagercrantz, U., Lascoux, M., 2014. Patterns of nucleotide diversity at photoperiod related genes in Norway Spruce [*Picea abies* (L.) Karst.]. PLoS One 9, e95306.

Kameyama, Y., Isagi, Y., Nakagoshi, N., 2001. Patterns and levels of gene flow in *Rhododendron metternichii* var. *hondoense* revealed by microsatellite analysis. Mol. Ecol. 10, 205–216.

Karlgren, A., Gyllenstrand, N., Clapham, D., Lagercrantz, U., 2013. FLOWERING LOCUS T/TERMINAL FLOWER1-like genes affect growth rhythm and bud set in Norway spruce. Plant Physiol. 163, 792–803.

Karthikeyan, M., Jayakumar, V., Radhika, K., Bhaskaran, R., Velazhahan, R., Alice, D., 2005. Induction of resistance in host against the infection of leaf blight pathogen (*Alternaria palandui*) in onion (*Allium cepa* var *aggregatum*). Indian J. Biochem. Biophys. 42, 371–377.

Kaufman, S., Smouse, P., Alvarez-Buylla, E., 1998. Pollen-mediated gene flow and differential male reproductive success in a tropical pioneer tree, *Cecropia obtusifolia* Bertol. (Moraceae): a paternity analysis. Heredity 81, 164–173.

Kawecki, T.J., Ebert, D., 2004. Conceptual issues in local adaptation. Ecol. Lett. 7, 1225–1241.

King, G.M., Gugerli, F., Fonti, P., Frank, D.C., 2013. Tree growth response along an elevational gradient: climate or genetics? Oecologia 173, 1587–1600.

Klein, E.K., Desassis, N., Oddou-Muratorio, S., 2008. Pollen flow in the wildservice tree, *Sorbus torminalis* (L.) Crantz. IV. Whole interindividual variance of male fecundity estimated jointly with the dispersal kernel. Mol. Ecol. 17, 3323–3336.

Klisz, M., Koprowski, M., Ukalska, J., Nabais, C., 2016. Does the genotype have a significant effect on the formation of intra-annual density fluctuations? A case study using *Larix decidua* from northern Poland. Front. Plant Sci. 7.

Kolář, T., Čermák, P., Trnka, M., Žid, T., Rybníček, M., 2017. Temporal changes in the climate sensitivity of Norway spruce and European beech along an elevation gradient in Central Europe. Agric. For. Meteorol. 239, 24–33.

Kopelman, N.M., Mayzel, J., Jakobsson, M., Rosenberg, N.A., Mayrose, I., 2015. CLUMPAK: a program for identifying clustering modes and packaging population structure inferences across *K*. Mol. Ecol. Resour. 15, 1179–1191.

Kremer, A., Potts, B.M., Delzon, S., 2014. Genetic divergence in forest trees: understanding the consequences of climate change. Funct. Ecol. 28, 22–36.

Kremer, A., Ronce, O., Robledo-Arnuncio, J.J., Guillaume, F., Bohrer, G., Nathan, R., Bridle, J.R., Gomulkiewicz, R., Klein, E.K., Ritland, K., *et al.*, 2012. Long-distance gene flow and adaptation of forest trees to rapid climate change. Ecol. Lett. 1–15.

Lagercrantz, U., Ryman, N., 1990. Genetic structure of Norway spruce (*Picea abies*): concordance of morphological and allozymic variation. Evolution 44, 38–53.

Lamedica, S., Lingua, E., Popa, I., Motta, R., Carrer, M., 2011. Spatial structure in four Norway spruce stands with different management history in the Alps and Carpathians. Silva Fenn. 45, 865–873.

Langlet, O., 1971. Two hundred years of genecology. Taxon 20, 653–721.

Latutrie, M., Mérian, P., Picq, S., Bergeron, Y., Tremblay, F., 2015. The effects of genetic diversity, climate and defoliation events on trembling aspen growth performance across Canada. Tree Genet. Genomes 11.

Lebourgeois, F., 2007. Climatic signal in annual growth variation of silver fir (*Abies alba* Mill.) and spruce (*Picea abies* Karst.) from the French Permanent Plot Network (RENECOFOR). Ann. For. Sci. 64, 333–343.

Lefcheck, J.S., 2016. *piecewiseSEM*: piecewise structural equation modelling in R for ecology, evolution, and systematics. Methods Ecol. Evol. 7, 573–579.

Legendre, P., Fortin, M.J., Borcard, D., 2015. Should the Mantel test be used in spatial analysis? Methods Ecol. Evol. 6, 1239–1247.

Legendre, P., Legendre, L., 2012. Numerical Ecology. Developments in Environmental Modelling. 3rd ed. vol. 24 Elsevier, Amsterdam.

Lenoir, J., Gégout, J.C., Marquet, P.A., de Ruffray, P., Brisse, H., 2008. A significant upward shift in plant species optimum elevation during the 20th century. Science 320, 1768–1771.

Leonarduzzi, C., Piotti, A., Spanu, I., Vendramin, G.G., 2016. Effective gene flow in a historically fragmented area at the southern edge of silver fir (*Abies alba* Mill.) distribution. Tree Genet. Genomes 12, 95.

Levanič, T., Gričar, J., Gagen, M., Jalkanen, R., Loader, N.J., McCarroll, D., Oven, P., Robertson, I., 2009. The climate sensitivity of Norway spruce [*Picea abies* (L.) Karst.] in the southeastern European Alps. Trees 23, 169–180.

Levins, R., 1968. Evolution in changing environments. Princeton University Press, New York.

Lewontin, R.C., Krakauer, J., 1973. Distribution of gene frequency as a test of the theory of the selective neutrality of polymorphisms. Genetics 74, 175–195.

Li, J., Li, H., Jakobsson, M., Li, S., Sjödin, P., Lascoux, M., 2012. Joint analysis of demography and selection in population genetics: where do we stand and where could we go? Mol Ecol 21:28–44.

Lian, C., Goto, S., Kubo, T., Takahashi, Y., Nakagawa, M., Hogetsu, T., 2008. Nuclear and chloroplast microsatellite analysis of *Abies sachalinensis* regeneration on fallen logs in a subboreal forest in Hokkaido, Japan. Mol. Ecol. 17, 2948–2962.

Linares, J.C., Camarero, J.J., Carreira, J.A., 2010. Competition modulates the adaptation capacity of forests to climatic stress: insights from recent growth decline and death in relict stands of the Mediterranean fir *Abies pinsapo*. J. Ecol. 98, 592–603.

Lind, B.M., Menon, M., Bolte, C.E., Faske, T.M., Eckert, A.J., 2018. The genomics of local adaptation in trees: are we out of the woods yet? Tree Genet. Genomes 14, 29.

Lindgren, K., Ekberg, I., Eriksson, G., 1977. External factors influencing female flowering in *Picea abies* (L.) Karst. Stu. For. Sue. 142.

Lloret, F., Keeling, E.G., Sala, A., 2011. Components of tree resilience: effects of successive low-growth episodes in old ponderosa pine forests. Oikos 120, 1909–1920.

Loarie, S.R., Duffy, P.B., Hamilton, H., Asner, G.P., Field, C.B., Ackerly, D.D., 2009. The velocity of climate change. Nature 462, 1052–1055.

Luu, K., Bazin, E., Blum, M.G.B., 2017. *pcadapt*: an R package to perform genome scans for selection based on principal component analysis. Mol. Ecol. Resour. 17, 67–77.

van der Maaten-Theunissen, M., van der Maaten, E., Bouriaud, O., 2015. pointRes: an R package to analyze pointer years and components of resilience. Dendrochronologia 35, 34–38.

Macalady, A.K., Bugmann, H., 2014. Growth-mortality relationships in piñon pine (*Pinus edulis*) during severe droughts of the past century: shifting processes in space and time. PLoS One 9, e92770.

Magini, E., Pellizzo, A., Proietti Placidi, A.M., Tonarelli, F., 1980. La Picea dell'Alpe delle Tre Potenze. Areale – caratteristiche – posizione sistematica. Ann. Accad. Sci. Forest. 29, 107–210.

Magri, D., Agrillo, E., Di Rita, F., Furlanetto, G., Pini, R., Ravazzi, C., Spada, F., 2015. Holocene dynamics of tree taxa populations in Italy. Rev. Palaeobot. Palynol. 218, 267–284.

Makinen, H., Nojd, P., Kahle, H., Neumann, U., Tveite, B., Mielikainen, K., Rohle, H., Spiecker, H., 2002. Radial growth variation of Norway spruce (*Picea abies* (L.) Karst.) across latitudinal and altitudinal gradients in central and northern Europe. For. Ecol. Manag. 171, 243–259.

Martinez Meier, A.G., Sanchez, L., Salda, G., Pastorino, M.J.M., Gautry, J.-Y., Gallo, L.A., Rozenberg, P., 2008. Genetic control of the tree-ring response of Douglas-fir (*Pseudotsuga menziesii* (Mirb.) Franco) to the 2003 drought and heat-wave in France. Ann. For. Sci. 65, 102–102.

McKenney, D.W., Pedlar, J.H., Lawrence, K., Papadopol, P., Campbell, K., Hutchinson, M.F., 2014. Change and evolution in the plant hardiness zones of Canada. BioScience 64: 341–350.

Meagher, T.R., Thompson, E., 1987. Analysis of parentage for naturally established seedlings of *Chamaelirium luteum* (Liliaceae). Ecology 68, 803–812.

Mencuccini, M., Martínez-Vilalta, J., Vanderklein, D., Hamid, H.A., Korakaki, E., Lee, S., Michiels, B., 2005. Size-mediated ageing reduces vigour in trees. Ecol. Lett. 8, 1183–1190.

Mihai, G., Mirancea, I., 2016. Age trends in genetic parameters for growth and quality traits in *Abies alba*. iForest 9, 954–959.

Miina, J., 2000. Dependence of tree-ring, earlywood and latewood indices of Scots pine and Norway spruce on climatic factors in eastern Finland. Ecol. Modell. 132, 259–273.

Montwé, D., Isaac-Renton, M., Hamann, A., Spiecker, H., 2016. Drought tolerance and growth in populations of a wide-ranging tree species indicate climate change risks for the boreal north. Glob. Chang. Biol. 22, 806–815.

Moran, E.V., Clark, J.S., 2012. Causes and consequences of unequal seedling production in forest trees: a case study in red oaks. Ecology 93, 1082–1094.

Morgan, M.T., Conner, J.K., 2001. Using genetic markers to directly estimate male selection gradients. Evolution 55, 272–281.

Mosca, E., González-Martínez, S.C., Neale, D.B., 2014. Environmental versus geographical determinants of genetic structure in two subalpine conifers. New Phytol. 201, 180–192.

Mosca, E., Eckert, A.J., Di Pierro, E.A., Rocchini, D., La Porta, N., Belletti, P., Neale, D.B., 2012. The geographical and environmental determinants of genetic diversity for four alpine conifers of the European Alps. Mol. Ecol. 21, 5530–5545.

Motta, R., Ascoli, D., Corona, P., Marchetti, M., Vacchiano, G., 2018. Silviculture and wind damages. The storm "Vaia." Foresta@ 15, 94–98.

Nakagawa, S., Schielzeth, H., 2013. A general and simple method for obtaining R^2 from generalized linear mixed-effects models. Methods Ecol. Evol. 4, 133–142.

Namroud, M.-C., Beaulieu, J., Juge, N., Laroche, J., Bousquet, J., 2008. Scanning the genome for gene single nucleotide polymorphisms involved in adaptive population differentiation in white spruce. Mol. Ecol. 17, 3599–3613.

Nehrbass-Ahles, C., Babst, F., Klesse, S., Nötzli, M., Bouriaud, O., Neukom, R., Dobbertin, M., Frank, D., 2014. The influence of sampling design on tree-ring-based quantification of forest growth. Glob. Chang. Biol. 20, 2867–2885.

Nystedt, B., Street, N.R., Wetterbom, A., Zuccolo, A., Lin, Y.C., Scofield, D.G., Vezzi, F., Delhomme, N., Giacomello, S., Alexeyenko, A., *et al.*, 2013. The Norway spruce genome sequence and conifer genome evolution. Nature 497, 579–584.

Obeso, J.R., 2002. The costs of reproduction in plants. New Phytol. 155, 321–348.

Oddou-Muratorio, S., Gauzere, J., Bontemps, A., Rey, J.-F., Klein, E.K., 2018a. Tree, sex and size: ecological determinants of male vs. female fecundity in three *Fagus sylvatica* stands. Mol. Ecol. 27, 3131–3145.

Oddou-Muratorio, S., Petit, C., Journé, V., Lingrand, M., Magdalou, J.-A., Hurson, C., Garrigue, J., Davi, H., Magnanou, E., 2018b (bioRxiv). Crown defoliation decreases reproduction and wood growth in a marginal European beech population. http://dx.doi.org/10.1101/474874

Oddou-Muratorio, S., Klein, E.K., 2008. Comparing direct vs. indirect estimates of gene flow within a population of a scattered tree species. Mol. Ecol. 17, 2743–2754.

Oddou-Muratorio, S., Klein, E.K., Austerlitz, F., 2005. Pollen flow in the wildservice tree, *Sorbus torminalis* (L.) Crantz. II. Pollen dispersal and heterogeneity in mating success inferred from parent-offspring analysis. Mol. Ecol. 14, 4441–4452.

Oksanen, J., Guillaume Blanchet, F., Friendly, M., Kindt, R., Legendre, P., McGlinn, D., Minchin, P.R., O'Hara, R.B., Simpson, G.L., Solymos, P., *et al.*, 2018. *vegan*: Community Ecology. R package version 2.4-6. https://CRAN.R-project.org/package=vegan

Pakkanen, A., Nikkanen, T., Pulkkinen, P., 2000. Annual variation in pollen contamination and outcrossing in a *Picea abies* seed orchard. Scand J Forest Res 15, 399–404.

Parmesan, C., 2006. Ecological and evolutionary responses to recent climate change. Annu. Rev. Ecol. Evol. Syst. 37, 637–669.

Parmesan, C., Yohe, G., 2003. A globally coherent fingerprint of climate change impacts across natural systems. Nature 421, 37–42.

Partanen, J., Koski, V., Hänninen, H., 1998. Effects of photoperiod and temperature on the timing of bud burst in Norway spruce (*Picea abies*). Tree Physiol. 18, 811–816.

Paule, L., Lindgren, D., Yazdani, R., 1993. Allozyme frequencies, outcrossing rate and pollen contamination in *Picea abies* seed orchards. Scand J Forest Res 8, 8–17.

Pavy, N., Gagnon, F., Rigault, P., Blais, S., Deschênes, A., Boyle, B., Pelgas, B., Deslauriers, M., Clément, S., Lavigne, P. *et al.*, 2013. Development of high-density SNP genotyping arrays for white spruce (*Picea glauca*) and transferability to subtropical and nordic congeners. Mol. Ecol. Resour. 13, 324–336.

Peakall, R., Smouse, P.E., 2012. GenALEx 6.5: Genetic analysis in Excel. Population genetic software for teaching and research-an update. Bioinformatics 28, 2537–2539.

Petit, R.J., Hampe, A., 2006. Some evolutionary consequences of being a tree. Annu. Rev. Ecol. Evol. Syst. 37, 187–214.

Petit, R.J., El Mousadik, A., Pons, O., 1998. Identifying populations for conservation on the basis of genetic markers. Conserv. Biol. 12, 844–855.

Pew, J., Muir, P.H., Wang, J., Frasier, T.R., 2015. related: An R package for analysing pairwise relatedness from codominant molecular markers. Mol. Ecol. Resour. 15, 557–561.

Pfeiffer, A., Olivieri, A., Morgante, M., 1997. Identification and characterization of microsatellites in Norway spruce (*Picea abies* K.). Genome 40, 411–419.

Pinheiro, J.C., Bates, D.M., 2000. Mixed-effects models in S and S-PLUS. Springer, New York.

Pinheiro, J., Bates, D., DebRoy, S., Sarkar, D., R Core Team, 2018. nlme: Linear and Nonlinear Mixed Effects Models. R package version 3.1-137. https://CRAN.R-project.org/package=nlme

Piotti, A., Leonardi, S., Buiteveld, J., Geburek, T., Gerber, S., Kramer, K., Vettori, C., Vendramin, G.G., 2012. Comparison of pollen gene flow among four European beech (*Fagus sylvatica* L.) populations characterized by different management regimes. Heredity 108, 322–331.

Piotti, A., Leonardi, S., Piovani, P., Scalfi, M., Menozzi, P., 2009. Spruce colonization at treeline: where do those seeds come from? Heredity 103, 136–145.

Piussi, P., 1979. Nuovi studi sulla rinnovazione naturale delle peccete nella Val di Fiemme. Mem. Mus. Tridentino Sci. Nat. 23, 113–169.

Pluess, A.R., Frank, A., Heiri, C., Lalagüe, H., Vendramin, G.G., Oddou-Muratorio, S., 2016. Genome-environment association study suggests local adaptation to climate at the regional scale in *Fagus sylvatica*. New Phytol. 210, 589–601.

Primicia, I., Camarero, J.J., Janda, P., Čada, V., Morrissey, R.C., Trotsiuk, V., Bače, R., Teodosiu, M., Svoboda, M., 2015. Age, competition, disturbance and elevation effects on tree and stand growth response of primary *Picea abies* forest to climate. For. Ecol. Manage. 354, 77–86.

Pritchard, J.K., Stephens, M., Donnelly, P., 2000. Inference of population structure using multilocus genotype data. Genetics 155, 945–959.

Prunier, J., GÉrardi, S., Laroche, J., Beaulieu, J., Bousquet, J., 2012. Parallel and lineage-specific molecular adaptation to climate in boreal black spruce. Mol. Ecol. 21, 4270–4286.

Pukkala, T., Hokkanen, T., Nikkanen, T., 2010. Prediction models for the annual seed crop of Norway spruce and Scots pine in Finland. Silva Fenn. 44, 629–642.

Pukkala, T., 1987. Siementuotannon vaikutus kuusen ja männyn vuotuiseen kasvuun (Effect of seed production on the annual growth of *Picea abies* and *Pinus sylvestris*). Silva Fenn. 21, 145–158.

Quesada, T., Parisi, L.M., Huber, D.A., Gezan, S.A., Martin, T.A., Davis, J.M., Peter, G.F., 2017. Genetic control of growth and shoot phenology in juvenile loblolly pine (*Pinus taeda* L.) clonal trials. Tree Genet. Genomes 13, 65.

R Core Team (2018). R: A language and environment for statistical computing. R Foundation for Statistical Computing, Vienna, Austria. https://www.R-project.org/

Ravazzi, C., 2002. Late Quaternary history of spruce in southern Europe. Rev. Palaeobot. Palynol. 2002 120, 131-177.

Redmond, M.D., Kelsey, K.C., Urza, A.K., Barger, N.N., 2017. Interacting effects of climate and landscape physiography on piñon pine growth using an individual-based approach. Ecosphere 8 e01681.

Rellstab, C., Zoller, S., Walthert, L., Lesur, I., Pluess, A.R., Graf, R., Bodénès, C., Sperisen, C., Kremer, A., Gugerli, F., 2016. Signatures of local adaptation in candidate genes of oaks (*Quercus* spp.) with respect to present and future climatic conditions. Mol. Ecol. 25, 5907–5924.

Rellstab, C., Gugerli, F., Eckert, A.J., Hancock, A.M., Holderegger, R., 2015. A practical guide to environmental association analysis in landscape genomics. Mol. Ecol. 24, 4348–4370.

Ribeiro Jr, P.J., Diggle, P.J., 2016. *geoR*: analysis of geostatistical data. R package version 1.7-5.2. https://CRAN.R-project.org/package=geoR

Rita, A., Borghetti, M., Todaro, L., Saracino, A., 2016. Interpreting the climatic effects on xylem functional traits in two Mediterranean oak species: the role of extreme climatic events. Front. Plant Sci. 7, 1126.

Ritland, K., 1996. Estimators for pairwise relatedness and individual inbreeding coefficients. Genet. Res. 67, 175-185.

Ritland, K., Ritland, C., 1996. Inferences about quantitative inheritance based on natural population structure in the yellow monkeyflower, *Mimulus guttatus*. Evolution 50, 1074–1082.

Ritland, K., 2000. Marker-inferred relatedness as a tool for detecting heritability in nature. Mol. Ecol. 9, 1195–1204.

Robledo-Arnuncio, J.J., Unger, G.M., 2018. Measuring viability selection from prospective cohort mortality studies: a case study in maritime pine. Evol. Appl. doi: 10.1111/eva.12729.

Rousset, F., 2008. GENEPOP'007: A complete re-implementation of the GENEPOP software for Windows and Linux. Mol. Ecol. Resour. 8, 103–106.

Rozas, V., 2015. Individual-based approach as a useful tool to disentangle the relative importance of tree age, size and inter-tree competition in dendroclimatic studies. iForest 8, 187–194.

Ruiz Daniels, R., Taylor, R.S., Serra-Varela, M.J., Vendramin, G.G., González-Martínez, S.C., Grivet, D., 2018. Inferring selection in instances of long-range colonization: the Aleppo pine (*Pinus halepensis*) in the Mediterranean Basin. Mol. Ecol. 27, 3331–3345.

Rungis, D., Bérubé, Y., Zhang, J., Ralph, S., Ritland, C.E., Ellis, B.E., Douglas, C., Bohlmann, J., Ritland, K., 2004. Robust simple sequence repeat markers for spruce (*Picea* spp.) from expressed sequence tags. Theor. Appl. Genet. 109, 1283–1294.

Sato, T., 2004. Size-dependent sex allocation in hermaphroditic plants: the effects of resource pool and self-incompatibility. J Theor. Biol., 227, 265–275.

Savolainen, O., Lascoux, M., Merilä, J., 2013. Ecological genomics of local adaptation. Nat. Rev. Genet. 14, 807–820.

Savolainen, O., Pyhäjärvi, T., Knürr, T., 2007. Gene flow and local adaptation in trees. Annu. Rev. Ecol. Evol. Syst. 38, 595–619.

Scalfi, M., Mosca, E., Di Pierro, E.A., Troggio, M., Vendramin, G.G., Sperisen, C., La Porta, N., Neale, D.B., 2014. Micro-and macro-geographic scale effect on the molecular imprint of selection and adaptation in Norway spruce. PLoS One 9, 1–22.

Schnabel, A., Nason, J.D., Hamrick, J.L., 1998. Understanding the population genetic structure of *Gleditsia triacanthos* L.: seed dispersal and variation in female reproductive success. Mol. Ecol. 7, 819–832.

Schoen, D.J., Stewart, S.C., 1986. Variation in male reproductive investment and male reproductive success in white spruce. Evolution 40, 1109–1120.

Schoville, S.D., Bonin, A., Francois, O., *et al.*, 2012. Adaptive genetic variation on the landscape: methods and cases. Ann. Rev. Ecol. Evol. System. 43, 23–43.

Schweingruber, F.H., 1988. Tree rings: basics and applications of dendrochronology. Kluwer Academic Publishers, Dordrecht.

Schweingruber, F.H., 1996. Tree Rings and Environment. Dendroecology. Paul Haupt AG Bern, Berne.

Scotti, I., Magni, F., Paglia, G.P., Morgante, M., 2002. Trinucleotide microsatellites in Norway spruce (*Picea abies*): Their features and the development of molecular markers. Theor. Appl. Genet. 106, 40–50.

Selkoe, K.A., Toonen, R.J., 2006. Microsatellites for ecologists: a practical guide to using and evaluating microsatellite markers. Ecol. Lett. 9, 615–629.

Silvertown, J., Franco, M., Perez-Ishiwara, R., 2001. Evolution of senescence in iteroparous perennial plants. Evol. Ecol. Res. 3, 393–412.

Smouse, P.E., Sork, V.L., 2004. Measuring pollen flow in forest trees: an exposition of alternative approaches. For. Ecol. Manage. 197, 21–38.

Smouse, P.E., Meagher, T.R., Lobak, C.J., 1999. Parentage analysis in *Chaemeclirium luteum* (L.) Gray (Liliaceae): why do some males have higher contributions? J. Evol. Biol. 12, 1069–1077.

Sork, V.L., Squire, K., Gugger, P.F., Steele, S.E., Levy, E.D., Eckert, A.J., 2016. Landscape genomic analysis of candidate genes for climate adaptation in a California endemic oak, *Quercus lobata*. Am. J. Bot. 103, 33–46.

Sork, V.L., Davis, F.W., Westfall, R., Flint, A., Ikegami, M., Wang, H., Grivet, D., 2010. Gene movement and genetic association with regional climate gradients in California valley oak (*Quercus lobata* Née) in the face of climate change. Mol. Ecol. 19, 3806–3823.

Steinitz, O., Troupin, D., Vendramin, G.G., Nathan, R., 2011. Genetic evidence for a Janzen-Connell recruitment pattern in reproductive offspring of *Pinus halepensis* trees. Mol. Ecol. 20, 4152–4164.

Stintzi, A., Heitz, T., Prasad, V., Wiedemann-Merdinoglu, S., Kauffmann, S., Geoffroy, P., Legrand, M., Fritig, B., 1993. Plant "pathogenesis-related" proteins and their role in defense against pathogens. Biochimie 75, 687–706.

Storey, J.D., Bass, A.J., Dabney, A., Robinson, D., 2015. qvalue: Q-value estimation for false discovery rate control. R package version 2.8.0. http://github.com/jdstorey/qvalue

Szeicz, J.M., MacDonald, G.M., 1994. Age dipendent tree-ring growth responses of subartic white spruce to climate. Can. J. For. Res. 24, 120–132.

Sutinen, R., Teirilä, A., Pänttäjä, M., Sutinen, M.-L., 2002. Distribution and diversity of tree species with respect to soil electrical characteristics in Finnish Lapland. Can. J. For. Res. 32, 1158–1170.

Taeger, S., Zang, C., Liesebch, M., Schneck, V., Menzel, A., 2013. Impact of climate and drought events on the growth of Scots pine (*Pinus sylvestris* L.) provenances. For. Ecol. Manag. 307, 30–42.

Tirén, L. 1935. Om granens kottsättning, des periodicitet och samband med temperature och nederbörd. Meddelanden från Statens Skogsforskningsinstitut 28, 413–518.

Tollefsrud, M.M., Kissling, R., Gugerli, F., Johnsen, Ø., Skrøppa, T., Cheddadi, R., Van Der Knaap, W.O., Latałowa, M., Terhürne-Berson, R., Litt, T., *et al.,* 2008. Genetic consequences of glacial survival and postglacial colonization in Norway spruce: combined analysis of mitochondrial DNA and fossil pollen. Mol. Ecol. 17, 4134–4150.

Trujillo-Moya, C., George, J.-P., Fluch, S., Geburek, T., Grabner, M., Karanitsch-Ackerl, S., Konrad, H., Mayer, K., Sehr, E.M., Wischnitzki, E., Schueler, S., 2018. Drought sensitivity of Norway spruce at the species' warmest fringe: quantitative and molecular analysis reveals high genetic variation among and within provenances. G3-Genes|Genomes|Genet. 8, 1225–1245.

Tuomi, J., Hakala, T., Haukioja, E., 1983. Alternative concepts of reproductive efforts, costs of reproduction and selection in life hystory evolution. Am. Zool. 23, 25–34.

Unger, G.M., Konrad, H., Geburek, T., 2011. Does spatial genetic structure increase with altitude? An answer from *Picea abies* in Tyrol, Austria. Plant Syst. Evol. 292, 133–141.

Venables, W.N., Ripley, B.D., 2002. Modern applied statitics with S. Springer Ferlag, NewYork.

Vendramin, G.G., Lelli, L., Rossi, P., Morgante, M., 1996. A set of primers for the amplification of 20 chloroplast microsatellites in Pinaceae. Mol. Ecol. 5, 595–598.

Vescovi, E., Ammann, B., Ravazzi, C., Tinner, W., 2010. A new Late-glacial and Holocene record of vegetation and fire history from Lago del Greppo, northern Apennines, Italy. Veg. Hist. Archaeobot. 19, 219–233.

Viglas, J.N., Brown, C.D., Johnstone, J.F., 2013. Age and size effects on seed productivity of northern black spruce. Can. J. For. Res. 43, 534–543.

de Villemereuil, P., Frichot, É., Bazin, É., François, O., Gaggiotti, O.E., 2014. Genome scan methods against more complex models: when and how much should we trust them? Mol. Ecol. 23, 2006–2019.

Vitti, J.J., Grossman, S.R., Sabeti, P.C., 2013. Detecting natural selection in genomic data. Annu. Rev. Genet. 47, 97–120.

Wang, J., 2007. Triadic IBD coefficients and applications to estimating pairwise relatedness. Genet. Res. 89, 135–153.

Wang, J., 2017. Estimating pairwise relatedness in a small sample of individuals. Heredity 119, 302–313.

Wang, T., O'Neill, G.A., Aitken, S.N., 2010. Integrating environmental and genetic effects to predict responses of tree populations to climate. Ecol Appl 20,153–163.

Weir, B.S., Anderson, A.D., Hepler, A.B., 2006. Genetic relatedness analysis: modern data and new challenges. Nat. Rev. Genet. 7, 771–780.

Williams, G.C., 1966. Adaptation and natural selection. Princeton University Press, New York.

Wilson, R.J.S., Hopfmüller, M., 2001. Dendrochronological investigations of Norway spruce along an elevational transect in the Bavarian Forest, Germany. Dendrochronologia 19, 67–69.

Xie, C.Y., Knowles, P., 1994. Mating system and effective pollen immigration in a Norway spruce (*Picea abies* (L.) Karst.) plantation. Silvae Genet 43, 48–51.

Younginger, B.S., Sirová, D., Cruzan, M.B., Ballhorn, D.J., 2017. Is biomass a reliable estimate of plant fitness? Appl. Plant Sci. 5, 1600094.

Zapata, J.M., Martínez-García, V., Lefebvre, S., 2007. Phylogeny of the TRAF/MATH domain. In: TNF Receptor Associated Factors (TRAFs). Springer.

Zimin, A., Stevens, K.A., Crepeau, M.W., Holtz-Morris, A., Koriabine, M., Marcais, G., Puiu, D., Roberts, M., Wegrzyn, J.L., de Jong, P.J., *et al.*, 2014. Sequencing and assembly of the 22-Gb loblolly pine genome. Genetics 196, 875–890.

Zuur, A.F., Ieno, E.N., Walker, N., Saveliev, A.A., Smith, G.M., 2009. Mixed Effects Models and Extensions in Ecology with R. Springer, New York.

Zuur, A.F., Ieno, E.N., Elphick, C.S., 2010. A protocol for data exploration to avoid common statistical problems. Methods Ecol. Evol. 1, 3–14.

Appendix 1

ID[a]	SNP	Scaffold	Gene	Type	Probe
1	0.10267.01.11641.contigContig1.154	MA.139238	MA.139238g0010	NonSyn	T/C
2	08Pg04341e.2	MA.135525	MA.135525g0010	Intron	T/A
3	08pg08102j	MA.89683	MA.89683g0010	Syn	A/C
4	08pg15170h	MA.101422	MA.101422g0010	NonSyn	A/G
5	AP2L3.2319	MA.2193	MA.2193g0020	Intron	A/G
6	c74958.g1.i1.1765.HT	MA.10428140		Intergenic	T/C
7	c80226.g1.i1.820.HT	MA.10436298		Intergenic	T/G
8	c89584.g2.i1.197	MA.90007		Intergenic	A/C
9	CDF1.merged.p1.469	MA.2474564	MA.2474564g0010	Syn	A/G
10	CL1414Contig1.01.11984.contigContig2.201	MA.133096	MA.133096g0010	Intron	T/A
11	CL22Contig1.934	MA.30402	MA.30402g0010	Syn	A/G
12	CL3444Contig1.02.9029.contigContig1.407	MA.49382	MA.49382g0010	Intron	A/C
13	CL697Contig1.1468	MA.12670		Intergenic	C/G
14	CL866Contig1.01.10993.contigContig1.209	MA.10234164	MA.10234164g0010	Intron	A/G
15	CL995Contig1.252	MA.124514		Intergenic	A/C
16	FCL1104Contig1.834	MA.4218		NA	T/C
17	FCL1156Contig1.373	MA.10435905	MA.10435905g0030	Syn	T/C
18	FCL1488Contig1.1814	MA.37369	MA.37369g0010	Syn	A/G
19	FCL1522Contig1.865	MA.10427843		NA	T/G
20	FCL164Contig1.1221	MA.59480	MA.59480g0010	Syn	T/C
21	FCL1942Contig1.292	MA.10426376		Intergenic	T/C
22	FCL1947Contig1.1181	MA.657535			T/C
23	FCL2232Contig1.745	MA.7211			T/C
24	FCL697Contig1.1758	MA.109548		Intergenic	T/C
25	GCAT.2.0.GQ0131.B3.H20.EPB.03	MA.8519251	MA.8519251g0010	NonSyn	T/A
26	GCAT.2.0.GQ0172.B3.r.H11.EPB.06	MA.58914	MA.58914g0010	Intron	A/G
27	GCAT.2.0.GQ02010.B3.r.E06.EPB.02	MA.10427662	MA.10427662g0010	Syn	A/G
28	GQ00410.P08.1.111	MA.2784169	MA.2784169g0010	NonSyn	A/G
29	GQ0046.B3.E02.1.777	MA.10426168	MA.10426168g0010	Syn	A/C
30	GQ0062.A21.1.168	MA.68129	MA.68129g0010	Syn	T/C
31	GQ0082.C07.1.844	MA.10426168	MA.10426168g0010	Syn	A/G
32	GQ01312.B05.2.453	MA.913693	MA.913693g0010	NonSyn	A/C
33	GQ0207.I07.1.41	MA.59732	MA.59732g0010	Syn	A/G
34	GQ0256.F18.1.547	MA.185096	MA.185096g0010	Syn	G/C
35	GQ02803.I06.3.2091	MA.10433428		Intergenic	T/A
36	GQ02805.H15.1.75	MA.10430373		Intergenic	T/C
37	GQ02811.M07.1.118	MA.10436794		Intergenic	T/G
38	GQ02818.M02.1.334	MA.93052	MA.93052g0010	Syn	A/G
39	GQ02830.K01.1.272	MA.57955	MA.57955g0010	NonSyn	T/C
40	GQ02901.G01.3.181	MA.91105		Intergenic	A/G
41	GQ02907.H19.1.164	MA.10431084			A/G
42	GQ03102.M11.1.991	MA.19866		Intergenic	A/G
43	GQ03104.H16.1.718	MA.8230652		Intergenic	T/C
44	GQ03109.J19.1.782	MA.10427740		Intergenic	A/C
45	GQ03109.L07.1.719	MA.295515		Intergenic	T/C
46	GQ03110.O16.1.1413	MA.2382		Intergenic	T/C
47	GQ03111.D17.1.1106	MA.10426088		Intergenic	A/G

48	GQ03111.P07.1.80	MA.74264	MA.74264g0020	Syn	T/C
49	GQ03114.H08.1.159	MA.58159	MA.58159g0010	NonSyn	T/C
50	GQ03116.D16.1.66	MA.363801	MA.363801g0010	Syn	T/C
51	GQ03201.F12.1.693	MA.5933		Intergenic	T/C
52	GQ03209.H09.1.774	MA.58340		Intergenic	A/G
53	GQ03224.A01.1.188	MA.75636	MA.75636g0010	Syn	T/C
54	GQ03230.M01.1.766	MA.10434080	MA.10434080g0010	NonSyn	A/G
55	GQ03237.D15.1.370	MA.121869		Intergenic	A/G
56	GQ03407.I03.1.21	MA.55851	MA.55851g0010	NonSyn	T/C
57	GQ03412.L23.1.1340	MA.942991		NA	T/C
58	GQ03414.P13.2.1203	MA.10436085		Intergenic	A/G
59	GQ03604.O12.1.630	MA.8396769			A/G
60	GQ03605.F01.2.643	MA.15776			A/G
61	GQ03614.F14.1.1273	MA.8910932		Intergenic	A/G
62	GQ03702.D08.1.1408	MA.10228148	MA.10228148g0010	Syn	A/G
63	GQ03712.F05.1.170	MA.141	MA.141g0010	NonSyn	A/G
64	GQ03716.M20.1.928	MA.9130892		Intergenic	T/C
65	GQ03719.P11.1.1591	MA.10433955	MA.10433955g0020	Intron	A/G
66	GQ03815.P06.1.1333	MA.92132	MA.92132g0010	Syn	A/G
67	GQ03819.E08.1.554	MA.281207			T/C
68	GQ03912.E20.1.589	MA.14427	MA.14427g0010	Syn	T/C
69	GQ04001.H11.3.589	MA.10433187	MA.10433187g0010	Syn	T/C
70	GQ04013.J19.4.1537	MA.10434838		Intergenic	T/C
71	MA.10219080g0010.579.C.T	MA.10219080	MA.10219080g0010	Syn	T/C
72	MA.103581g0010.6996.C.T	MA.103581	MA.103581g0010	Syn	T/C
73	MA.10430155g0010.2606.T.G	MA.10430155	MA.10430155g0010	Intron	T/G
74	MA.10430492g0030.1681.A.T	MA.10430492	MA.10430492g0030	NonSyn	T/A
75	MA.115536g0010.2534.A.C	MA.115536	MA.115536g0010	NonSyn	A/C
76	MA.654072g0010.1774.G.T	MA.654072	MA.654072g0010	NonSyn	A/C
77	MA.7133366g0010.479.T.C	MA.7133366	MA.7133366g0010	Syn	A/G
78	MA.91554g0010.2937.C.T	MA.91554	MA.91554g0010	Syn	T/C
79	MA.96461g0010.2684.T.C	MA.96461	MA.96461g0010	Intron	T/C
80	NODE.2238.length.196.cov.80.989799.117	MA.10434331		Intergenic	T/G
81	NODE.32475.length.733.cov.91.013641.619	MA.4671		Intergenic	A/G
82	NODE.4223.length.996.cov.63.923695.391	MA.10435805	MA.10435805g0010	Syn	A/G
83	NODE.4953.length.1279.cov.202.146210.373	MA.10435489	MA.10435489g0010	Syn	A/G
84	P03706.2	MA.124661	MA.124661g0010	Intron	A/G
85	P04801.5	MA.41523	MA.41523g0010	Intron	A/G
86	P06971.3	MA.104065	MA.104065g0020	Syn	A/G
87	P07840F1.3	MA.9889985		Intergenic	T/C
88	P3747.3	MA.93259	MA.93259g0010	Intron	T/C
89	pa08pg01018e	MA.212053			T/G
90	Pabies1391.224	MA.10591	MA.10591g0010	NonSyn	A/T
91	PabiesCry.823	MA.10428291	MA.10428291g0010	NonSyn	G/C
92	PabiesMYB2.3545	MA.115536	MA.115536g0010	NonSyn	A/G
93	PabiesSb62.472	MA.19619	MA.19619g0010	Syn	A/G
94	PabiesZTL.514	MA.70291	MA.70291g0010	Syn	A/G
95	paP08075.2	MA.394947	MA.394947g0010	Syn	T/C
96	PaPHYO.RIII336	MA.6718		Intergenic	A/C
97	PaPHYO.RIV211	MA.6809	MA.6809g0030	Intron	T/C

98	PBB.PF02309.12.1	MA.53529		Intergenic	T/A
99	PGLM0.0295	MA.10260690	MA.10260690g0010	NonSyn	A/G
100	PGLM1.1163	MA.88541	MA.88541g0010	NonSyn	T/C
101	PGLM2.0104	MA.10436040	MA.10436040g0020	Syn	T/C
102	PGLM2.0395	MA.7312	MA.7312g0010	Syn	A/C
103	PGLM2.0624	MA.10436947	MA.10436947g0010	NonSyn	T/C
104	PGLM2.0690	MA.182569	MA.182569g0020	Syn	A/C
105	PGLM2.0812	MA.12354		Intergenic	A/C
106	PGLM2.1030	MA.140984	MA.140984g0020	Syn	T/C
107	PGLM2.1091	MA.953992		Intergenic	C/G
108	SB18.506	MA.14940	MA.14940g0020	Syn	T/G
109	SB18.686	MA.14940		Intergenic	A/C
110	SPA2.1601	MA.101443	MA.101443g0010	Intron	A/G
111	ss538946232	MA.134110		Intergenic	T/C
112	WS.2.0.GQ0013.BR.1.M07.3.171	MA.10430608	MA.10430608g0010	Syn	A/G
113	WS.2.0.GQ00410.B3.L15.1.478	MA.7457516		Intergenic	T/C
114	WS.2.0.GQ02828.B7.G06.1.930	MA.10436842		Intergenic	A/G
115	WS00841.F23.1.82	MA.10431591		Intergenic	T/G
	02739.B22.2345	MA.14534	MA.14534g0010	Intron	A/C
	FCL116Contig1.249	MA.4907	MA.4907g0010	NonSyn	T/C
	FCL1399Contig1.562	MA.1170922		Intergenic	A/G
	FCL1727Contig1.865	MA.60257		Intergenic	A/C
	GQ0013.BR.1.A19.18.422	MA.10436059	MA.10436059g0010	NonSyn	T/C
	GQ0031.B3.r.N13.1.1306	MA.10431764		Intergenic	T/G
	GQ01313.K05.3.371	MA.9139232		Intergenic	A/G
	GQ0202.C02.1.71	MA.18326		Intergenic	T/C
	GQ02814.E08.1.259	MA.623831	MA.623831g0010	Syn	T/C
	GQ03112.C10.1.583	MA.60257	MA.60257g0010	Syn	A/G
	GQ03210.O01.1.1242	MA.10431764		Intergenic	A/G
	GQ03304.M18.1.273	MA.39167	MA.39167g0010	NonSyn	T/C
	GQ03308.J05.1.1406	MA.30905	MA.30905g0010	Syn	T/C
	GQ03326.H03.1.842	MA.10229417		Intergenic	T/C
	GQ03607.I03.1.292	MA.8420140		Intergenic	A/C
	MA.10434099g0020.1498.A.G	MA.10434099	MA.10434099g0020	Syn	A/G
	PGLM2.0334	MA.918722	MA.918722g0010	Syn	T/C
	PTC9341	MA.5950	MA.5950g0010	Intron	A/G
	ss538953158	MA.82939		Intergenic	T/C
	WS.2.0.GQ0222.B7.B17.1.379	MA.100136	MA.100136g0010	Syn	T/G

[a]The SNP ID was reported only for the 115 SNP loci that were retained after the filtering procedure.